**Western Australia School of Mines: Minerals, Energy and Chemical Engineering**

# Data driven modelling of biomass pyrolysis

**Ruturaj Jayant Sawant**

**This thesis is presented for the Degree of**

**Doctor of Philosophy**

**Curtin University**

**And**

**University of Aberdeen**

**April 2024**

# Declaration

To the best of my knowledge this thesis contains no work previously published, unless where due acknowledgement is given.

This thesis contains no material which has been accepted for the award of any other degree or diploma in any university.

12/04/2024

# Acknowledgements

researcher, and a good friend. Discussions with him helped me understand the basics of artificial neural networks and coding in python. I hope the Sawant-Thosar correlation is not too far in the future!

I have learnt from the past work of my peers. A great deal of work has been carried out with regards to biomass pyrolysis. The current work learns from it and tries to further it a bit. Some of the associated challenges have been addressed over the course of PhD work and the learnings from the work have contributed towards this thesis. Due credit has been given wherever possible in this work.

# Abstract

Biomass pyrolysis is one of the processes for deriving fuel and value-added platform chemicals from a renewable carbonaceous feedstock having a carbon neutral to carbon positive process potential. Biomass pyrolysis has been studied for over 60 years, however it has started receiving greater scientific and commercial interest in recent years, especially in lieu of subsea crude oil dependence and as an option to aid the green energy transition.

The aim-objective of this work was to gain a deeper understanding of the factors governing the phenomena of biomass pyrolysis to obtain consistent and relevant kinetic parameters which would help facilitate the development of robust reactor and particle scale models.

One of the major challenges in kinetic modelling as well as reactor design and product yield prediction is the inherently heterogeneous nature of biomass as a solid feedstock. This heterogeneity is not captured in most commonly used kinetic methods. As a result, there is a general lack of robustness and fidelity when calculating kinetic parameters using conventional methods for reactor and process design. Another source of inconsistencies and confusion is the difference in nature of slow pyrolysis and fast pyrolysis and a dearth of qualitative and quantitative understanding of factors determining it. Slow pyrolysis is characterized by lumped reaction mechanism as opposed to fast pyrolysis in which constituent elements undergo discrete degradation. The possibility and benefits of dynamic reactor control specifically in case of fast pyrolysis is also dealt with in our work.

In this work, a series of experiments were performed to elucidate the nature of slow pyrolysis and fast pyrolysis and study the factors influencing the rate of pyrolysis. A critical review of existing methods for determination of kinetic parameters and the limits of their applicability for biomass pyrolysis has also been addressed. Based on the understanding gained, biochemical chemical characterization of 10 locally sourced biomass samples was carried out and the composition of their structural carbohydrates (viz. cellulose, hemicellulose, lignin etc) was determined. Since the inorganics present in biomass make biomass pyrolysis an inherently autocatalytic process, the inorganic and elemental composition of all 10 samples was also calculated. TGA experiments were performed at various linear heating rates and particle sizes not just for the 10 biomass samples, but also for pure cellulose, hemicellulose and lignin samples.

The generated experimental data was used to link the composition of biomass to its relevant kinetic parameters. Comparison between kinetic parameters from conventional methods and proposed method has shown to support our thesis. An attempt to combine model fitting method with model free methods to obtain Arrhenius type kinetic parameters has also been made and shows some promise within applicable limits. Further, machine learning approaches such as artificial neural networks have been implemented to develop predictive models which not just capture the inherent heterogeneity of biomass but also give decent predictive

capabilities across length and time scales. Elucidation of the phenomena of biomass pyrolysis and factors governing it along with proposed predictive model makes it possible to integrate consistent kinetics with particle scale and reactor scale models with improved fidelity. Lastly, this work hopes to be a contribution which would help in realizing the commercial and operational potential of biomass pyrolysis.

# Contents

# Chapter 1 Understanding Biomass Pyrolysis

*In this chapter, the concept of biomass pyrolysis is introduced along with various engineering (physio-chemical) aspects related to the process. Historical development of scientific and technological advancements brought about through various studies on biomass pyrolysis is also discussed. Factors influencing the modelling and experimental work necessary for commercialisation and operability of biomass pyrolysis process are also reviewed. A short discussion regarding the major challenges inhibiting the general maturity of biomass pyrolysis as a viable technology is included. Despite the associated challenges, the potential and promise shown by biomass pyrolysis and applicability that it finds in today's global energy scenario has been summarized. The environmental aspects and techno-economic considerations associated with biomass pyrolysis along with various conjugate and affiliated thermochemical processes has also been addressed. Finally, a brief literature review is given which discusses major contributions by various authors/research groups, major phenomena which govern and determine the nature of biomass pyrolysis process and various engineering considerations necessary for design and optimization of the process.*

## 1.1 Introduction

Biomass fast pyrolysis is one of the techniques of converting biomass into utilizable fuel forms or relevant platform chemicals. The process of pyrolysis can be explained as thermal treatment of a feedstock in an inert (oxygen free) atmosphere. Non-reactive gas such as Nitrogen, Argon or Helium is used to achieve inert conditions while simultaneously serving as carrier agent for the volatiles produced during pyrolysis reaction. Pyrolysis of a carbonaceous feedstock is carried out to convert the feedstock into a crude-oil dominant fraction (+ char) as opposed to a syngas dominant fraction (+ char) which occurs during combustion. The quality and quantity of each of the said fractions is determined by the **process conditions** and **composition of biomass**. In other words, the process conditions together with the composition of biomass determine not just the kinetics of reaction process but also determine the yield of each fraction quantitatively and qualitatively[1–3].

Process conditions are determined first and foremost by the reactor type and design. This determines the scale and physical boundary conditions of the process. Table 1 and 2 show some of the common reactor types in use and their details. Chapter 5 of this thesis deals with this aspect in more detail. The variables temperature, pressure and carrier gas flow rate determine the dynamic control of the process. In most common pyrolysis applications, pressure is kept constant. However, both vacuum and high-pressure pyrolysis operations have been reported. Throughout our work, we have dealt only with constant pressure conditions. The temperature control of pyrolysis process can either be at isothermal (constant temperature) conditions or at non-isothermal (varying temperature) conditions. For isothermal processes, the temperature is kept constant at $T_{max}$ and pyrolysis kinetics is essentially the relationship between degree of conversion and reaction time. Non-isothermal pyrolysis is performed either at a variable or a constant heating rate. In our work, we have used multiple linear heating-rates to elucidate the relationship between temperature and degree of conversion. The reaction kinetics is then a function not just of time but also of temperature. Effect of reactor temperature conditions on biomass pyrolysis and the methods associated with determination of reaction kinetics are discussed in detail in chapter 2 and chapter 3 of the thesis. The carrier gas flowrate essentially determines the residence time of particle in reaction regime and as such also influences the degree of conversion/reaction of feedstock particles.

Feedstock composition is determined both chemically and physically. A chemically homogenous feedstock (single compound or polymer) usually has uniform conversion profile under pyrolysis conditions. Biomass, however, is a highly heterogeneous feedstock compositionally. Its structure is depicted in Figure 1. Its main constituent blocks are the polymers cellulose, hemicellulose and lignin. Protein, lipids and inorganics are the minor constituents on biomass. Cellulose is a crystalline polysaccharide consisting of n-glucose monomers linked with 1,4- β glucoside bond. This provides cellulose with a degree of linearity in its structure. Cellulose, therefore, decomposes within a specific thermal range. Hemicellulose is an amorphous polysaccharide consisting of units of mainly xylose and arabinose. Lignin is three-dimensional cross-linked polymer consisting of units of phenyl propane. Both hemicellulose and lignin decompose over a broader range of temperature. It is easier to decompose hemicellulose than to decompose lignin.[4,5] Conversion kinetics of biomass pyrolysis is closely linked to the compositional make-up of each biomass feedstock. The complexity in modeling conversion kinetics arises due to distinct yet overlapping regimes of cellulose, hemicellulose and lignin conversion under heat treatment conditions.[1,4] The complexity in prediction of yields is further compounded due to the primary and secondary reactions between gas phase products of the three polymers and the inherent autocatalytic nature of biomass at elevated temperature conditions.[6,7]
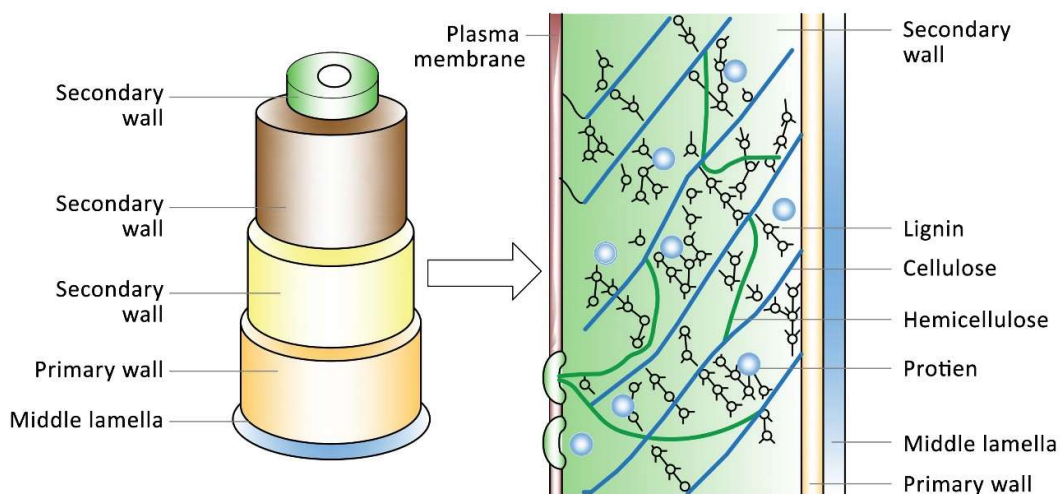
*Figure 1 Structural representation of biomass sample*

The process conditions and the feed composition are intimately linked to the yield quality and quantity of pyrolysis products. As such, the commercial application of yield fractions and required upgrading is determined to a large extent by process conditions and composition of biomass. There have been several attempts at modelling this relationship between feedstock composition, process conditions and yield distribution for biomass pyrolysis over the years with varying degrees of satisfaction. There are several thermochemical techniques to convert biomass into utilizable fuel forms or value-added chemical. The current work focusses specifically on fast pyrolysis process for biomass conversion. A brief overview of biomass pyrolysis process along with some prevalent conjugate pathways is shown in Figure 2. Prior efforts and related work carried out by various authors and research groups is reviewed at the end of this chapter.

Growing environmental concerns and problems associated with dependence on crude oil make it pertinent to look at alternative green energy sources. Biomass pyrolysis is one such technology. It has been around for almost 50 years but has started gaining more attention recently.[3,8] A brief overview of global energy production and global energy consumption is shown in Figures 3 and 4.
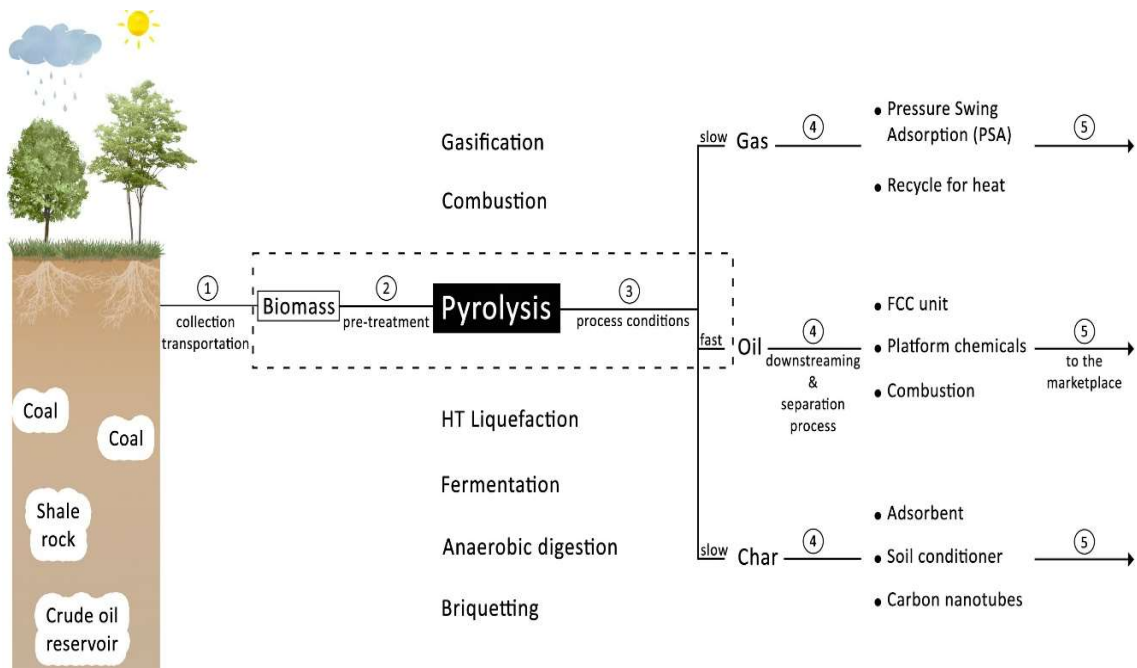
*Figure 2 Overview of conversion processes for carbonaceous feedstock, specifically biomass*
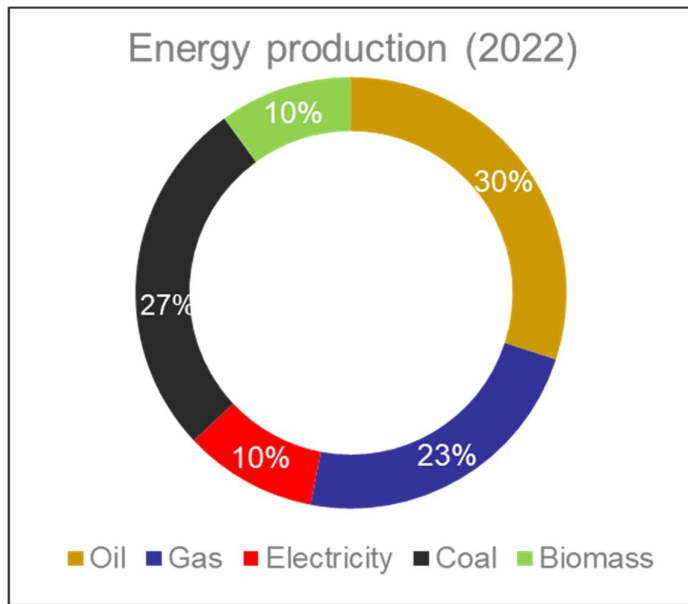


*Figure 3 Overview of global energy production[9]*

## 1.2 Literature review

There is abundance of literature available on thermochemical conversion of various feedstock. The process pyrolysis has been studied adjacent with studies delving into gasification. In the same vein, the study of kinetics of biomass pyrolysis is derived at least in part through the study into devolatilization of coal. However, there are specificities which make biomass pyrolysis quite unique. Biomass pyrolysis route can be adopted to produce char, crude-oil or gas depending upon process conditions.

### 1.2.1 Process conditions

Process conditions which determine and define pyrolysis are temperature, pressure, residence time/reaction time. The effect of pressure has not been included in this study and pressure is assumed to be constant (atmospheric pressure) for all our considerations. There have been some investigations [10–12] into effect of pressure on biomass pyrolysis, but it is tricky to carry out and is beyond the scope of this study. Broadly speaking, low pressure conditions seem to favour devolatilization and higher pressures seem to favour charring.

### I.    Temperature

The effect of temperature is the most well studied and well understood aspect of biomass pyrolysis. For a given pyrolysis process, the temperature could either be constant (isothermal conditions) or variable (non-isothermal conditions). When biomass is introduced in a pre-heated reactor at constant temperature, the process is considered isothermal. When biomass is fed to the reactor prior to heat ramping, the process is considered non-isothermal. It is important, however, to note that if the particle size of biomass is large enough for a thermal gradient to be effective within a particle, the particle scale process should be considered non-isothermal. This aspect will be discussed again towards the end of the thesis. The optimal operating temperature for biomass pyrolysis intended for oil production is ~500-600 $^\circ$C range. Higher operating temperatures than this lead to promotion of charring reactions and char + syngas is obtained. Operating temperatures lower than this lead to persistence of a plastic phase which is ionized and promotes charring and cracking reactions.[3,13,14]

In case of non-isothermal conditions, a heating rate is employed to heat up the biomass sample to desired temperature. The heating-rate is usually constant, and a lot of kinetic studies have been performed using constant (multiple) heating rates. There are number of studies which study the non-isothermal kinetics of biomass pyrolysis for a variety of samples which have been reviewed comprehensively.[2,8,15–18] Slower heating rates imply lower $\Delta T/\Delta t$ values, whereas faster heating rates imply higher $\Delta T/\Delta t$ values. Generally speaking, slower the heating rate, more lumped is the process. A review of literature reveals that most kinetic studies have been performed for slow heating rates, however fast pyrolysis has gained interest over recent years. Traditionally, biomass was thermally processed either via torrefaction or to generate low quality combustion oil and char. This had applications in electricity generation as well.

Generation of pyrolysis oil (from biomass) with the intention of integration with petrochemical industry for fuel and value-added chemical generation has found recent interest.[19–21] Studies focused on this have increased over recent years. Published literature tells us that to ensure maximizing pyrolysis oil fraction quantitatively and qualitatively, it is necessary to ensure fast heating rates, a kinetically controlled reaction regime and endothermic process control.[22–25] However, we also see that there are difficulties associated in achieving high quality oil yield. Especially for large scale operations to be commercially viable. Another thing to note is that in most works, the conversion of biomass during pyrolysis is the function of Temperature (only). *It is observed during the course of this work that while this temperature relationship is largely okay in case of homogenous compounds, it can lead to erroneous results in case of biomass pyrolysis. Incorporating the dependence of composition along with temperature is beneficial for designing biomass pyrolysis reactors and is one of the contributions of this work*. The current work tries to address some these fast pyrolysis aspects along the way.

## II.      Residence time

In case there is a carrier gas transporting the volatiles, the residence time is determined by the carrier gas flowrate. Wherein there is no carrier gas, usually a mechanical transport or batch process is assumed. In such cases, it is rather difficult to achieve short residence times (~2-5 seconds) and such reactors are not suited for achieving fast pyrolysis conditions. An inert carrier gas provides for a decent control over vapour residence time and can be used to achieve vapour residence times of ~2-5 seconds which are preferable for fast pyrolysis conditions.[26–28] Residence time is usually not of concern in case of batch processes or slow pyrolysis processes.

## III.      Feedstock properties

Cellulose, hemicellulose and lignin along with protein and ash constitute the components of biomass responsible for determining the chemical interactions during pyrolysis and subsequently the composition of bio-oil. Cellulose is a crystalline polysaccharide consisting of n-glucose monomers linked with 1,4- β glucoside bond. This provides cellulose with a degree of linearity in its structure. Cellulose, therefore, decomposes within a specific thermal range. Hemicellulose is an amorphous polysaccharide consisting of units of mainly xylose and arabinose. Lignin is three-dimensional cross-linked polymer consisting of units of phenylpropane. Both hemicellulose and lignin decompose over a broader range of temperature. It is easier to decompose hemicellulose than to decompose lignin. These individual thermal decomposition characteristics, their respective gas-phase (volatile) chemistries and the interactions between the primary and secondary gas phase components play a significant role in determination of bio-oil composition.[2,4]
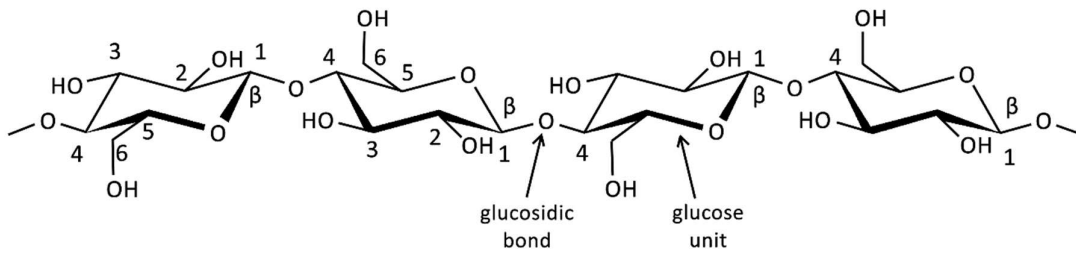
*Figure 4 Cellulose polysaccharide structure*
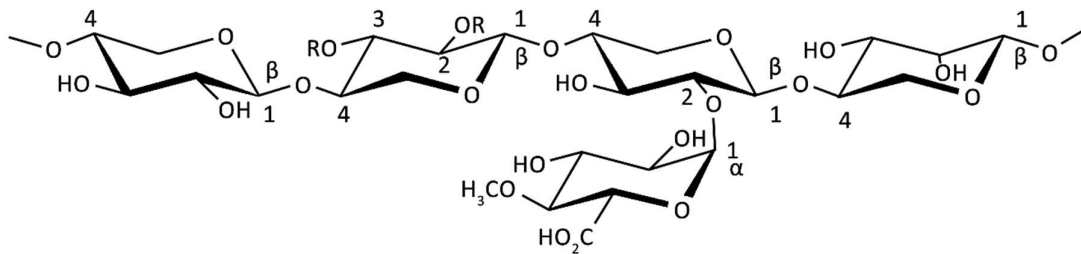


*Figure 5 Xylan (hemicellulose) of hardwoods*
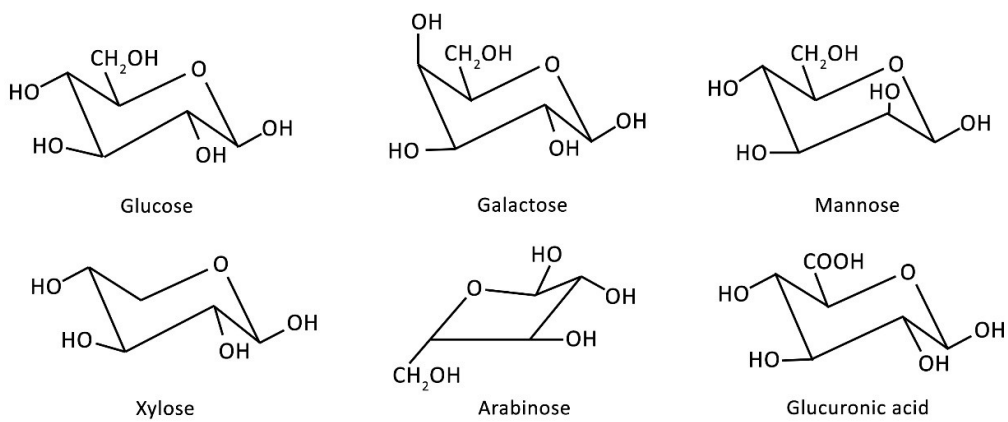


*Figure 6 Major monosaccharides which constitute cellulose and hemicellulose polysaccharides*
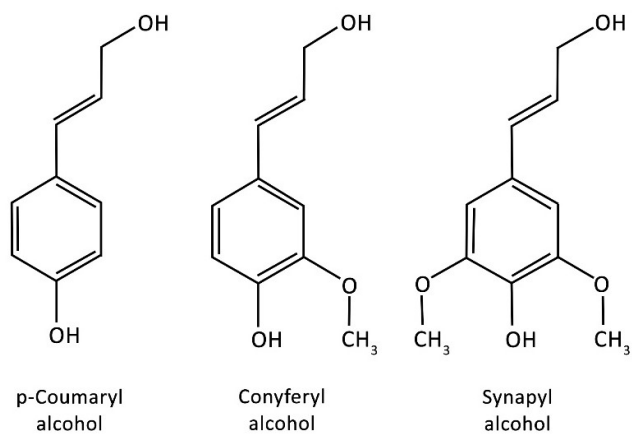
*Figure 7 Lignin monomers*
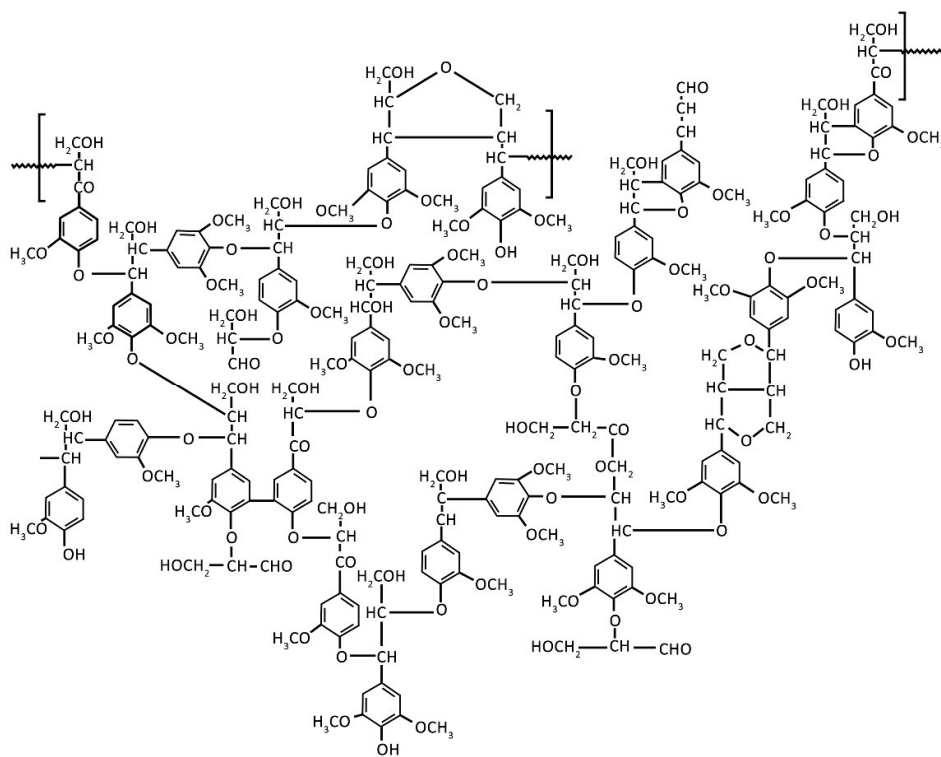


*Figure 8 Hardwood lignin structure*
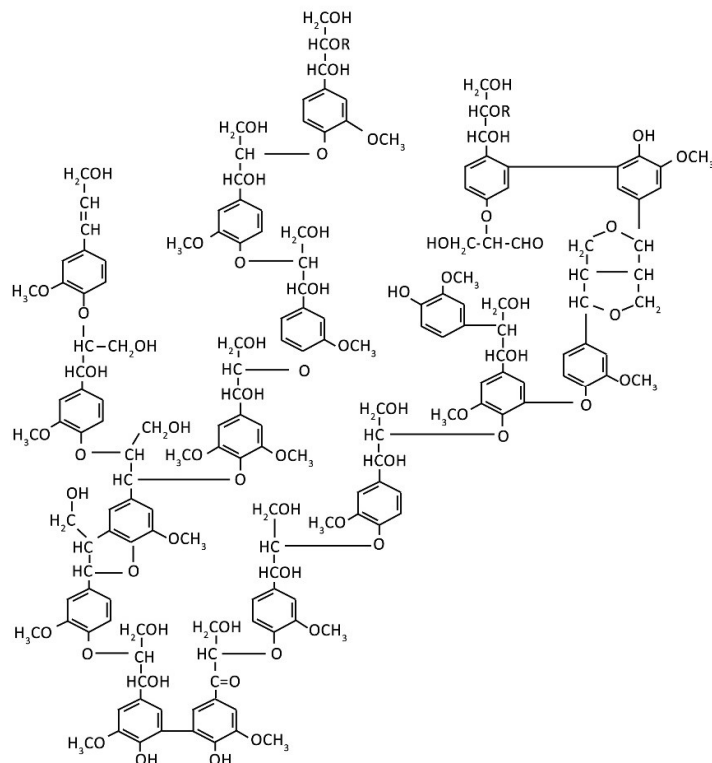
Figure 9 Softwood lignin structure

Thus, in this work, TGA datasets will serve as the basis of training the predictive model and for calculating the kinetic parameters of biomass samples for fast pyrolysis. Comprehensive TGA analysis of ten biomass samples have been carried out. TGA experiments for each biomass sample were carried out at five heating rates (250 K/min, 100 K/min, 50 K/min, 20 K/min, 5 K/min), two sample sizes (1 mg and 0.25 mg) and three particle size range (250 – 300 μm, 106 – 150 μm and below 45 μm). The sample size and particle size range were chosen to ensure that devolatilization occurs in purely kinetically controlled regime. Every sample was run in triplicates to check for repeatability. The generated 900 datasets will be used to comprehensively calculate the kinetic parameters for biomass samples as well as for training the predictive model. [1]

---

[1] *Juxtaposing coal gasification and biomass gasification/pyrolysis to understand the context of early studies in biomass pyrolysis- The fundamental idea behind biomass pyrolysis could be found in the process of natural crude formation and investigations in the process of coal gasification to generate energy/meet energy demand. The process of crude formation is essentially the conversion of solid carbon-based matter into hydrocarbon fractions under natural conditions. This process is over extremely long-time scales, at higher than atmospheric pressure and with entropy controlled conversion kinetics. Biomass pyrolysis could also be considered as a process of converting solid carbon-based matter into liquid hydrocarbons (plus*

## 1.2.2 Kinetic methods

Kinetic studies for biomass pyrolysis follow either a lumped approach or follow an approach involving individual specie based discretised yield models, both of which are based either on a mechanistic methodology or an empirical methodology. A mechanistic model is based on incorporating as much knowledge about a reaction mechanism into it for determining reaction kinetics. It can have predictive capabilities such as prediction of composition and yield. The more knowledge about reaction pathways and interconnectedness can one incorporate into it the better would be the predictive accuracy of mechanistic model. On the other hand, when the system under study is complex and hardly anything is known about its structural connectivity and functional mechanisms, yet one has to produce hypotheses about it one often relies on empirical models. They may incorporate some mechanistic assumptions so that they may look realistic.

The approach adopted in this work could be considered mechanistic but with transient nature on account of the dynamism of neural networks.

Till date, majority of these approaches are derived from kinetic investigations into thermal behaviour of wood, coal or synthetically generated polymers for varied applications. Most approaches assume that the Arrhenius form parameterized in terms of activation energy and other factors is sufficient to describe the pyrolysis behaviour of biomass. Arrhenius equation basically gives temperature dependence of a reaction. In this work, we see that the Arrhenius equation and only temperature dependence is insufficient to accurately describe biomass pyrolysis over temperature and time scales. We also present a kinetic approach suitable for biomass pyrolysis by incorporating feedstock composition dependence over time and temperature scale in kinetic reaction model. [2]

---

*some syngas and char), since it is most often a high temperature process. The kinetics of this thermochemical conversion is enthalpy driven. Biomass pyrolysis process can be carried out over longer time scales (slow pyrolysis) or shorter time scales (fast pyrolysis).*

[2] *The Arrhenius equation is analogous to its thermodynamic counterpart Eyring equation. Eyring equation is an analytical model whereas Arrhenius equation is an empirical model. For solid state reaction, as temperature of system is increased the entropy of solid feedstock starts to increase. The entropy of solid feedstock increases until it reaches the entropy of activation, at which the solid inert state undergoes phase change and a reactive plastic state or a fluid state is reached. This entropy of activation in thermodynamic theory is analogous to the activation energy in kinetic theory.*

## 1.2.3 Heat transfer and Mass transfer

Heat transfer and mass transfer effects over temperature and time scale are one of the lesser understood aspects of biomass pyrolysis.[29] The phenomena should be understood at particle scale and also at reactor scale to develop comprehensive models accounting for multiscale aspects. Smaller particles would have lesser internal thermal gradients and kinetic control of reaction is possible. With larger particle sizes, the internal thermal gradient is large and a diffusion reaction with secondary and tertiary cracking is present. One measure of gaining insight into these factors is to make use of dimensionless numbers. Three relevant dimensionless numbers and their significance is discussed here briefly. This is also touched upon in chapter 5.

Biot number $\quad Bi = \frac{hD}{\lambda}$ $\hspace{6cm}$ 1.1

Pyrolysis number 1 $\quad Py_1 = \frac{\lambda}{kC_pD^2\rho}$ $\hspace{4cm}$ 1.2

Pyrolysis number 2 $\quad Py_2 = \frac{h}{kC_pD\rho}$ $\hspace{4cm}$ 1.3

Where, *h: convective heat transfer coefficient (Wm$^{-2}$K$^{-1}$) ; D: characteristic length (m) (either particle diameter or length of reactor)  ; λ: thermal conductivity( Wm$^{-1}$K$^{-1}$)  ; $C_p$: specific heat capacity of biomass particle (J Kg$^{-1}$ K$^-$)$^1$ ; k: reaction rate coefficient (s$^{-1}$)  ; ρ: density of particle (kg m$^{-3}$)*

The range and values of these dimensionless numbers determines the operating regime of reaction.


## 1.2.4 Down-streaming, Upgradation, Process integration

Down-streaming, upgradation and process integration are crucial aspects of biomass pyrolysis process. However, these aspects are beyond the scope of the current work and are not dealt with in detail in this work. A brief overview of these aspects and their role in process is presented below.

Collection and phase separation: Since pyrolysis vapours are reactive and vapour phase reactions are known to occur, it is important to condense the vapours, separate various phase fractions and inhibit reactivity of crude-oil. Condensable vapours are usually passed through a cyclone separator to remove solid char particles from vapours. A shell and tube type heat exchanger is generally employed to condense the vapours and obtain crude fraction. Other approaches such as solvent quenching and in-situ catalytic treatment are also employed in certain cases. The non-condensable fraction is usually recycled to meet a portion of energy demand for the pyrolysis reactor, or it can be processed in a pressure swing adsorption system to separate individual component gases.

The high amount of elemental oxygen in biomass leads to formation of oxygenated compounds with poor fuel properties. Catalytic deoxygenation or hydrogenation is performed either in situ or ex situ to improve the fuel properties and make it petro-chemical compatible. Such an oil fraction could be processed within fluid catalytic cracking units of petrochemical infrastructure. [16,30,31]

A review of literature available on biomass pyrolysis throws light on the major challenges and possible solutions. Several authors have pointed towards the need for both concerted efforts at linking the available know how on biomass pyrolysis to help realise its commercial and technical promise and towards the need for adopting unique approaches to circumvent near certain pitfalls and difficulties associated in modelling biomass pyrolysis. [1, 4–6]
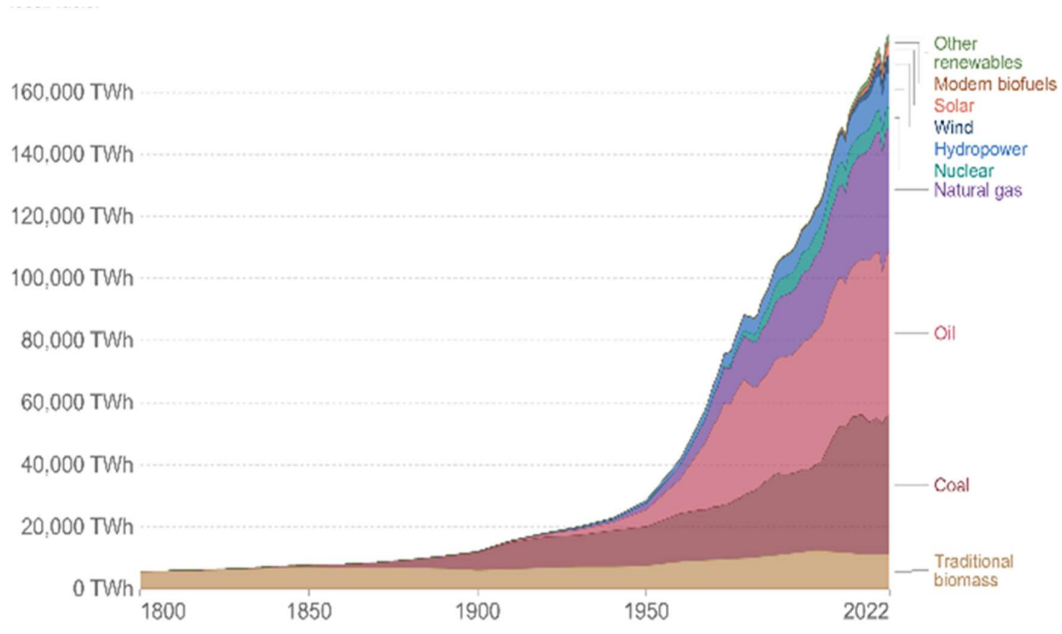


*Figure 10 Overview of global energy consumption [33]*

1.2.5 Promise and potential of biomass pyrolysis

One of the major reasons for interest in biomass pyrolysis is it the availability of feedstock and possibility of integrating the products into existing crude oil processing infrastructure. Biomass is the only renewable source for liquid fuels and chemicals that can be integrated within the existing crude processing infrastructure and oil-energy markets and has been studied now for decades. [29,32] Thermochemical conversion of biomass can technically utilise the entire plant as feedstock rather than utilise just the simple sugars which is the case with biological conversion. The reaction process timescale in case of thermochemical conversion ranges from

18

a few seconds to a few minutes, as compared to fermentation based processes which occur over days. The US department of energy has set a goal of replacing around 30% of transportation fuel with biofuel [32] (mainly bioethanol and biodiesel).

As such, biomass pyrolysis has the potential to assuage load on crude oil demand and use while being a carbon neutral process. Biomass pyrolysis is usually performed to convert lignocellulosic biomass into a bio-oil consisting of diverse chemicals (phenols, alcohols, furans, ketones, acids, etc.), bio-char, a solid product made up of residual carbon and syngas. Syngas is most often used to meet the partial energy requirements of the pyrolysis process. Although bio –oil has commercially relevant chemicals, it is also used as fuel (after necessary down-streaming operations) as it has a heating value of around 20 MJ/kg. Bio-char has potential to be used as soil-conditioner and commercial grade adsorbent.[34,35]

Further, biomass pyrolysis systems are not as capital intensive as other non-conventional renewable energy systems and the bio-oil obtained via pyrolysis can be blended with vacuum gas oil in fluid catalytic cracking units of oil refineries. Proper utilization of char for carbon sequestering purposes and elimination of NOx and SOx emissions would help reduce the adverse effects associated with production of crude oil and other associated products. Furthermore, there is yet not completely explored potential of co-pyrolysis, especially biomass and plastic-like waste.[36,37] Lastly, there is also a potential for hydrogen or lower hydrocarbons generation using biomass pyrolysis.[38,39]

Despite the need and promise held by biomass pyrolysis, it has found little success at large scale commercial operation due to a host of interlinked and difficult to overcome inherent issues associated with feedstock and process control. Some of the major challenges are discussed briefly in the next section and the aspects covered within the scope of current work are highlighted.

1.2.6 Factors impeding commercial and operational realization of biomass pyrolysis

I. **Multiscale and multiphase nature of feedstock, process and products**
   a. *Multiscale aspects*

One of the issues associated with biomass pyrolysis is the variance of phenomena as the scale of operation changes.[4] The multiscale nature of biomass pyrolysis is observed mainly in two aspects. First aspect is the multiscale nature of the feedstock and the second aspect is the multiscale nature of reaction process. The feedstock at microscopic/cellular level is inherently multi-scale in nature. The length-scale of cellulose polymer/structural carbohydrates (along with its structure) is quite different from the length-scales and structures of hemicellulose and lignin. At the macroscopic level, that particle size of feedstock is also important. [40]

The multiscale nature at cellular level is beyond our control. However, pre-treatment and size reduction can help us control or mitigate this effect a bit. Larger the particle size, longer would be the required residence time for complete conversion/reaction. This leads to larger particles undergoing charring and (secondary and tertiary) cracking reactions which contribute to a greater proportion of char and non-condensable gases. As such, in larger particle sizes the reaction would be diffusion controlled and exothermic reactions would be promoted. When the particle size is small enough for the reaction to be kinetically controlled, endothermic reactions would be promoted, and oil yield would be greater. This implies devolatization reactions as opposed to charring and cracking reactions.

In terms of reactor, the multiscale aspect is observed during the scale up of process. The phenomena of biomass pyrolysis at a small-scale/lab-scale is different from the phenomena of biomass pyrolysis at commercial scale/large scale. It is because of these reasons that the reactor design and process optimization at lab scale cannot be extrapolated to large scale operations and doing so would yield vastly different product profiles than as predicted. It can thus be said that biomass pyrolysis is essentially multiscale in nature due to the multiscale properties of its structural carbohydrates. This multiscale aspect can be either exemplified/magnified or it can be mitigated and minimized based on feedstock pre-treatment, size reduction and modelling and design considerations. Developing models capable of such multiscale predictions is important especially when considering scale-up. Our work discusses these aspects in chapter 2 and 3 and chapter 4 discusses a novel modelling approach suited for such multiscale predictive modelling.

The physical pre-treatment (drying and size reduction) carried out for current work is discussed in later section.

### b. Multiphase aspects

The phase change phenomena involved in biomass pyrolysis is relatively less understood. There have been efforts to understand the phase change occurring during pyrolysis. During biomass pyrolysis, a solid feedstock is converted in three fractions (solid char, liquid oil and syngas) of different phases. The composition and quantity of these said fractions is a result of process conditions and feedstock composition and this dual dependence makes studying these phenomena concretely a challenge. [29]

As discussed earlier, exothermic control of reaction would promote charring and gasification products, meaning a greater yield of solid and gas phase products. Whereas an endothermic controlled process within the kinetic regime would yield higher proportion of liquid phase products (condensed bio-oil). The phase change profiles for cellulose, hemicellulose and lignin are markedly different over time and temperature scales. The differential phase change characteristic of biomass constituents are not revealed to be of much importance during slow pyrolysis when highly lumped reaction assumptions work well. However, in case of fast

pyrolysis conditions, this differential phase change profile comes to fore much more. We discuss this in further detail in chapter 2 and 3. *Kinetic models capable of capturing this multiphase aspect with dynamic controlled have been recommended in this work to further utilize the potential of fast pyrolysis.*


## II.    Lack of consensus on reaction chemistry and mechanism

Most works classically were focussed on obtaining overall char, oil and gas yields via lumped kinetic modelling of biomass pyrolysis. These models gave little to no information about the composition and as such the quality of bio-oil. The speciation arising from primary and secondary reactions was not delineated. To study the reaction mechanism of biomass pyrolysis are different temperature and heating rate conditions to figure out the resulting oil yield compositions, a knowledge of thermal decomposition mechanism of cellulose, hemicellulose and lignin is required. Also, the effect of inorganics on reaction process of these structural carbohydrates is preferred.  There is not a complete knowledge about reaction mechanism of pure cellulose, hemicellulose and lignin especially at fast pyrolysis conditions. Furthermore, their vapour phase chemistries and interaction are even less understood. These interactions are important to study since they determine the product composition to a degree. Initial investigations about pyrolysis mechanisms of pure cellulose, hemicellulose and lignin were carried out by Patwardhan et al.[41–43] The identified species from polysaccharide pyrolysis could be broadly classified into low-molecular weight compounds, furan/pyran ring derivatives and anhydro sugars. Major compounds detected from cellulose fast pyrolysis were formic acid (~7 wt%), glycoaldehyde (~7 wt%), levoglucosan compounds (~62 wt%) and char (~5 wt%). The work revealed that product formation from primary pyrolysis reactions is competitive in nature rather than sequential. The group also studied the effect of inorganic salts on pure cellulose pyrolysis and specie formation. The study showed that inorganic salt concentrations as low as 0.005 mmoles/g of cellulose were sufficient to significantly alter pyrolysis product speciation. Inorganic salts and ash catalysed primary reactions that led to formation of lower molecular weight compounds (formic acid, acetol and glycoaldehyde in particular). As a result of competitive reactions, lower levoglucosan yields were observed. Effect of certain cations and anions on pyrolysis of pure cellulose was also studied. The work showed that careful control of mineral content could be used to alter the composition of bio-oil.

Studies on primary pyrolysis of hemicellulose show that the major products are $CO_2$, formic acid, char, DAXP2, xylose, acetol, CO, 2-furaldehyde and AXP in decreasing order of abundance. Inorganic salts were found to increase the formation of char and $CO_2$ along with 2-furaldehyde. This was accompanied by a decrease in yield of other dehydration products. Decaboxylation was observed to be one of the preliminary steps of hemicellulose

decomposition. Dehydration products : DAXP1, DAXP2, AXP and 2-furaldehyde had highest yield ~350-450 °C.[44,45]

Studies into lignin pyrolysis show that the primary reaction products are phenol, 4-vinyl phenol, 2-methoxy-4-vinyl phenol and 2,6-dimethoxy phenol. These compounds could be grouped together as monomeric phenolic compounds. Condensation of lignin pyrolytic vapours showed re-oligomerization of monomeric products during condensation which was facilitated by acetic acid. Temperature is shown to play a major role in determining the product speciation. The study shows possibility of selectively obtaining monomeric phenolic compounds from dynamic control of pyrolysis process.[46–48]

Cracking reactions generate anhydro-oligosaccharides while subsequent reactions produce levoglucosan from these anhydro-oligosaccharides. Eventually, cracking of anhydro-oligosaccharides is eclipsed by levoglucosan producing reactions. These reactions compete with other reactions that produce light oxygenates and non-condensable gases. Initial rate of cracking is much faster than levoglucosan generation from end-chain LPRs. This result should not be surprising considering the plethora of potential cracking sites in long-chain anhydro-oligosaccharides (equal to DP minus two) compared to the small number of sites for end-chain reactions (two per anhydro-oligosaccharide molecule regardless of DP). [49,50]
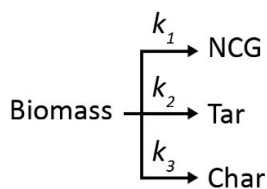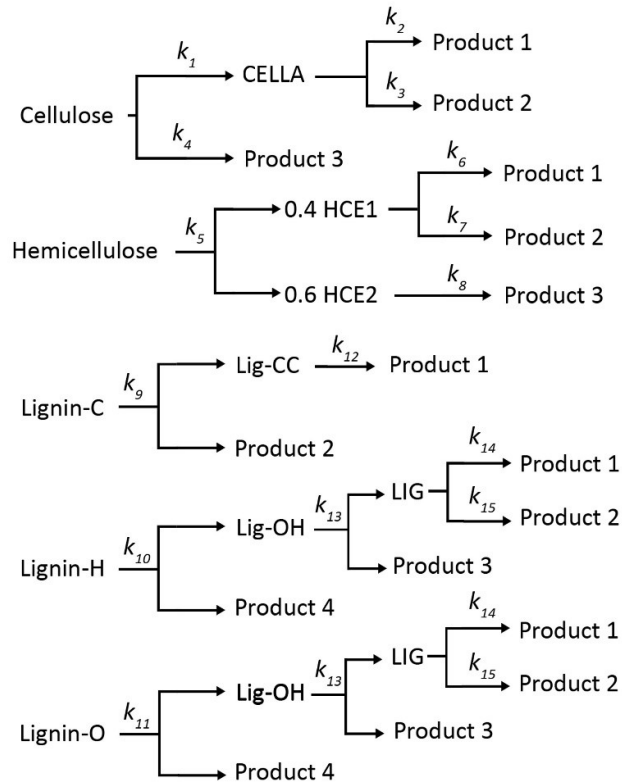


*Figure 11 Shafizadeh's scheme (1976)*

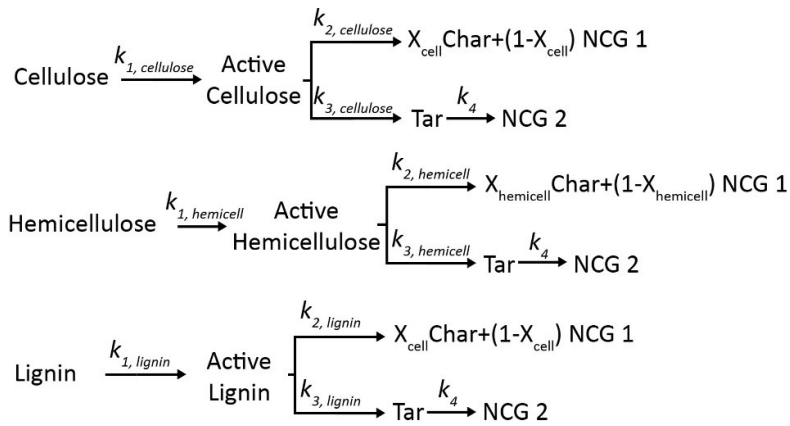*Figure 12 Ranzi's scheme (2008)*



*Figure 13 Briodo and Shafizadeh (1975) + Miller and Belan (1997)*

## 1.2.7 Techno economic aspects

Techno-economic assessment shows that fast pyrolysis fuel has the potential to compete with and eventually replace petroleum based fuels in future. However, due to various difficulties as stated earlier, only a handful of fast pyrolysis plants are able to operate commercially over sustained time-scales.[51] In terms of product fuel cost, fast pyrolysis has been reported to be competitive with biological and gasification conversion technologies.[32] As far as thermochemical conversion processes are considered, pyrolysis chemistry is observable within gasification and combustion as well. The peculiarity of pyrolysis (fast and slow) is the conversion of solid biomass into a denser crude liquid form which is better for transportation, storage and integration into consumable fuel forms. However, crude pyrolysis oil is not stable and without appropriate collection and downstream treatment, it would continue to react and change its viscosity, acidy and chemical composition. The down-streaming, upgradation and process integration aspects are touched upon briefly in this chapter, however, their detailed study lies outside the scope of this thesis work.

Some of the leading reactor technologies for pyrolysis are review by Perkins et al and presented in table below. The review covers relevant organizations and their technologies aimed at realizing fast pyrolysis for specific commercial purposes. The reactors currently in use for fast pyrolysis are fluidized bed reactor, rotating cone reactor and their modified versions. The pyrolysis oil derived from these reactors and processes is different from conventional petroleum oil and requires significant upgrading to be compatible with petroleum based combustion system. Else, the pyrolysis oil finds use in industrial combustion processes.

| Organisation | Technology supplier | Location | Reactor type | Feed rate (tpd) | Status |
|---|---|---|---|---|---|
| **RTI International** | RTI | USA | Bubbling fluidized bed | 1 | Operational |
| **Ensyn** | Ensyn | Canada | Circulating transported bed | 2 | Operational |
| **Union Fenosa** | RTI, University of Waterloo | Spain | Fluidized bed | 5 | Shutdown |
| **PyTec** | PyTec | Germany | Ablative reactor | 6 | |
| **DynaMotive** | DynaMotive | Canada | Bubbling fluidized bed | 11 | |

| | | | | | |
|---|---|---|---|---|---|
| **Karlsruhe Institute Technology** | KIT/Lurgi | Germany | Twin screw | 12 | Operational |
| **Genting** | BTG | Malaysia | Rotating cone | 48 | |
| **AbriTech** | AbriTech | Canada | Auger reactor | 50 | |
| **Pyrovac** | Pyrovac | Canada | Vacuum | 93 | Shut down |
| **Empyro** | BTG | Netherland | Rotating cone | 120 | Operational |
| **Fortum** | VTT/Valmet | Finland | Circulating fluidized bed | 274 | Operational |

*Table 1.1 Selected commercial fast pyrolysis reactor systems[51]*

There have been efforts in commercializing biomass based production systems to mitigate the dependence on petroleum based energy production systems with the view of to help reduce the cost of energy and for environmental purposes. However high operating costs labour costs and lack of government subsidies plus the small scale of biomass based power systems make it more expensive and such commercial operations have been very limited in the success that they have found. Some authors have reviewed and presented efforts and technologies dedicated to realizing this. Some of the earlier approaches or energy systems were for power (electricity) generation via gasification and pyrolysis. [52]

## 1.2.8 Life cycle analysis

The highly variable operating range of biomass pyrolysis leading to vastly different product fraction yields dependent on process conditions. The down-streaming and further applications of the obtained products are also vastly different and have differing environmental impacts. As such defining the scope of the life cycle analysis (cradle to grave or cradle to gate) is important. Recommendations for the same are discussed in some recent works. Due to a lack of uniformity in process conditions and associated energy and environmental impacts, it is reported that there is a lack of systemic standardized approach in dealing with life cycle analysis of biomass pyrolysis.[53] The application of char in carbon capture technologies plays a role in carbon negative economy as well. The potential of char for carbon sequestering has been noted as well. Such applications of char are looked upon favourably while assessing environmental impacts of the process. Wherein, pyrolysis oil is the major product, the process is comparable with coal gasification and conventional petroleum technologies, in terms of its environmental impacts. Multiple studies have found that in terms of greenhouse gas emissions (GHG impact factor), biomass pyrolysis is better than coal gasification and similar petrochemical processes. Some studies have also found that biomass pyrolysis has potential in reducing the global warming potential (GWP) amongst related

energy production systems. Although more systemic and detailed research into the same is advised. Amongst various biomass feedstocks, forest residues seem to fare better than most other options in terms of environmental impacts. Biomass co-pyrolysis with municipal solid waste or other waste streams (such as waste tyres) contribute negatively in terms of environmental impacts. Whereas co-pyrolysis and integration with processes such as anaerobic digestion improve the environmental impacts of the process.[53–57]

Overall, it could be said that biomass pyrolysis is neither inherently beneficial nor detrimental in terms of environmental impact as compared to its conjugate thermochemical energy production systems. That being said, biomass pyrolysis holds potential to meet energy demand while reducing the environmental impacts. To realise this potential, understanding the phenomena and designing reactors for optimized process control is essential. This would also facilitate a more comprehensive understanding of the environmental impacts throughout the process of biomass pyrolysis.[58,59]

# Aim and objective of current work

*The objective of the current work is to gain a deeper understanding of biomass pyrolysis with the aim of developing kinetic models suitable for fast pyrolysis reactor design and process control.*

Figure 14 gives a graphical overview of the work carried out for thesis.

| reactor | Advantages | Disadvantages | Dominant mode of heat transfer |
|---|---|---|---|
| Fluidized bed reactor | Continuous operation. Reasonable heat-transfer and mixing. Accurate temperature control. Suitable for scale-up | Blockage and accumulation issues during feeding and operation. Expensive pre-treatment process. Sophisticated equipment requiring high technical maintenance. | Convection, conduction |
| Auger reactor | Higher control over residence time. Wide feedstock handling capacity. Resistant to clogging and winding. Robust and compact structurally. Carrie gas is not essential. | Susceptible to wear and tear. Low heat transfer efficiency. Issues in scaling up. | Conduction |

| | | | |
|---|---|---|---|
| Free-fall reactor | Simple equipment. Decent scale-up range. No necessity of carrier gas. | Low heat transfer efficiency. Difficult to control residence time. | Convection, conduction |
| Ablative reactor | Can handle feedstock without extensive pre-treatment. | Low heat transfer rates. Complex reactor design and structure. | Conduction |
| Rotating cone reactor | Heat transfer driven. Carrier gas is not essential. | Expensive and complicated design. Difficulties in scale-up. | Conduction |
| Fixed bed reactor | Simlple reactor setup. Low cost and easy to operate. Can handle wide range of feedstock | Not suited for continuous operation. Insufficient heat transfer rates. Severe scale-up limitation. Low liquid yield. | Conduction |
| | | | |

*Table1-2Advantages and disadvantages of commonly used reactors for fast pyrolysis[17]*

| Order-based $f(\alpha) = (1-\alpha)^n$ | First-order $(Or1)n = 1$ | $1 - \alpha$ | $-ln(1-\alpha)$ |
|---|---|---|---|
| | First-order $(Or2)n = 2$ | $(1-\alpha)^2$ | $(1-\alpha)^{-1} - 1$ |
| | First-order $(Or3)n = 3$ | $(1-\alpha)^3$ | $[(1-\alpha)^{-2} - 1]/2$ |
| Diffusional | 1-D diffusion (D1) | $1/2\alpha$ | $\alpha^2$ |
| | 2-D diffusion (D2) | $[-ln(1-\alpha)]^{-1}$ | $\alpha + (1-\alpha)ln(1-\alpha)$ |
| | 3-D diffusion-Jander (D3) | $[(3/2)(1-\alpha)^{2/3}]$ $/[1 - (1-\alpha)^{1/3}]$ | $[1 - (1-\alpha)^{1/3}]^2$ |
| | Ginstling-Brounshtein (D4) | $[(3/2)(1-\alpha)^{1/3}]$ $/[1 - (1-\alpha)^{1/3}]$ | $(1 - 2\alpha/3) - (1-\alpha)^{2/3}$ |
| Nucleation | Avrami-Erofeev (A2) | $2(1-\alpha)[-ln(1-\alpha)]^{1/2}$ | $[-ln(1-\alpha)]^{1/2}$ |
| | Avrami-Erofeev (A3) | $3(1-\alpha)[-ln(1-\alpha)]^{1/3}$ | $[-ln(1-\alpha)]^{1/3}$ |
| | Avrami-Erofeev (A15) | $1.5(1-\alpha)[-ln(1-\alpha)]^{1/3}$ | $[-ln(1-\alpha)]^{2/3}$ |
| | Avrami-Erofeev (A4) | $4(1-\alpha)[-ln(1-\alpha)]^{3/4}$ | $[-ln(1-\alpha)]^{1/4}$ |
| Geometrical contraction | Contracting area (G2) | $2(1-\alpha)^{1/2}$ | $1 - (1-\alpha)^{1/2}$ |
| | Contracting volume (G3) | $3(1-\alpha)^{1/3}$ | $1 - (1-\alpha)^{1/3}$ |
| Power law | 2/3-Power law (P23) | $(2/3)\alpha^{-1/2}$ | $\alpha^{3/2}$ |
| | 2-Power law (P2) | $2\alpha^{1/2}$ | $\alpha^{1/2}$ |
| | 3-Power law (P3) | $3\alpha^{1/3}$ | $\alpha^{1/3}$ |
| | 4-Power law (P4) | $4\alpha^{1/4}$ | $\alpha^{1/4}$ |
| Random scission model | L=2 | $f(\alpha) = 2(\alpha^{1/2} - \alpha)$ | l |

*Table 1-3 Various models for model fitting approach [60]*
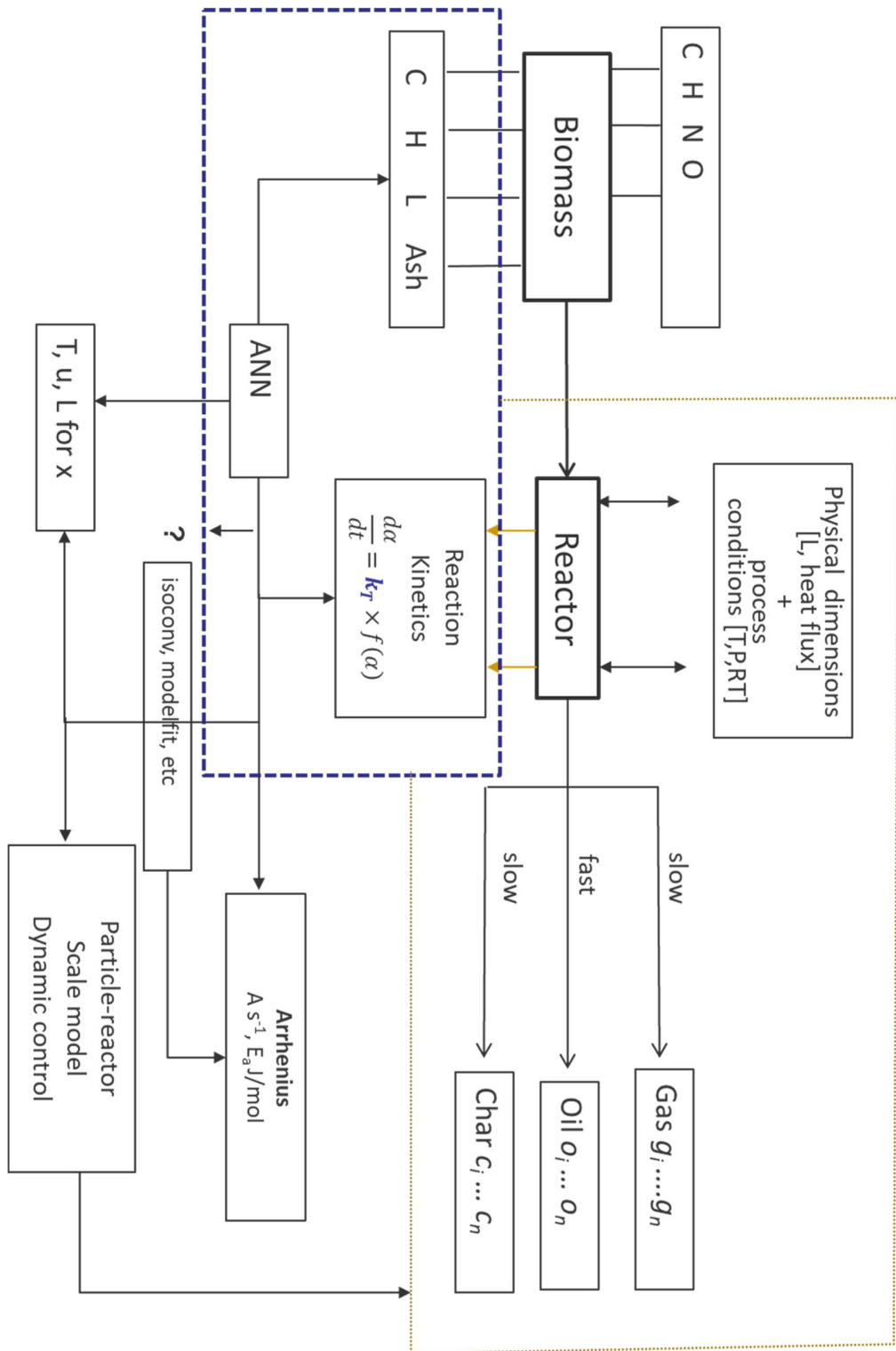
*Figure 14 Graphical overview of thesis work*

| No. | Method | Expression |
|-----|--------|-----------|
| 1 | Friedman method | $ln\left(\beta\dfrac{d\alpha}{dT}\right) = \ln(k_o f(\alpha)) - \dfrac{E_o}{RT}$ |
| 2 | FWO method | $ln(\beta) = \ln\left(\dfrac{k_o E}{Rg(\alpha)}\right) - 5.331 - 1.052\dfrac{E}{RT}$ |
| 3 | KAS method | $ln\left(\dfrac{\beta}{T^2}\right) = \ln\left(\dfrac{k_o R}{Eg(\alpha)}\right) - \dfrac{E}{RT}$ |
| 4 | Kissinger method | $ln\left(\dfrac{\beta}{T^2{}_{max}}\right) = \ln\left(\dfrac{k_o R}{E}\right) - \dfrac{E}{RT_{max}}$ |
| 5 | Miura Maki method | $ln\left(\dfrac{\beta}{T^2}\right) = \ln\left(\dfrac{k_o R}{E)}\right) + 0.6045 - \dfrac{E_o}{RT}$ |

*Table 1-4 Model free or isoconversional approach*

# References

(1) Kostetskyy, P.; Broadbelt, L. J. Progress in Modeling of Biomass Fast Pyrolysis: A Review. *Energy Fuels* **2020**, *34* (12), 15195–15216. https://doi.org/10.1021/acs.energyfuels.0c02295.

(2) Sharma, A.; Pareek, V.; Zhang, D. Biomass Pyrolysis—A Review of Modelling, Process Parameters and Catalytic Studies. *Renew. Sustain. Energy Rev.* **2015**, *50*, 1081–1096. https://doi.org/10.1016/j.rser.2015.04.193.

(3) Wang, S.; Dai, G.; Yang, H.; Luo, Z. Lignocellulosic Biomass Pyrolysis Mechanism: A State-of-the-Art Review. *Prog. Energy Combust. Sci.* **2017**, *62*, 33–86. https://doi.org/10.1016/j.pecs.2017.05.004.

(4) Anca-Couce, A. Reaction Mechanisms and Multi-Scale Modelling of Lignocellulosic Biomass Pyrolysis. *Prog. Energy Combust. Sci.* **2016**, *53*, 41–79. https://doi.org/10.1016/j.pecs.2015.10.002.

(5) Debiagi, P. E. A.; Gentile, G.; Pelucchi, M.; Frassoldati, A.; Cuoci, A.; Faravelli, T.; Ranzi, E. Detailed Kinetic Mechanism of Gas-Phase Reactions of Volatiles Released from Biomass Pyrolysis. *Biomass Bioenergy* **2016**, *93*, 60–71. https://doi.org/10.1016/j.biombioe.2016.06.015.

(6) Pagano, M.; Hernando, H.; Cueto, J.; Moreno, I.; Serrano, D. P. Autocatalytic Properties of Biochar during Lignocellulose Pyrolysis Probed Using a Continuous Reaction System. *Catal. Today* **2023**, *418*, 114065. https://doi.org/10.1016/j.cattod.2023.114065.

(7) Zaror, C. A.; Pyle, D. L. Competitive Reactions Model for the Pyrolysis of Lignocellulose: A Critical Study. *J. Anal. Appl. Pyrolysis* **1986**, *10* (1), 1–12. https://doi.org/10.1016/0165-2370(86)85015-X.

(8) Shen, D.; Jin, W.; Hu, J.; Xiao, R.; Luo, K. An Overview on Fast Pyrolysis of the Main Constituents in Lignocellulosic Biomass to Valued-Added Chemicals: Structures, Pathways and Interactions. *Renew. Sustain. Energy Rev.* **2015**, *51*, 761–774. https://doi.org/10.1016/j.rser.2015.06.054.

(9) *World Energy Statistics | Enerdata*. https://yearbook.enerdata.net/ (accessed 2023-11-26).

(10) Pecha, M. B.; Terrell, E.; Montoya, J. I.; Stankovikj, F.; Broadbelt, L. J.; Chejne, F.; Garcia-Perez, M. Effect of Pressure on Pyrolysis of Milled Wood Lignin and Acid-Washed Hybrid Poplar Wood. *Ind. Eng. Chem. Res.* **2017**, *56* (32), 9079–9089. https://doi.org/10.1021/acs.iecr.7b02085.

(11) Pecha, M. B.; Montoya, J. I.; Ivory, C.; Chejne, F.; Garcia-Perez, M. Modified Pyroprobe Captive Sample Reactor: Characterization of Reactor and Cellulose Pyrolysis at Vacuum and Atmospheric Pressures. *Ind. Eng. Chem. Res.* **2017**, *56* (18), 5185–5200. https://doi.org/10.1021/acs.iecr.7b00463.

(12) Pecha, M. B.; Montoya, J. I.; Chejne, F.; Garcia-Perez, M. Effect of a Vacuum on the Fast Pyrolysis of Cellulose: Nature of Secondary Reactions in a Liquid Intermediate. *Ind. Eng. Chem. Res.* **2017**, *56* (15), 4288–4301. https://doi.org/10.1021/acs.iecr.7b00476.

(13) Lede, J.; Diebold, J. P.; Peacocke, G. V. C.; Piskorz, J. The Nature and Properties of Intermediate and Unvaporized Biomass Pyrolysis Materials. In *Developments in Thermochemical Biomass Conversion: Volume 1 / Volume 2*; Bridgwater, A. V., Boocock, D. G. B., Eds.; Springer Netherlands: Dordrecht, 1997; pp 27–42. https://doi.org/10.1007/978-94-009-1559-6_2.

(14) Jerzak, W.; Reinmöller, M.; Magdziarz, A. Estimation of the Heat Required for Intermediate Pyrolysis of Biomass. *Clean Technol. Environ. Policy* **2022**, *24* (10), 3061–3075. https://doi.org/10.1007/s10098-022-02391-1.

(15) Wang, S.; Dai, G.; Yang, H.; Luo, Z. Lignocellulosic Biomass Pyrolysis Mechanism: A State-of-the-Art Review. *Prog. Energy Combust. Sci.* **2017**, *62*, 33–86. https://doi.org/10.1016/j.pecs.2017.05.004.

(16) Gea, S.; Hutapea, Y. A.; Piliang, A. F. R.; Pulungan, A. N.; Rahayu, R.; Layla, J.; Tikoalu, A. D.; Wijaya, K.; Saputri, W. D. A Comprehensive Review of Experimental Parameters in Bio-Oil Upgrading from Pyrolysis of Biomass to Biofuel Through Catalytic Hydrodeoxygenation. *BioEnergy Res.* **2023**, *16* (1), 325–347. https://doi.org/10.1007/s12155-022-10438-w.

(17) Cai, W.; Luo, Z.; Zhou, J.; Wang, Q. A Review on the Selection of Raw Materials and Reactors for Biomass Fast Pyrolysis in China. *Fuel Process. Technol.* **2021**, *221*, 106919. https://doi.org/10.1016/j.fuproc.2021.106919.

(18) Mohan, D.; Pittman, C. U. Jr.; Steele, P. H. Pyrolysis of Wood/Biomass for Bio-Oil: A Critical Review. *Energy Fuels* **2006**, *20* (3), 848–889. https://doi.org/10.1021/ef0502397.

(19) Solantausta', Y.; BRIDGWATERb, A. T.; Beckman, D. FEASIBILITY OF POWER PRODUCTION WITH PYROLYSIS AND GASIFICATION SYSTEMS.

(20) Chiaramonti, D.; Oasmaa, A.; Solantausta, Y. Power Generation Using Fast Pyrolysis Liquids from Biomass. *Renew. Sustain. Energy Rev.* **2007**, *11* (6), 1056–1086. https://doi.org/10.1016/j.rser.2005.07.008.

(21) Chiaramonti, D.; Oasmaa, A.; Solantausta, Y. Fast Pyrolysis Oil for Power Generation. In *GT2006*; Volume 2: Aircraft Engine; Ceramics; Coal, Biomass and Alternative Fuels; Controls, Diagnostics and Instrumentation; Environmental and Regulatory Affairs, 2006; pp 325–332. https://doi.org/10.1115/GT2006-90245.

(22) Gomez, C.; Velo, E.; Barontini, F.; Cozzani, V. Influence of Secondary Reactions on the Heat of Pyrolysis of Biomass. *Ind. Eng. Chem. Res.* **2009**, *48* (23), 10222–10233. https://doi.org/10.1021/ie9007985.

(23) Reyes, L.; Abdelouahed, L.; Mohabeer, C.; Buvat, J.-C.; Taouk, B. Energetic and Exergetic Study of the Pyrolysis of Lignocellulosic Biomasses, Cellulose, Hemicellulose and Lignin. *Energy Convers. Manag.* **2021**, *244*, 114459. https://doi.org/10.1016/j.enconman.2021.114459.

(24) Anca-Couce, A.; Scharler, R. Modelling Heat of Reaction in Biomass Pyrolysis with Detailed Reaction Schemes. *Fuel* **2017**, *206*, 572–579. https://doi.org/10.1016/j.fuel.2017.06.011.

(25) Di Blasi, C. Kinetic and Heat Transfer Control in the Slow and Flash Pyrolysis of Solids. *Ind. Eng. Chem. Res.* **1996**, *35* (1), 37–46. https://doi.org/10.1021/ie950243d.

(26) Marathe, P. S.; Westerhof, R. J. M.; Kersten, S. R. A. Effect of Pressure and Hot Vapor Residence Time on the Fast Pyrolysis of Biomass: Experiments and Modeling. *Energy Fuels* **2020**, *34* (2), 1773–1780. https://doi.org/10.1021/acs.energyfuels.9b03193.

(27) Shen, Q.; Wu, H. Rapid Pyrolysis of Biochar Prepared from Slow and Fast Pyrolysis: The Effects of Particle Residence Time on Char Properties. *Proc. Combust. Inst.* **2023**, *39* (3), 3371–3378. https://doi.org/10.1016/j.proci.2022.07.119.

(28) Mayor, J. R.; Williams, A. Residence Time Influence on the Fast Pyrolysis of Loblolly Pine Biomass. *J. Energy Resour. Technol.* **2011**, *132* (041801). https://doi.org/10.1115/1.4003004.

(29) Pecha, M. B.; Arbelaez, J. I. M.; Garcia-Perez, M.; Chejne, F.; Ciesielski, P. N. Progress in Understanding the Four Dominant Intra-Particle Phenomena of Lignocellulose Pyrolysis: Chemical Reactions, Heat Transfer, Mass Transfer, and Phase Change. *Green Chem.* **2019**, *21* (11), 2868–2898. https://doi.org/10.1039/C9GC00585D.

(30) Bu, Q.; Lei, H.; Zacher, A. H.; Wang, L.; Ren, S.; Liang, J.; Wei, Y.; Liu, Y.; Tang, J.; Zhang, Q.; Ruan, R. A Review of Catalytic Hydrodeoxygenation of Lignin-Derived Phenols from Biomass Pyrolysis. *Bioresour. Technol.* **2012**, *124*, 470–477. https://doi.org/10.1016/j.biortech.2012.08.089.

(31) De, S.; Saha, B.; Luque, R. Hydrodeoxygenation Processes: Advances on Catalytic Transformations of Biomass-Derived Platform Chemicals into Hydrocarbon Fuels. *Bioresour. Technol.* **2015**, *178*, 108–118. https://doi.org/10.1016/j.biortech.2014.09.065.

(32) Mettler, M. S.; Vlachos, D. G.; Dauenhauer, P. J. Top Ten Fundamental Challenges of Biomass Pyrolysis for Biofuels. *Energy Environ. Sci.* **2012**, *5* (7), 7797. https://doi.org/10.1039/c2ee21679e.

(33) Ritchie, H.; Rosado, P.; Roser, M. Energy Production and Consumption. *Our World Data* **2023**.

(34) Oyebanji, J. A.; Okekunle, P. O.; Lasode, O. A.; Oyedepo, S. O. Chemical Composition of Bio-Oils Produced by Fast Pyrolysis of Two Energy Biomass. *Biofuels* **2018**, *9* (4), 479–487. https://doi.org/10.1080/17597269.2017.1284473.

(35) Li, P.; Shi, X.; Wang, X.; Song, J.; Fang, S.; Bai, J.; Zhang, G.; Chang, C.; Pang, S. Bio-Oil from Biomass Fast Pyrolysis: Yields, Related Properties and Energy Consumption Analysis of the Pyrolysis System. *J. Clean. Prod.* **2021**, *328*, 129613. https://doi.org/10.1016/j.jclepro.2021.129613.

(36) Uzoejinwa, B. B.; He, X.; Wang, S.; El-Fatah Abomohra, A.; Hu, Y.; Wang, Q. Co-Pyrolysis of Biomass and Waste Plastics as a Thermochemical Conversion Technology for High-Grade Biofuel Production: Recent Progress and Future Directions Elsewhere Worldwide. *Energy Convers. Manag.* **2018**, *163*, 468–492. https://doi.org/10.1016/j.enconman.2018.02.004.

(37) Wang, Z.; Burra, K. G.; Lei, T.; Gupta, A. K. Co-Pyrolysis of Waste Plastic and Solid Biomass for Synergistic Production of Biofuels and Chemicals-A Review. *Prog. Energy Combust. Sci.* **2021**, *84*, 100899. https://doi.org/10.1016/j.pecs.2020.100899.

(38) Czernik, S.; Evans, R.; French, R. Hydrogen from Biomass-Production by Steam Reforming of Biomass Pyrolysis Oil☆. *Catal. Today* **2007**, *129* (3–4), 265–268. https://doi.org/10.1016/j.cattod.2006.08.071.

(39) Lopez, G.; Santamaria, L.; Lemonidou, A.; Zhang, S.; Wu, C.; Sipra, A. T.; Gao, N. Hydrogen Generation from Biomass by Pyrolysis. *Nat. Rev. Methods Primer* **2022**, *2* (1), 20. https://doi.org/10.1038/s43586-022-00097-8.

(40) Lu, H.; Ip, E.; Scott, J.; Foster, P.; Vickers, M.; Baxter, L. L. Effects of Particle Shape and Size on Devolatilization of Biomass Particle. *Fuel* **2010**, *89* (5), 1156–1168. https://doi.org/10.1016/j.fuel.2008.10.023.

(41) Patwardhan, P. R.; Satrio, J. A.; Brown, R. C.; Shanks, B. H. Influence of Inorganic Salts on the Primary Pyrolysis Products of Cellulose. *Bioresour. Technol.* **2010**, *101* (12), 4646–4655. https://doi.org/10.1016/j.biortech.2010.01.112.

(42) Patwardhan, P. R.; Dalluge, D. L.; Shanks, B. H.; Brown, R. C. Distinguishing Primary and Secondary Reactions of Cellulose Pyrolysis. *Bioresour. Technol.* **2011**, *102* (8), 5265–5269. https://doi.org/10.1016/j.biortech.2011.02.018.

(43) Patwardhan, P. R.; Satrio, J. A.; Brown, R. C.; Shanks, B. H. Product Distribution from Fast Pyrolysis of Glucose-Based Carbohydrates. *J. Anal. Appl. Pyrolysis* **2009**, *86* (2), 323–330. https://doi.org/10.1016/j.jaap.2009.08.007.

(44) Patwardhan, P. R.; Brown, R. C.; Shanks, B. H. Product Distribution from the Fast Pyrolysis of Hemicellulose. *ChemSusChem* **2011**, *4* (5), 636–643. https://doi.org/10.1002/cssc.201000425.

(45) Hu, B.; Zhang, W.-M.; Guo, X.-W.; Liu, J.; Yang, X.; Lu, Q. Experimental and Computational Study on Xylan Pyrolysis: The Pyrolysis Mechanism of Main Branched Monosaccharides. *Fuel Process. Technol.* **2024**, *253*, 107989. https://doi.org/10.1016/j.fuproc.2023.107989.

(46) Patwardhan, P. R.; Brown, R. C.; Shanks, B. H. Understanding the Fast Pyrolysis of Lignin. *ChemSusChem* **2011**, *4* (11), 1629–1636. https://doi.org/10.1002/cssc.201100133.

(47) Ojha, D. K.; Viju, D.; Vinu, R. Fast Pyrolysis Kinetics of Alkali Lignin: Evaluation of Apparent Rate Parameters and Product Time Evolution. *Bioresour. Technol.* **2017**, *241*, 142–151. https://doi.org/10.1016/j.biortech.2017.05.084.

(48) Zhou, S.; Pecha, B.; van Kuppevelt, M.; McDonald, A. G.; Garcia-Perez, M. Slow and Fast Pyrolysis of Douglas-Fir Lignin: Importance of Liquid-Intermediate Formation on the Distribution of Products. *Biomass Bioenergy* **2014**, *66*, 398–409. https://doi.org/10.1016/j.biombioe.2014.03.064.

(49) Mettler, M. S.; Paulsen, A. D.; Vlachos, D. G.; Dauenhauer, P. J. The Chain Length Effect in Pyrolysis: Bridging the Gap between Glucose and Cellulose. *Green Chem.* **2012**, *14* (5), 1284. https://doi.org/10.1039/c2gc35184f.

(50) Lu, Q.; Hu, B.; Zhang, Z.; Wu, Y.; Cui, M.; Liu, D.; Dong, C.; Yang, Y. Mechanism of Cellulose Fast Pyrolysis: The Role of Characteristic Chain Ends and Dehydrated Units. *Combust. Flame* **2018**, *198*, 267–277. https://doi.org/10.1016/j.combustflame.2018.09.025.

(51) Perkins, G.; Bhaskar, T.; Konarova, M. Process Development Status of Fast Pyrolysis Technologies for the Manufacture of Renewable Transport Fuels from Biomass. *Renew. Sustain. Energy Rev.* **2018**, *90*, 292–315. https://doi.org/10.1016/j.rser.2018.03.048.

(52) Wang, T.; Huang, H.; Yu, C.; Fang, K.; Zheng, M.; Luo, Z. Understanding Cost Reduction of China's Biomass Direct Combustion Power Generation—A Study Based on Learning Curve Model. *J. Clean. Prod.* **2018**, *188*, 546–555. https://doi.org/10.1016/j.jclepro.2018.03.258.

(53) Ou, L.; Cai, H. Dynamic Life-Cycle Analysis of Fast Pyrolysis Biorefineries: Impacts of Feedstock Moisture Content and Particle Size. *ACS Sustain. Chem. Eng.* **2020**, *8* (16), 6211–6221. https://doi.org/10.1021/acssuschemeng.9b06836.

(54) Fan, J.; Kalnes, T. N.; Alward, M.; Klinger, J.; Sadehvandi, A.; Shonnard, D. R. Life Cycle Assessment of Electricity Generation Using Fast Pyrolysis Bio-Oil. *Renew. Energy* **2011**, *36* (2), 632–641. https://doi.org/10.1016/j.renene.2010.06.045.

(55) Han, J.; Elgowainy, A.; Dunn, J. B.; Wang, M. Q. Life Cycle Analysis of Fuel Production from Fast Pyrolysis of Biomass. *Bioresour. Technol.* **2013**, *133*, 421–428. https://doi.org/10.1016/j.biortech.2013.01.141.

(56) Iribarren, D.; Peters, J. F.; Dufour, J. Life Cycle Assessment of Transportation Fuels from Biomass Pyrolysis. *Fuel* **2012**, *97*, 812–821. https://doi.org/10.1016/j.fuel.2012.02.053.

(57) Peters, J. F.; Iribarren, D.; Dufour, J. Life Cycle Assessment of Pyrolysis Oil Applications. *Biomass Convers. Biorefinery* **2015**, *5* (1), 1–19. https://doi.org/10.1007/s13399-014-0120-z.

(58) Xu, C.; Hong, J.; Chen, J.; Han, X.; Lin, C.; Li, X. Is Biomass Energy Really Clean? An Environmental Life-Cycle Perspective on Biomass-Based Electricity Generation in China. *J. Clean. Prod.* **2016**, *133*, 767–776. https://doi.org/10.1016/j.jclepro.2016.05.181.

(59) Yang, Q.; Zhou, H.; Bartocci, P.; Fantozzi, F.; Mašek, O.; Agblevor, F. A.; Wei, Z.; Yang, H.; Chen, H.; Lu, X.; Chen, G.; Zheng, C.; Nielsen, C. P.; McElroy, M. B. Prospective Contributions of Biomass Pyrolysis to China's 2050 Carbon Reduction and Renewable Energy Goals. *Nat. Commun.* **2021**, *12* (1), 1698. https://doi.org/10.1038/s41467-021-21868-z.

(60) Dhyani, V.; Bhaskar, T. Kinetic Analysis of Biomass Pyrolysis. In *Waste Biorefinery*; Elsevier, 2018; pp 39–83. https://doi.org/10.1016/B978-0-444-63992-9.00002-1.

# Chapter 2 Experimental work and preliminary investigations

*In this chapter, sample collection and pre-treatment are discussed followed by description of experimental methods and results. This later serves as basis for kinetic calculations and predictive model training. The influence of various parameters such as particle-size, temperature, heating rate, residence time, composition and reaction time-scale on weight loss kinetics and nature of process have also been investigated for collected biomass samples. TGA and DTG modelling results based on experiments performed are also presented along with its theoretical and mathematical basis.*

## 2.1 Sample collection and pre-treatment

All the samples were collected from Perth, Western Australia. Malleewood samples were predominantly tree barks. The wood samples were obtained as pieces of blocks.  Pinecone and pine-needles were from Curtin university campus. Lupin shells were given by GRDC Curtin university. The sample size reduction was performed using rotating knife mill. The milled samples were kept in an oven at 110 °C for 24 hours. The samples were then passed through a vibrating sieve machine. Particle size within the ranges of 250 μm – 300 μm; 106 μm – 150 μm; <45 μm were chosen for TGA runs. Particle size of < 60 μm was chosen for analytical experiments. The samples were chosen based on global and regional availability of woody biomass and other samples were chosen to add variability to aid with predictive model training. Such a sample selection ensures a closer fidelity to real case scenarios in predictive models as opposed to predictive models trained on simulated data. Particle size and sample size were chosen in order to limit mass transfer and heat transfer limitations and ensure that the process occurs under kinetic (reaction) control regime.  The physical pre-treatment was done to ensure moisture free basis and kinetic control within TGA mass loss reactions. Pure cellulose was purchased from Sigma Aldrich (<85 μm particle size). Hemicellulose was xylan separated from cotton (particle size <65 um). Lignin (alkali) was purchased from Sigma Aldrich.

## 2.2 Feedstock characterization

The inherent heterogeneity of biomass and its implications in reaction modelling and process design have been reviewed in chapter 1. As such it is crucial to develop models which would account for this inherent heterogeneity. For developing such models, we need reliable feedstock characterization. In the current work, 10 locally sourced naturally occurring biomass samples have been characterized. The elemental composition and structural carbohydrate composition of these biomass samples has been determined experimentally (Table 2.1 and Table 2.2). A comprehensive analysis of feedstock composition would facilitate the integration

of biomass heterogeneity into newer pyrolysis models, which has been one of the shortcomings of existing kinetic models describing biomass fast pyrolysis. Figure 2.2, presented later, shows the biochemical compositional cluster of selected biomass samples.

There are some works dedicated specifically for analysing and determining the composition of lignocellulosic biomass samples.[1–4]

In our work we determine the composition of structural carbohydrates and lignin of the 10 biomass samples. The laboratory analytical procedure prescribed by NREL is followed determining the composition.[5,6] This procedure uses two-step acid hydrolyses to break the carbohydrates into their sugars which are then quantified using HPLC. Cellulose is calculated from the amount of glucose in the hydrolysate, whereas xylose and arabinose quantities are indicative of hemicellulose.[6] The hydrolysate stream also contains acid soluble lignin, thus measuring its UV absorbance at a wavelength specified by NREL (in this case 240nm) helps in determining the acid soluble lignin part. Insoluble fraction of biomass after two stage acid hydrolysis majorly is the acid insoluble lignin. Acid insoluble fraction of lignin also contains ash and protein which too were determined using an NREL specified method. The ash content of biomass samples was also determined using the NREL prescribed laboratory analytical procedures. [6–9,9,10]


## 2.3 TGA runs

Biomass pyrolysis is essentially the conversion of solid feedstock into condensable, non-condensable and solid products. The study of the rate of this conversion gives us insights into the kinetics of the said reaction. Thermogravimetric analyser is an analytical instrument which is capable of minutely tracking the mass loss of a sample over variable time-scales and temperature scales. TGA is commonly used to study the mass loss behaviour of biomass and other solid state fuel precursors since it generates mass loss curves in relatively short time (depending upon the heating program) and can reproduce the phenomena of pyrolysis with reasonable fidelity given proper sample preparation and TGA reaction conditions.[11–15] For the current work Perkin Elmer TGA 8000 was used for performing all mass loss experiments. Argon was used as the inert sweeping gas at 20 ml/min flowrate. Alumina ceramic pan with size ~100 µL or ф7.2×8.6mm dimensions are used for the TGA runs. TGA runs of well measured and well prepared samples produces good quality mass loss data with respect to time and temperature.[16–19]

The specific benefit of using TGA is the ability to subject the sample to a series of isothermal and non-isothermal regimes and study the effect of those on mass loss properties. General overview of heating programs used for the current work is given below.

The TGA was programmed to run with following steps with the intention of achieving steady state in separate temperature regimes during heat ramp up and to ensure pyrolysis process is initiated on moisture free basis:

1. Hold for 2 min at 35°C
2. Heat from 20°C to 100°C at 25°C/min
3. Hold for 10 min at 100°C
4. Heat from 100°C to 850°C at the decided heating rate ( 5°C/min - 250°C/min)
5. Hold for 20 min at 850°C
6. Cool from 850°C to 50°C at 200°C/min
7. Hold for 10 min at 50°C

Multiple heating rates of 5°C/min, 20°C/min, 50°C/min, 100°C/min and 250°C/min within temperature range 100°C -  850°C are used for this work. This provides mass loss data for a wide range of heating rates. Multiple heating rates also aid in improving the consistency of kinetic calculations.


## 2.4 Kinetic theory

Arrhenius equation is an empirical correlation that relates the reaction co-efficient (or constant in cases) with the activation energy and frequency factor. This co-relation is based on the Transition state theory, which in turn is an advancement of the collision theory.[20]

For a thermally stipulated solid state reaction, according to collision theory, as the temperature is increased, the amount of energy being provided to (and such being absorbed by) the solid reactant increases. As the energy absorbed increases, so does the energy of atoms constituting the material. This increases the frequency of collision between constituting atoms. This continues until the frequency of collisions of constituent and the energy contained in them is so large that a phase change and/or a chemical reaction occurs. The point at which this conversion is about to occur is called as the transition state point. The energy barrier between reactant state and transition state is considered as the activation energy for that reaction.[21] There is no direct method to calculate the frequency or pre-exponential factor. It is largely a theoretical concept with valid physical justification. It is usually resolved to obtain sensible activation energy and reaction coefficient values.[22]

For homogenous feedstock having simple reaction mechanism, resolving kinetic parameters and obtaining sensible kinetic data is well established.[23] In case of heterogenous cross-linked complex feedstock with multiple parallel, simultaneously competing inter-reactive  reaction systems the validity of Arrhenius kinetic parameters justified via collision and transition state theory has been questioned but not disproved.[21,24,25]

In our work, to study the reaction kinetics of biomass pyrolysis we use a hybrid approach in which both model-free /isoconversional approach and model fitting approach are used to gain insights into reaction kinetics and mechanism. Methods using model-fitting approach [26–28], model-free approach[29–33] or a combination of the two methods[34–37] can be found in literature.[27,38] We present the understanding, use and limitations of these methods (current chapter) and propose a novel approach with predictive capabilities suited for reactor design and process control (chapter 4).

$$\frac{d\alpha}{dt} = k_T \times f(\alpha)$$

2.1

$$k_T = A \times exp^{\left[\frac{-E_a}{RT}\right]}$$

2.2

Where $\{A \rightarrow frequency\ factor\left(\frac{1}{s}\right);\ E_a \rightarrow Activation\ energy\left(\frac{kJ}{mol}\right);$

$R \rightarrow gas\ constant(\frac{J}{K.mol}); T \rightarrow Temperature\ (K)\}$

Equation 2.1 shows the basic form of reaction order based relationship,:

$$\frac{-dC}{dt} = k_T \times C^n$$

2.3

Where $C \rightarrow concentration\ (\frac{mol}{dm^3});\ n \rightarrow order\ of\ reaction$

Whereas,

$$\alpha = \frac{m_0 - m_i}{m_0 - m_f}$$

2.4

Where $m_0 \rightarrow initial\ mass\ ;\ m_f \rightarrow final\ mass$

Similarly, for concentration[3]

---

[3] 1. A*ssuming reaction model to be a function of conversion implies that at different conversions there will be different activation energies. 2: TGA gives mass loss data which needs to be converted to degree of conversion, ref fig 2.14*

$$\alpha = \frac{C_0 - C}{C_0}$$

2.5

Isolating C from equation 2.5 and substituting in equation 2.3,

$$\frac{d\alpha}{dt} = k'_T(1 - \alpha)^n$$

2.6

Where $\ k'_T = \ C_0^{n-1} k_T$

Equation 2.6 is the basic equation of homogenous kinetics. Comparing it against equation 2.1 suggests that homogenous kinetics can be described by simple reaction model,

$$f(\alpha) = (1 - \alpha)^n$$

2.7

This is the reaction order model approach. Table 1.3 shows a variety of commonly used reaction order model forms.

Under isothermal conditions, Temperature T is a constant.

As such, in equation 2.1, the rate of reaction is directly proportional to $f(\alpha)$:

$$\frac{d\alpha}{dt} = constant \times f(\alpha)$$

2.8

 It may be assumed that $k_T \ \rightarrow constant$ for homogenous feedstock and isothermal temperature condition.However,

Under non-isothermal conditions, when temperature changes linearly with time,

$$\beta = \frac{dT}{dt} = \frac{\Delta T}{\Delta t}$$

2.9

For model-fitting approach, it is found that experimental data does not always follow a pre-defined model and efforts spent in fitting a given data to a model does not yield meaningful results nor does it help in identifying the reaction model.[27,39,40] Identification of reaction model becomes almost impossible when model fitting approach is used on data obtained under non-isothermal conditions with a single heating rate. [12,41–43]

As both α and $T$ vary simultaneously, a clean separation of $f(\alpha)$ and $k_T$ is not possible in equation 2.1. As such, whenever equation 2.1 is fitted to non-isothermal data, it is assumed that any inaccuracy in selecting the reaction model is compensated by the resulting inaccuracy in the rate constant.[31] As such, for a given experimental data, more than one set of $f(\alpha)$ and $k_T$ can fit the data, statistically speaking. The resulting rate constants give widely different pairs of Arrhenius parameters, E and A. They are considered to be linked via the so-called compensation effect,

$$\ln A_j = aE_j + b$$

2.10

Where 'j' denotes a particular reaction model $f_j(\alpha)$ that is used in model fitting method. A set of $\{f_j(\alpha), E_j, A_j\}$ is obtained as the kinetic triplet.

It has been recommended that single heating rates should be avoided for kinetic analysis of thermal processes while using model fitting as well as Isoconversional methods.[42,43]

Iso-conversional methods are called model-free approaches as Isoconversional kinetics takes its origin in the Isoconversional principle that allows one to eliminate the reaction model from kinetic computations.[31]

The principle states that the process rate at constant extent of conversion is only a function of temperature.

Taking logarithmic derivative of rate term in equation 2.1 at a specific(α,t)points gives,

$$\left\{\frac{\partial\left[\ln\frac{d\alpha}{dt}\right]}{\partial T^{-1}}\right\}_\alpha = \left\{\frac{\partial[\ln k_T]}{\partial T^{-1}}\right\}_\alpha + \left\{\frac{\partial[\ln f(\alpha)]}{\partial T^{-1}}\right\}_\alpha$$

2.11

Since, the value of α is constant, the right most term equals zero in equation 2.11

Therefore, from equation 2.2

$$\left\{\frac{\partial\left[\ln\frac{d\alpha}{dt}\right]}{\partial T^{-1}}\right\}_\alpha = \frac{-E_a}{R}$$

2.12

Thus, from equation 2.12 it is clear that activation energy can be determined without the need for assumption of reaction model.

Slope of $\alpha\ vs\ T\ curve\ at\ T_\alpha$ will give values of $\left(\frac{d\alpha}{dT}\right)_\alpha$ that can be converted into iso-conversional rate,

$$\left(\frac{d\alpha}{dt}\right)_\alpha = \left(\frac{d\alpha}{dT}\right)_\alpha \times \beta$$

2.13

The conversion (α) range recommended for kinetic studies from TGA based data is α = 0.05 to α = 0.95 with a step size of 0.05.[27]

In our work we have used Isoconversional methods to gain insights into the reaction mechanism and nature of biomass pyrolysis phenomena. We have also used a modified model-fitting approach. The details of iso-conversional methods and modified model fitting approach are discussed in chapter 3 and chapter 4 respectively.

All the TGA data for this work has been acquired over a time step of 0.125 seconds per mass data point. TGA 8000 by Perkin Elmer operated according to the program mentioned earlier generatedwith a small time step produces fine mas loss data curvesfor further mathematical modelling work. Figure 2.1 gives a graphical overview of pretreatment and other analytical experiments performed for biomass samples.
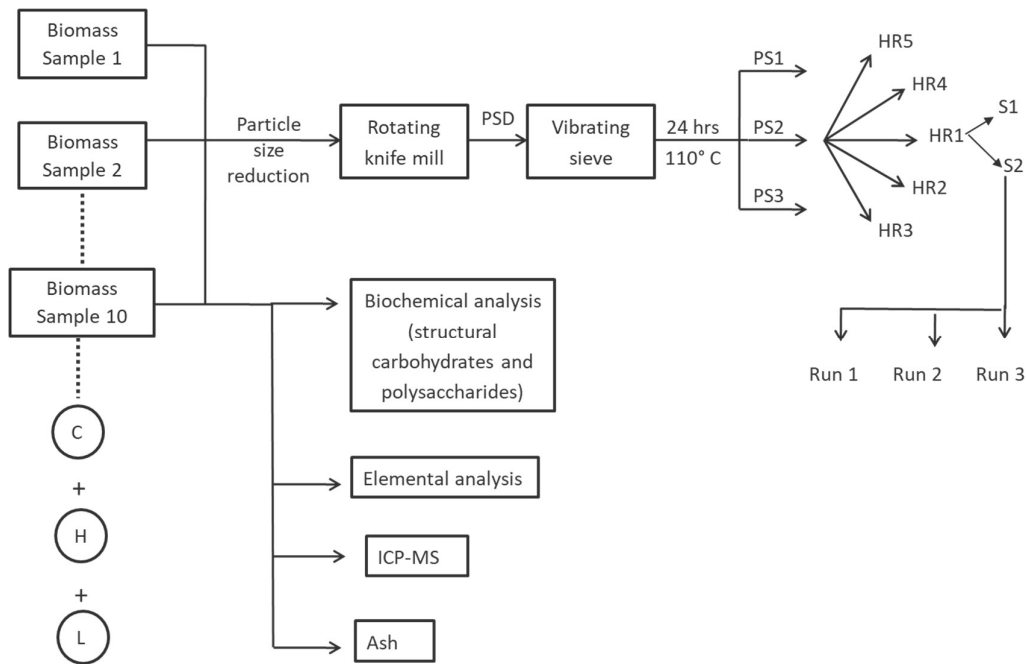


*Figure 2.1 Sample preparation overview; C:cellulose; H:hemicellulose; L:lignin (alkali); PSD:particel size distribution; HR:heating rate; PS: particle size; S:sample-size*

| Biomass | Carbon | Hydrogen | Nitrogen | Total | (O & inorganics) | H/C ratio |
|---|---|---|---|---|---|---|
| Malleewood | 45.0 | 5.3 | 0.19 | 50.5 | 49.4 | 1.4 |
| Jarrah | 48.1 | 5.3 | 0.06 | 53.5 | 46.4 | 1.3 |
| Pinewood | 46.2 | 5.7 | 0.11 | 52.0 | 47.9 | 1.5 |
| Merbau | 47.2 | 5.3 | 0.15 | 52.6 | 47.3 | 1.3 |
| Silvertop | 46.2 | 5.2 | 0.09 | 51.5 | 48.5 | 1.3 |
| Spotgum | 44.7 | 5.2 | 0.16 | 50.1 | 49.8 | 1.4 |
| Kapur | 46.6 | 5.4 | 0.13 | 52.2 | 47.8 | 1.4 |
| Lupin | 40.7 | 5.9 | 1.32 | 48.0 | 51.9 | 1.7 |
| Pinecone | 48.4 | 5.4 | 0.84 | 54.6 | 45.3 | 1.3 |
| Pineneedle | 46 .9 | 5.9 | 1.25 | 54.1 | 45.9 | 1.5 |

*Table 2-1 Elemental analysis of biomass samples. Values represented are wt%.*

| Biomass | Glucose (wt%) | Xylose (wt%) | Arabinose (wt%) |
|---|---|---|---|
| Malleewood | 32.49 | 17.27 | 1.16 |
| Jarrah | 36.65 | 9.77 | 0.10 |
| Pinewood | 44.32 | 20.82 | 1.38 |
| Merbau | 49.44 | 8.15 | 0.34 |
| Silvertop | 39.14 | 12.44 | 0.23 |
| Spotgum | 40.49 | 20.18 | 0.49 |
| Kapur | 45.14 | 9.25 | 0.10 |
| Lupin | 33.41 | 18.50 | 6.02 |
| Pinecone | 29.87 | 18.05 | 1.82 |

| | | | | | |
|---|---|---|---|---|---|
| Pineneedle | 17.88 | 10.77 | 2.43 | | |

*Table 2-2 Composition of cellulose and hemicellulose constituents for biomass samples*

| Biomass | Cellulose (wt%) | Hemicellulose (wt%) | AIL (wt%) | ASL (wt%) | Protein (wt%) | Ash (wt%) |
|---|---|---|---|---|---|---|
| Malleewood | 29.24 | 16.22 | 26.39 | 5.76 | 1.24 | 5.68 |
| Jarrah | 32.98 | 8.69 | 45.60 | 3.73 | 0.41 | 0.33 |
| Pinewood | 39.89 | 19.54 | 29.01 | 1.70 | 0.70 | 0.24 |
| Merbau | 44.50 | 7.47 | 40.63 | 3.65 | 0.94 | 1.05 |
| Silvertop | 35.23 | 11.15 | 33.82 | 13.40 | 0.59 | 0.04 |
| Spotgum | 36.44 | 18.19 | 31.41 | 6.81 | 1.03 | 0.90 |
| Kapur | 40.63 | 8.23 | 36.89 | 5.13 | 0.86 | 0.57 |
| Lupin | 30.07 | 21.57 | 3.76 | 3.19 | 8.25 | 2.46 |
| Pinecone | 26.89 | 17.49 | 39.79 | 2.02 | 5.26 | 1.04 |
| Pineneedle | 16.09 | 11.61 | 33.34 | 8.12 | 7.84 | 7.50 |

*Table 2-3 Strucutural carbohydrates and lignin composition of biomass samples; AIL:aicd insluble lignin; ASL:acid soluble lignin*
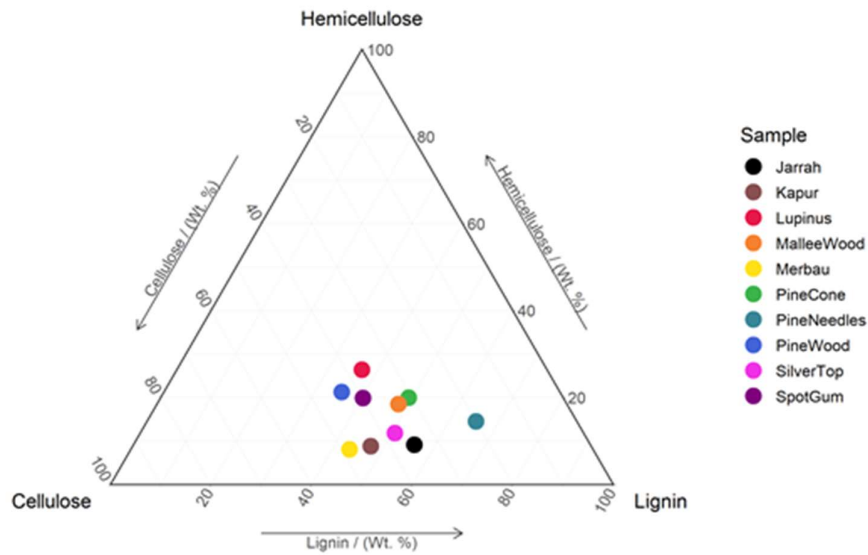
*Figure 2.2 Spatial distribution of cellulose, hemicellulose and lignin content of biomass samples*

## 2.5 Preliminary investigation and enquiry

### 2.5.1 Mallee wood

Figures *2.3 - 2.5* show the mass loss curves and derivative mass loss curves for mallee wood at 250 K/min heating rate. Mallee shows the first signs of decomposition around 250 °C, which corresponds to the initiation temperature for decomposition of lignin. This is a significant DTG peak, since mallee has significant amount of lignin. Lignin decomposition continues till 470 °C and coincides with hemicellulose decomposition range (~220 °C to 350 °C). There is a decrease in rate of mass loss in the temperature range of 300 to 350 °C, which corresponds to complete devolatilization of hemicellulose around 350 °C. The next and most significant mass loss peak coincides with cellulose decomposition range of ~320 °C to 450 °C. As evident from the mass loss curves, the major portion of devolatilization is complete with the decomposition of cellulose around 450 °C. The slight mass loss after that is the gradual decomposition of lignin which continues over the entire temperature range of process. The lower degree of decomposition of samples with particle size below 45 μm could be due to the presence of higher amount of inorganics in lower particle sizes due to sieving effects.
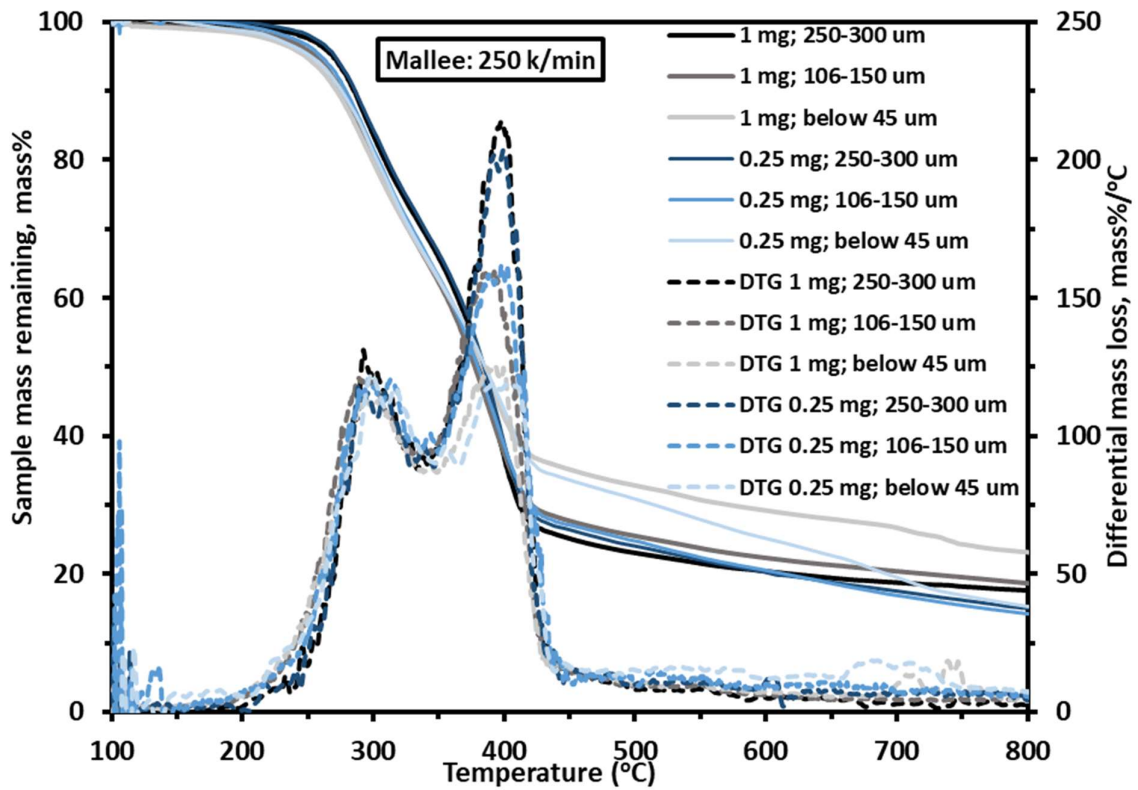
*Figure 2.3 Mass loss and derivative mass loss curves for mallee wood*
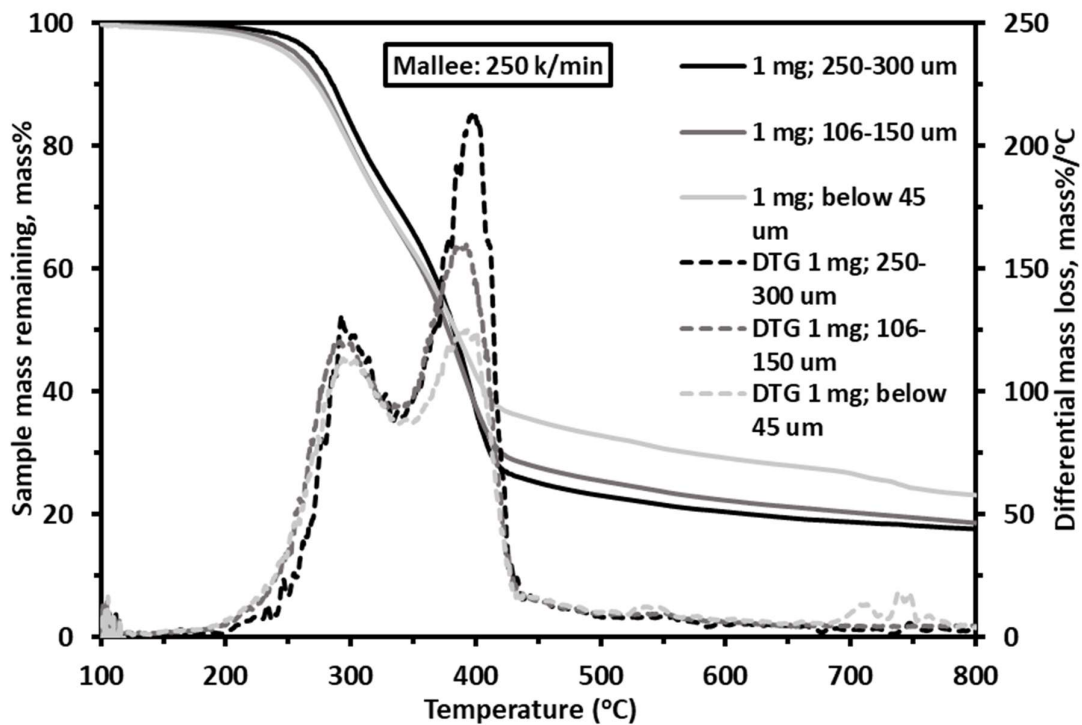


*Figure 2.4 Mass loss and derivative mass loss curves for mallee wood*
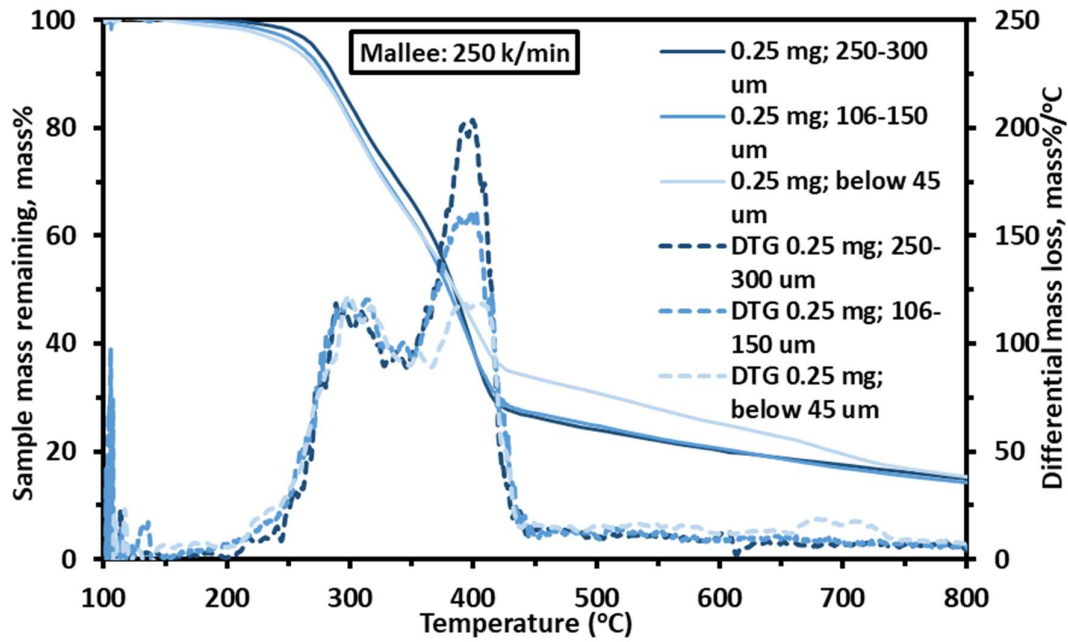
*Figure 2.5 Mass loss and derivative mass loss curves*

### 2.5.2 Jarrah wood
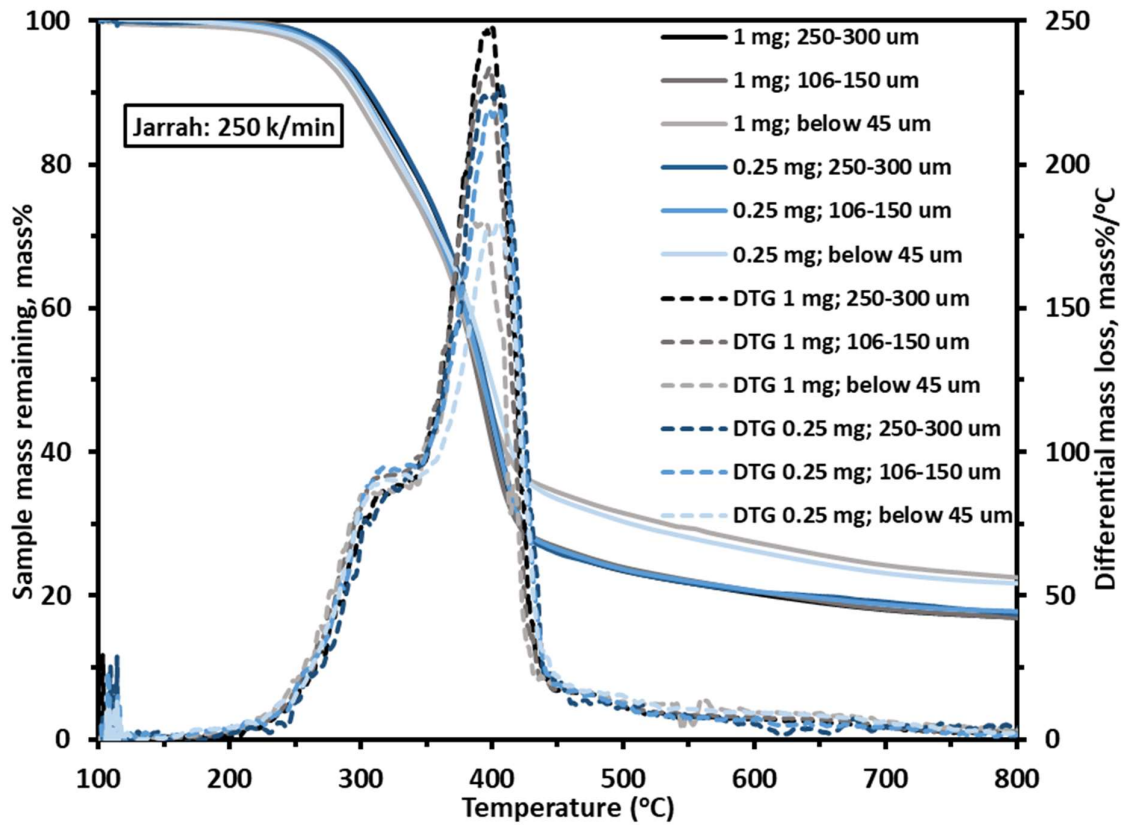


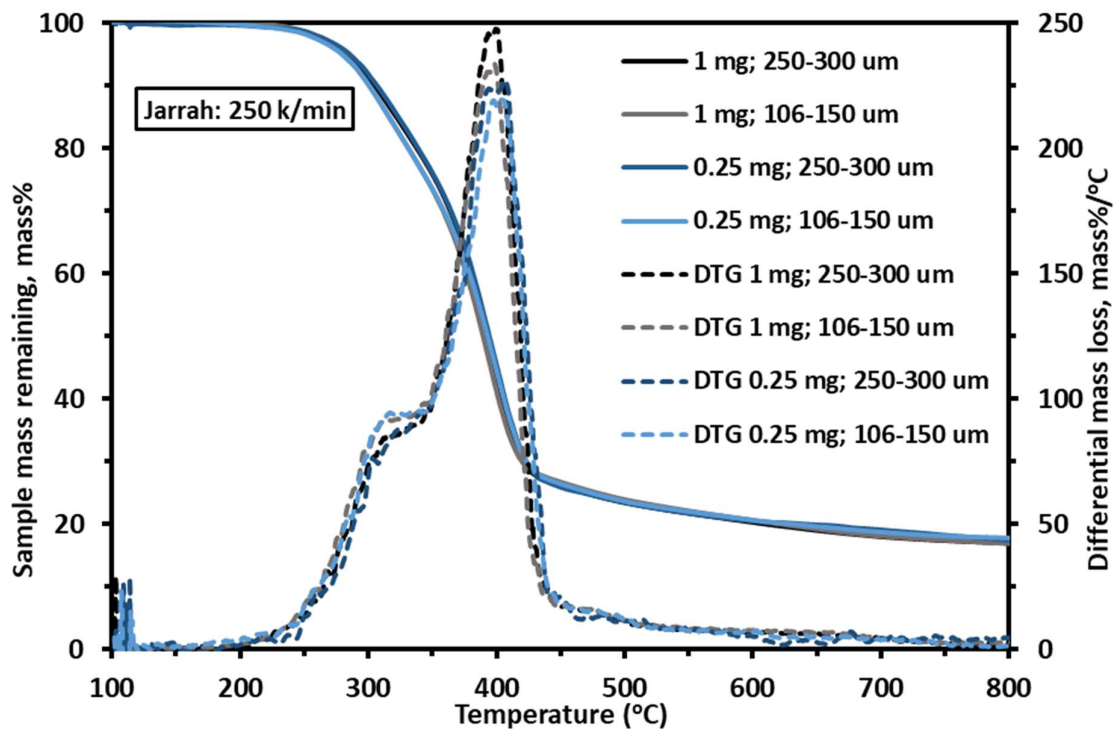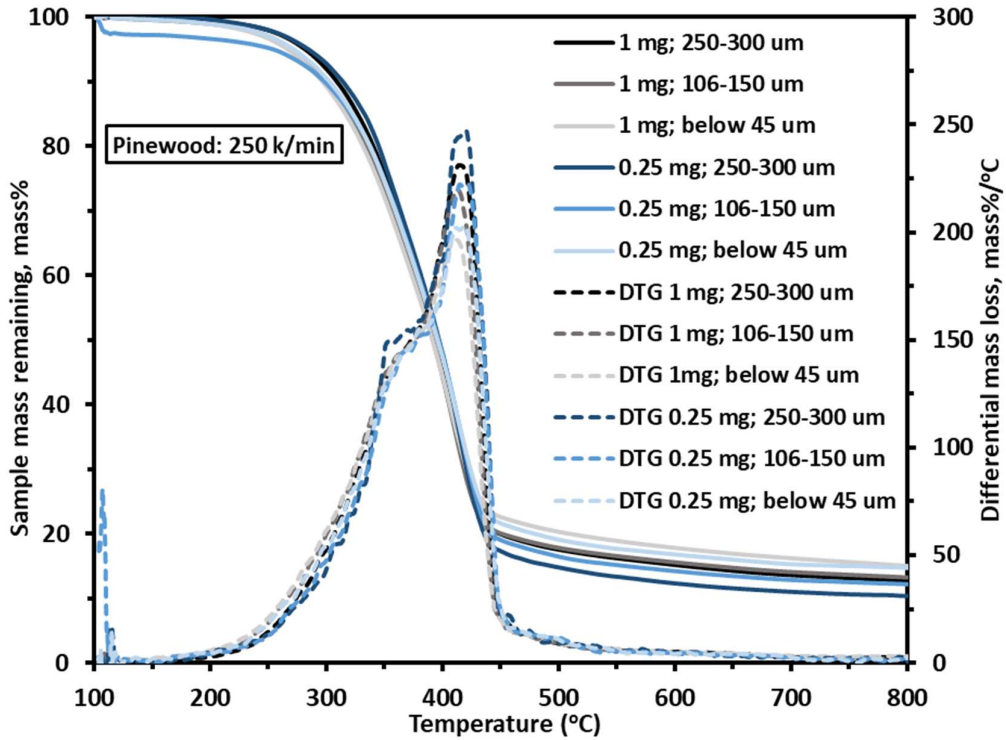*Figure 2.6 Mass loss and derivative mass loss curves for jarrah wood*

Figure 2.6 and Figure 2.7 show the mass loss curves and derivative mass loss curves for jarrah wood at 250 K/min heating rate. Jarrah shows the first signs of decomposition around 250 °C, which corresponds to the initiation temperature for decomposition of lignin. This is a significant DTG peak, since jarrah has significant amount of lignin. Jarrah has considerably lower amount of hemicellulose as compared to mallee and as such the rate of mass loss does not slow down, since hemicellulose isn't a significant contributor to the mass loss profile. As evident from the mass loss curves, majority of devolatilization occurs between 350 to 450 °C which is the range of cellulose decomposition. As is the case with mallee, the samples of particle size below 45 μm, devolatilize to a lesser extent in jarrah.



*Figure 2.7 Mass loss and derivative mass loss curves for jarrah wood*

### 2.5.3 Pine wood

Figure 2.8 and figure 2.9 show the mass loss characteristics of pinewood. Unlike mallee and jarrah, pinewood shows a sharp mass loss regime due to low composition of lignin in it. The mass loss starts with hemicellulose decomposition around 220 °C and continues steadily until ~320 °C. There is a sharp increase in % mass loss between 320 °C to 450 °C which coincides entirely with cellulose decomposition regime. The negligible mass loss after 450 °C and insignificant difference between the amount of final mass loss between different particle sizes, point towards a possible connection with lignin composition.

Figure 2.10 and figure 2.11 show the mass loss characteristics of merbau. Merbau has the highest cellulose content amongst the ten chosen biomass samples. Merbau also has a high lignin composition and a low hemicellulose composition. As a result, merbau has the first mass

loss peak around 220 °C which marks the starting temperature lignin decomposition, followed by another significant peak around 350 °C to coincide with cellulose decomposition. This mass loss continues sharply till 450 °C, after which there is a slight and steady mass loss corresponding to the remaining lignin decomposition after 470 °C. The overall decomposition of merbau is lesser than the previous biomass samples, which again point towards the role of lignin in determining the final mass loss percent.



*Figure 2.8 Mass loss and derivative mass loss curves for mallee wood*
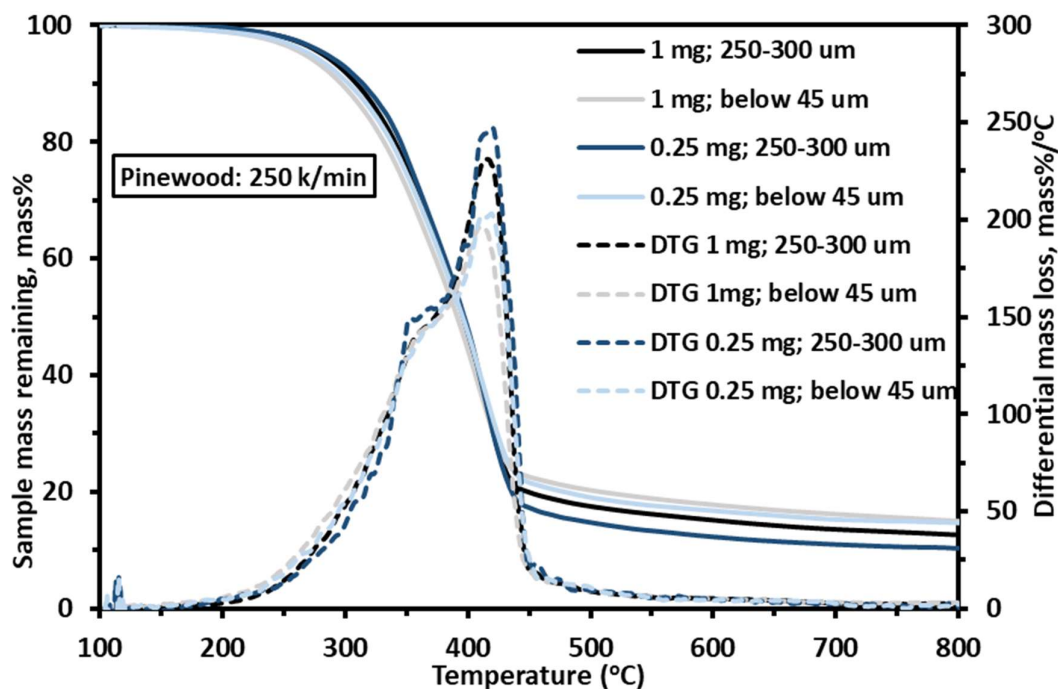
*Figure 2.9  Mass loss and derivative mass loss curves for pinewood*

### 2.5.4 Pinecone

Figure 2.10 shows the mass loss and derivative mass loss curves for pinecone. Pinecone has a comparatively high amount of lignin and low amount of cellulose. The amount of hemicellulose in pinecone is comparatively on the higher side. As such, there is a DTG peak at 220 °C followed by a steep increase in % mass loss till 350 °C which is precisely the range for hemicellulose decomposition. This is comparable to the contribution of cellulose in devolatilization in the case of pinecone. Since pinecone also contains a significant amount of lignin, the DTG peaks for % mass loss are comparatively broader in width.

Figure 2.11 shows the variation in mass loss and differential mass loss curves for pinecone at different heating rates. A comprehensive discussion on the effect of heating rates on TGA and DTG curves of biomass will be presented in future as part of a manuscript.
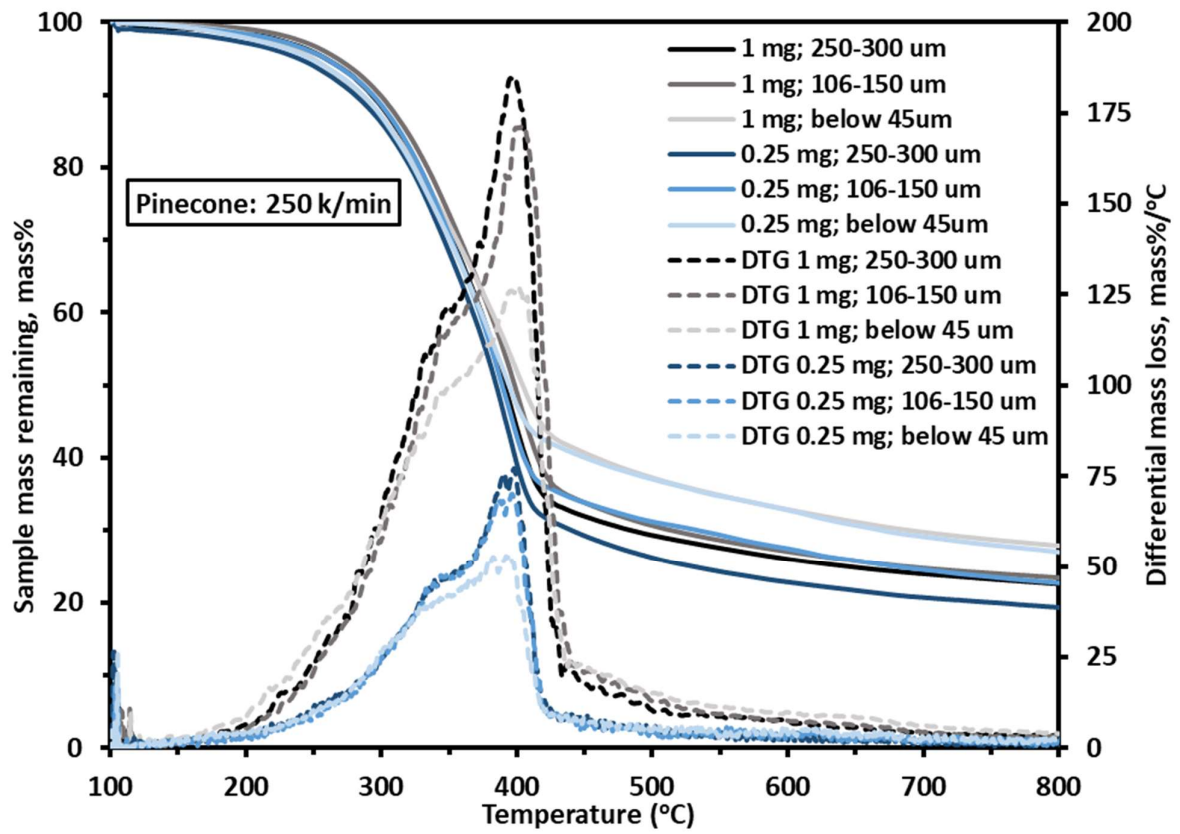
*Figure 2.10 Mass loss and derivative mass loss curves for pinecone*
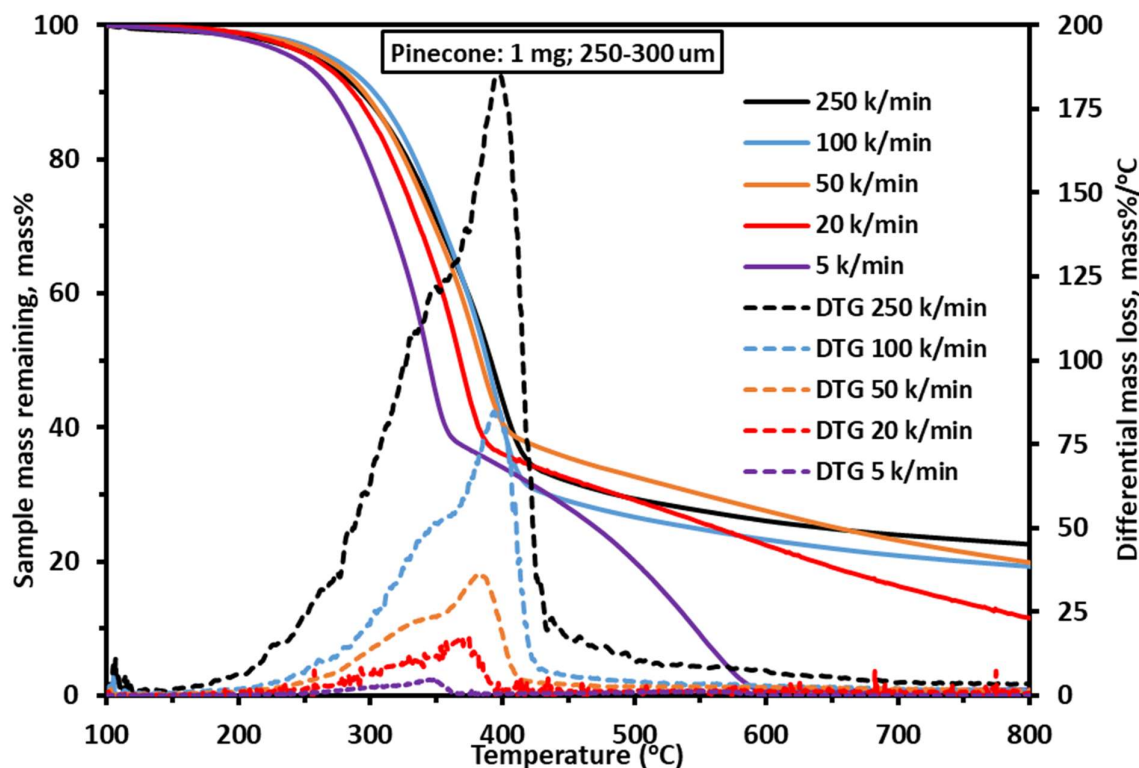
*Figure 2.11 Mass loss and derivative mass loss curves for pinecone at different heating rates*

### 2.5.5 Pine needle

Figure 2.12 shows the decomposition curves for pine needle. Pine needle has the least amount of cellulose amongst the selected biomass samples. As a result, the effect of hemicellulose and lignin on the decomposition curves is more pronounced in the case of pine needle. The DTG peak at 220 °C is more significant and so is the plateau at ~350 °C corresponding to hemicellulose degradation. The peak for cellulose decomposition is visibly less pronounced and there isn't a sharp slope corresponding to cellulose decomposition at 450 °C as is the case for other biomass samples. The effect of high proportion of lignin in biomass composition is evident from the wider width of the DTG peaks and by smaller DTG peaks corresponding to continuing lignin decomposition even after 450 °C.
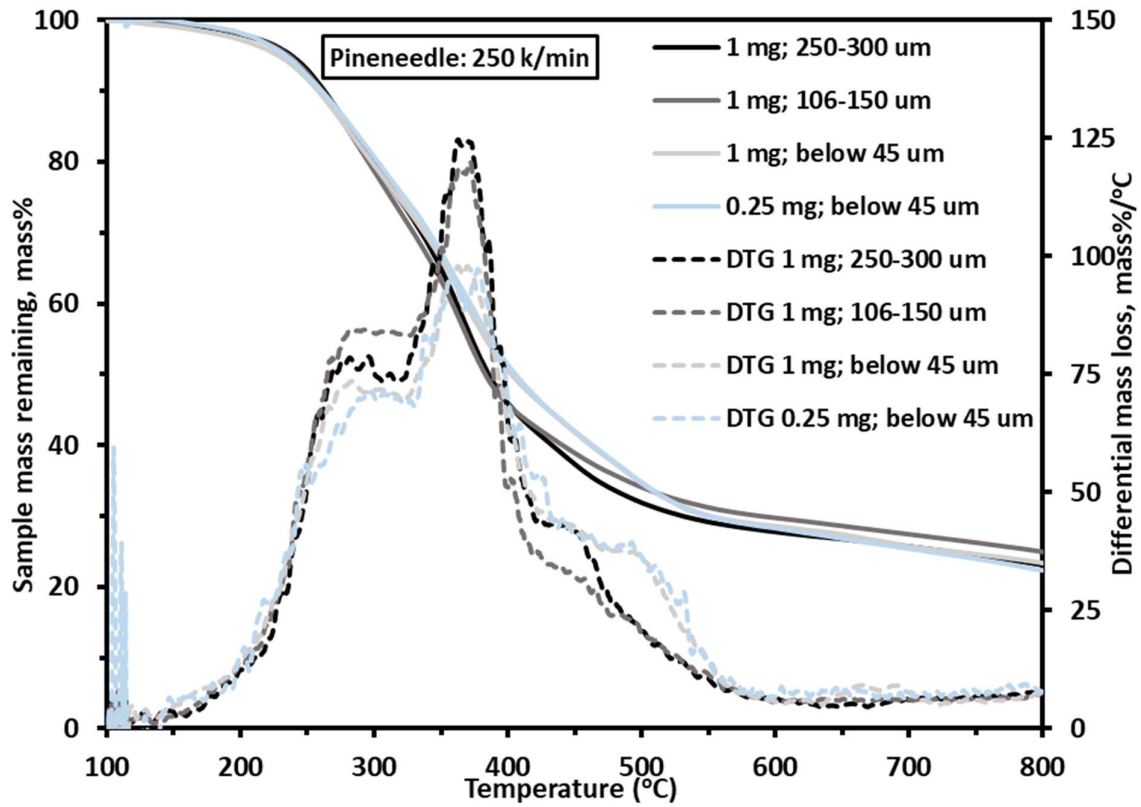
*Figure 2 Mass loss and derivative mass loss curves for pine-needle*
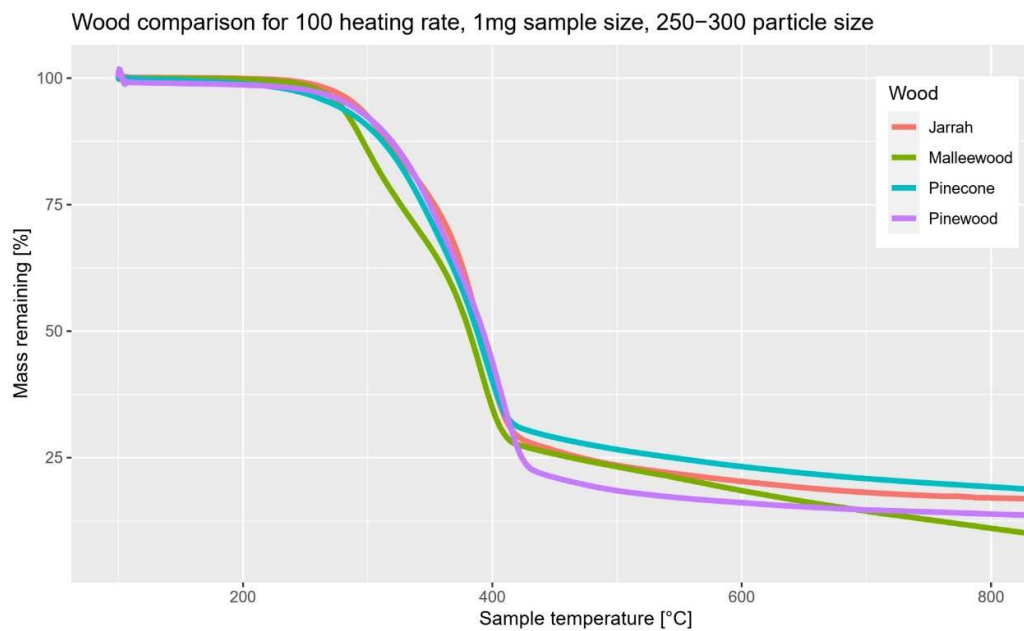


*Figure 2.13 Comparing mass loss profile of various wood samples*
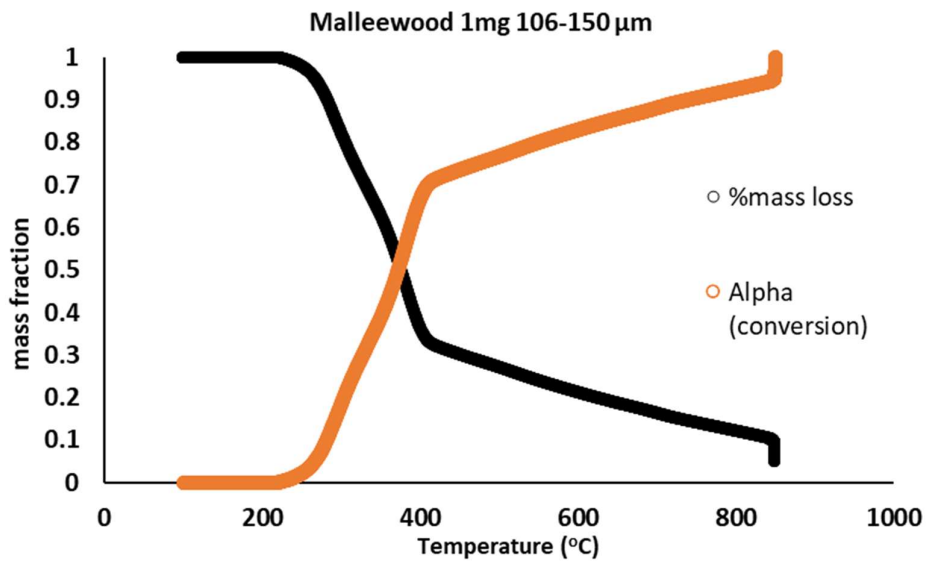
*Figure 2.14 mass loss and conversion relationship*
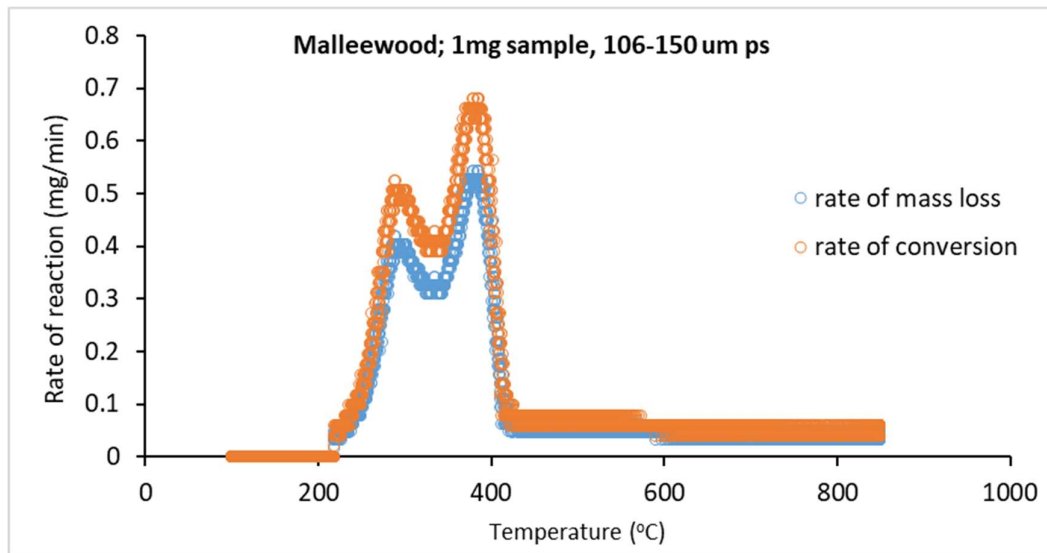


*Figure 2.15 Comparison between rate of mass loss and rate of conversion*
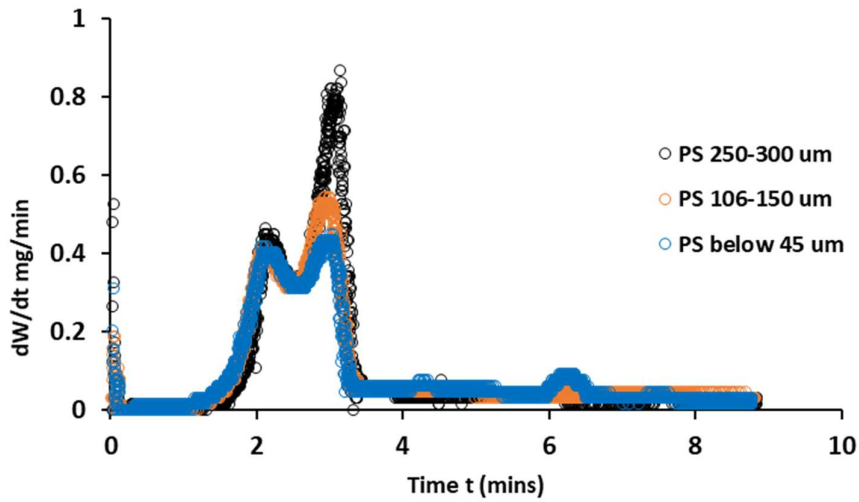
**2.6 Effect of Particle size on rate of reaction**



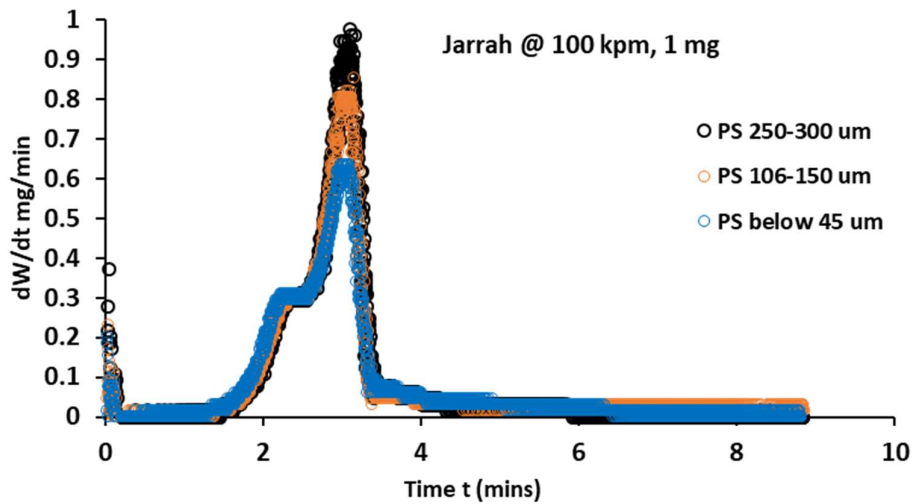*Figure 2.16 Effect of particle size on rate of mass loss; Malleewood 100 K/min*



*Figure 2.17 Effect of particle size on rate of mass loss, Jarrah 100 K/min*

**2.7 Effect of Temperature scale on progress of reaction**

*2.7.1 Slow pyrolysis*
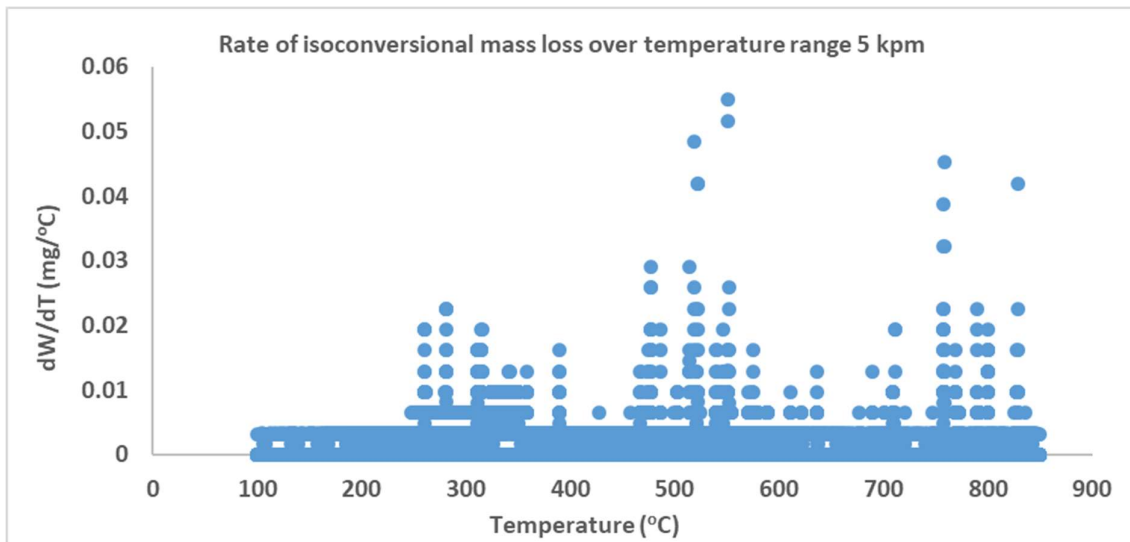
*Figure 2.18 Rate of mass loss @ 5 k/min or slow pyrolysis condition*

2.7.2 Fast pyrolysis
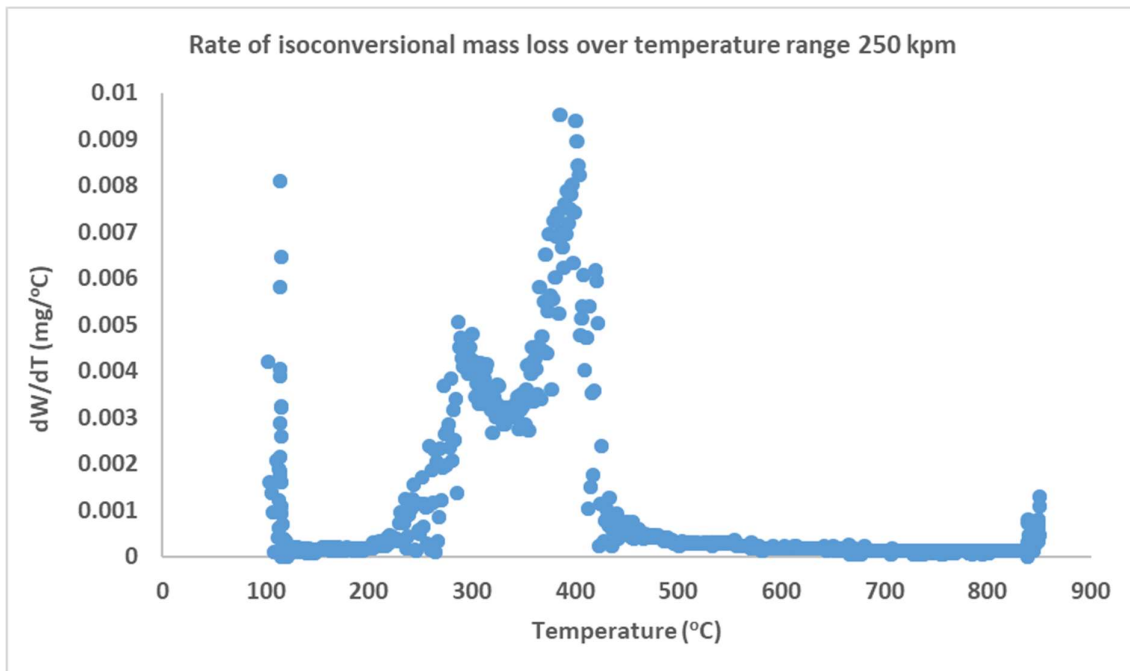


*Figure 2.19 Rate of mass loss at 250 K/min or (close to) fast pyrolysis conditions*

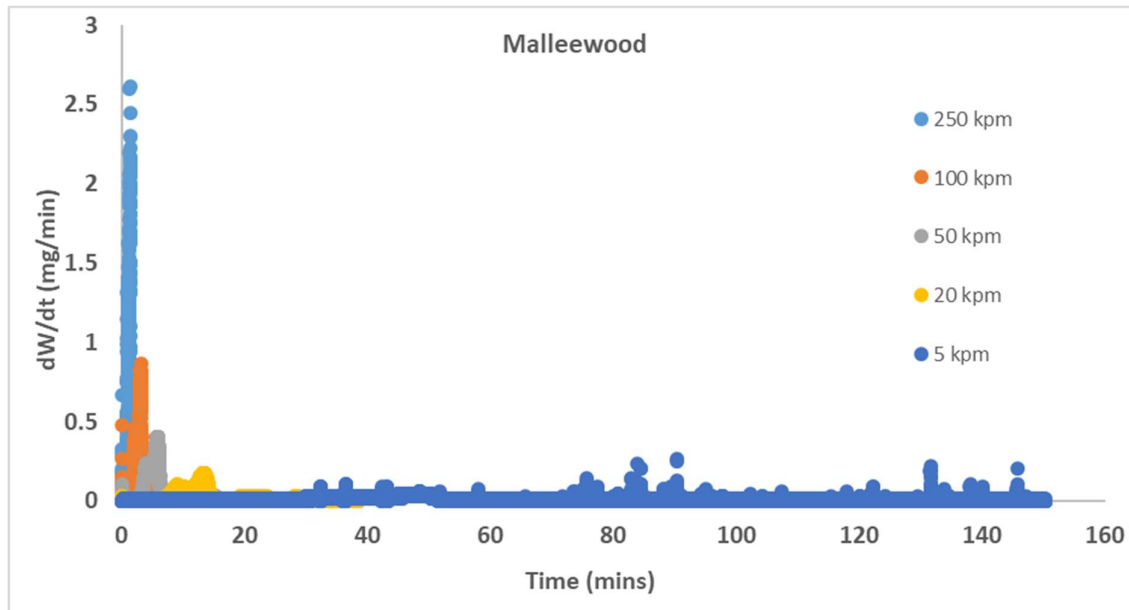## 2.8 Effect of Time scale of reaction progression



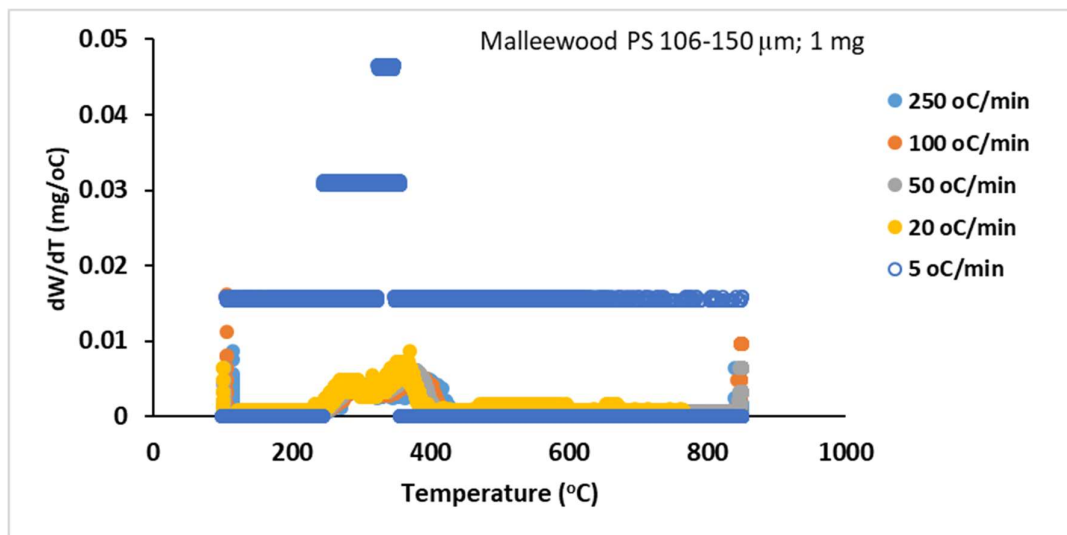*Figure 2.20 Rate of reactions at different heating rates*



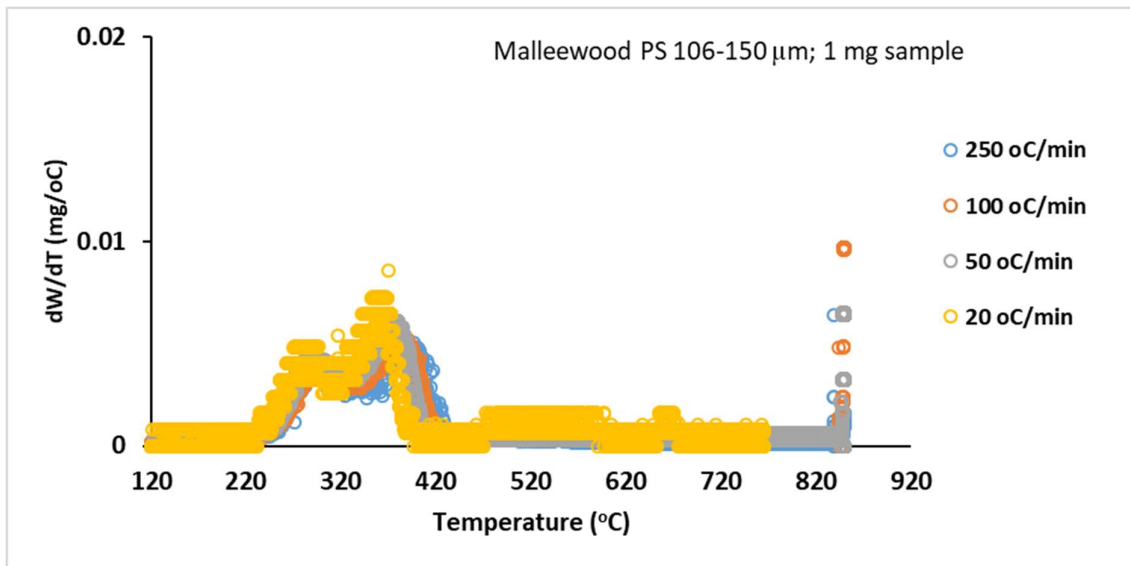*Figure 2.21 effect of heating rates over temperature scale*

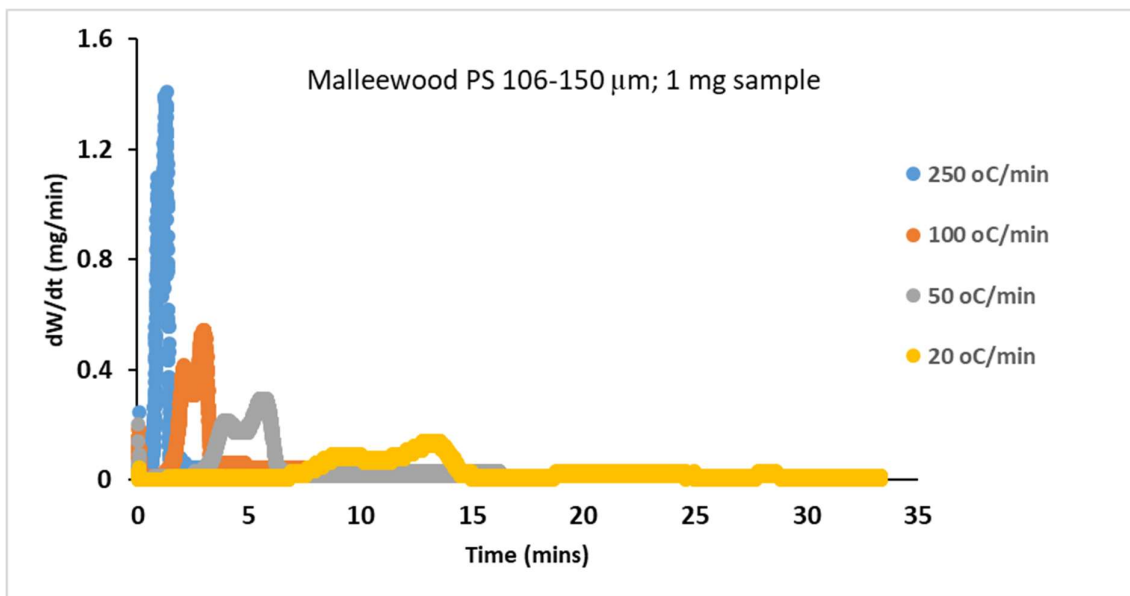*Figure 2.22 Rate of reaction across temperature scale*



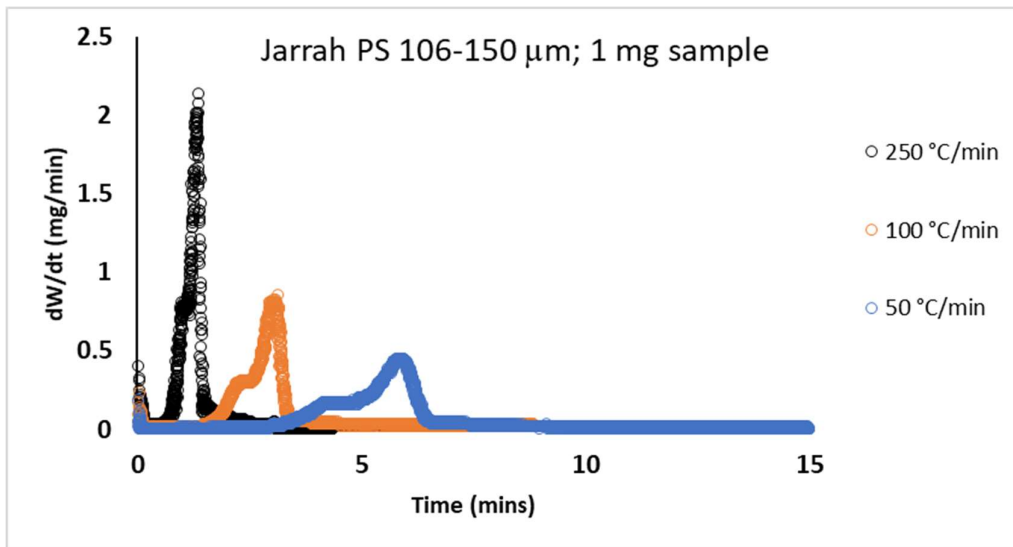*Figure 2.23 Rate of reaction across time-scale*
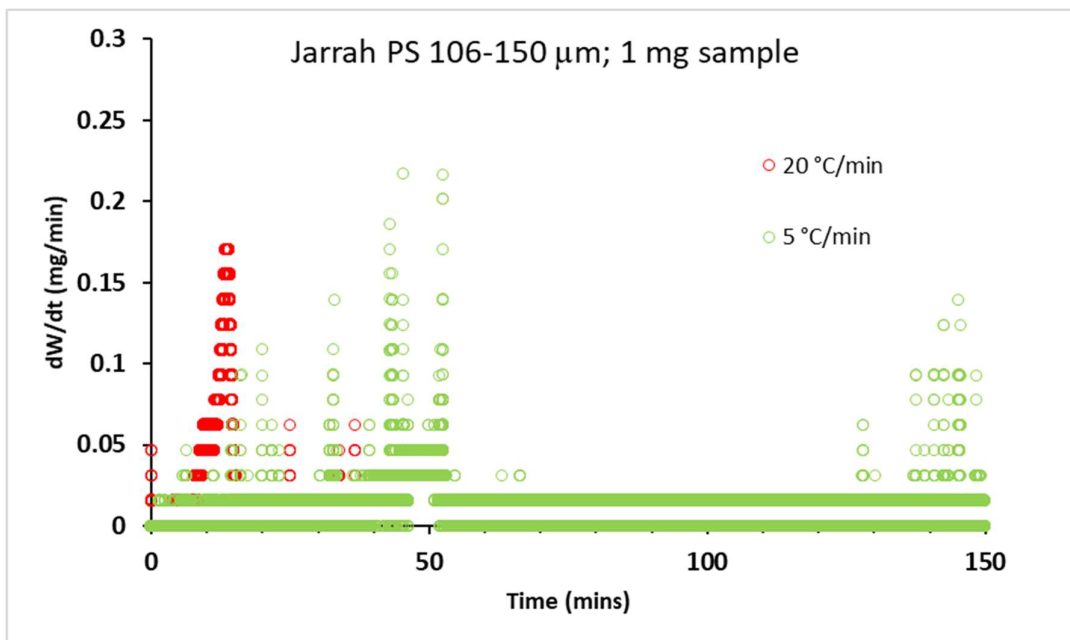
*Figure 2.24 Rate of mass loss across time scale*



*Figure 2.25 rate of mass loss for slower heating rates on time scale*

**2.9 Effect of heating rate – Heat transfer on pyrolysis reaction**
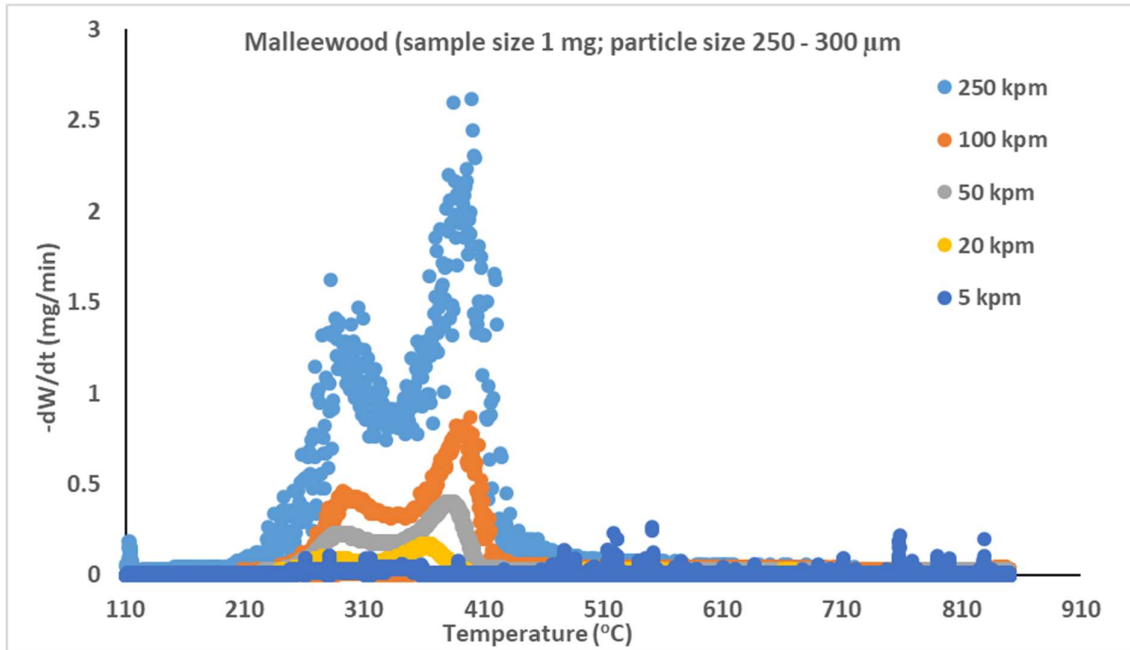


*Figure 2.26 Effect of heating rates on malleewood across temperature scale*

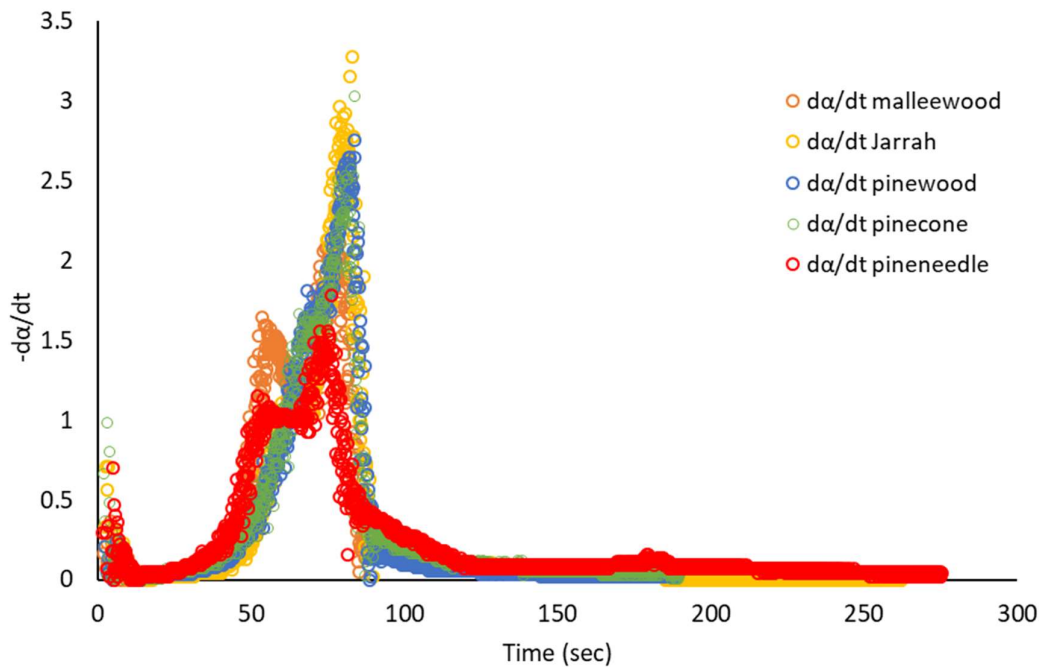**2.10 Effect of Composition and heterogeneity**



*Figure 2.27 Rate of mass loss for different biomass samples over time scale*
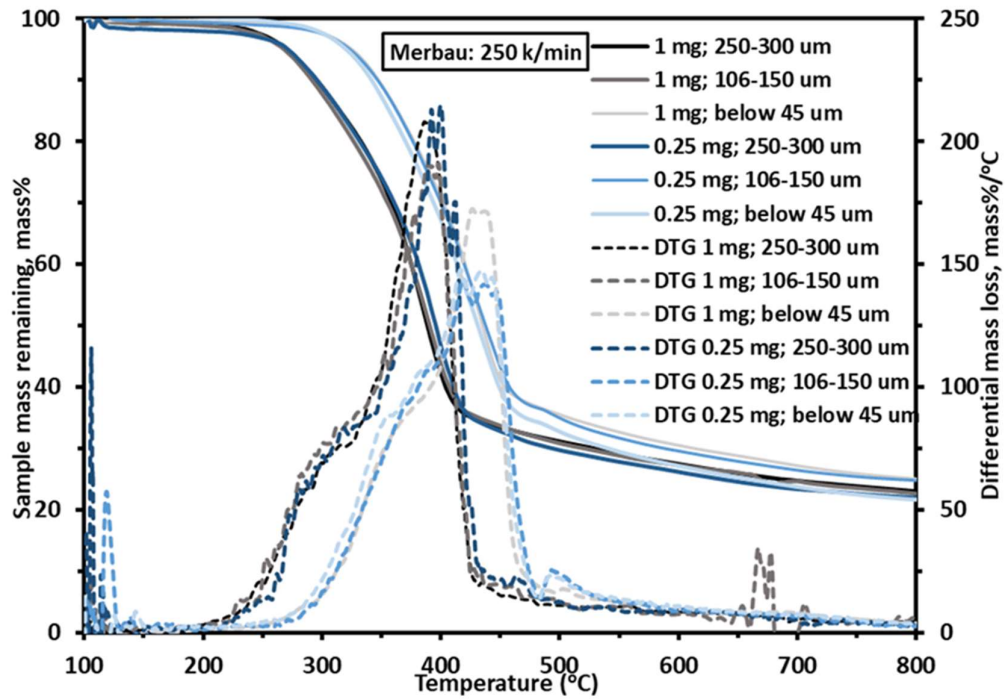
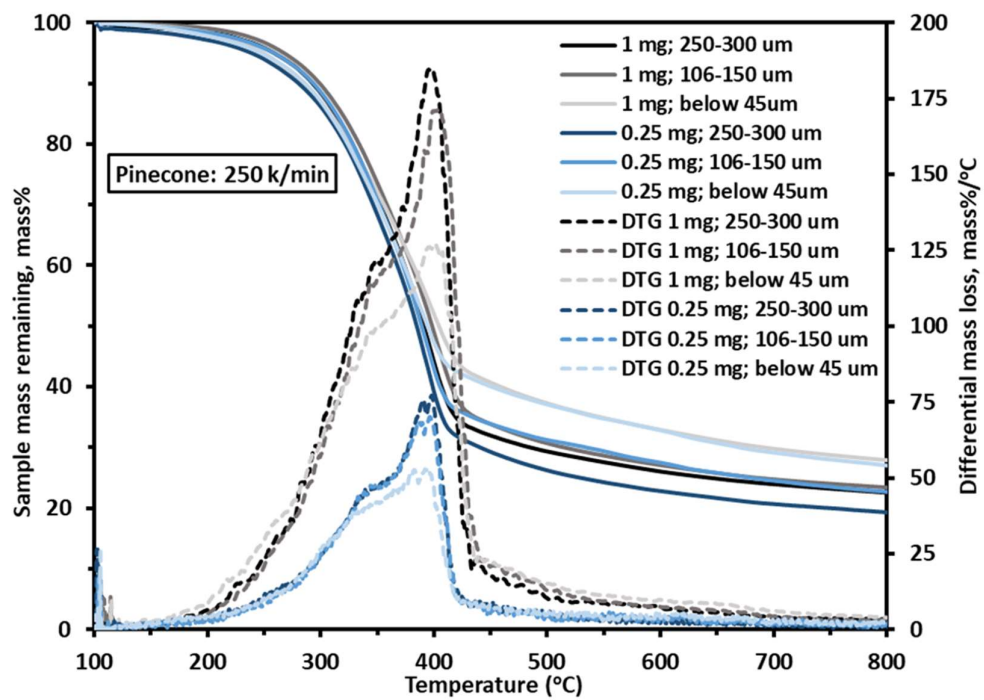*Figure 2.28 mass loss and rate of mass loss curves for merbau*



*Figure 2.29 mass loss and rate of mass loss curves for pinecone*

## 2.11 Mass balance tables

|  | Δt (sec) | Δm (mg) | % mass loss | ΔT (°K) |
|---|---|---|---|---|
| RT-100 hold | 855.8 | 0.06 | 6.79 | 63.8 |
| 100 - 200 C | 60.6 | -0.02 | -2.84 | 100.2 |
| 200 - 250 C | 11.3 | 0.016 | 1.84 | 50.1 |
| 250 - 300 C | 10.8 | 0.08 | 8.78 | 50.1 |
| 300 - 380 C | 17.2 | 0.28 | 32.17 | 79.8 |
| 380 - 500 C | 26.5 | 0.27 | 31.03 | 119.8 |
| 500 -600 C | 22.6 | 0.027 | 3.18 | 99.9 |
| 600 - 700 C | 23.1 | 0.02 | 2.42 | 100.4 |
| 700 -800 C | 23.1 | 0.01 | 1.21 | 99.6 |
| 800 - 850 C | 89.3 | 0.02 | 1.87 | 49.9 |
| 850 C hold | 474.8 | 0.12 | 13.53 | 0 |

*Table 2.4 Mass balance for Jarrah @ 250 K/min H.R; 106-150 μm ps, 1 mg sample*

|  | Δt (sec) | Δm (mg) | % mass loss | ΔT (°K) |
|---|---|---|---|---|
| RT-100 hold | 855.8 | 0.06 | 6.95 | 64.2 |
| 100 - 200 C | 1236.6 | 0.00 | 0 | 100 |
| 200 - 250 C | 598.1 | 0.03 | 3.51 | 50 |
| 250 - 300 C | 598.4 | 0.13 | 15.25 | 50 |
| 300 - 380 C | 957.7 | 0.39 | 45.33 | 80 |
| 380 - 500 C | 1437.7 | 0.06 | 6.51 | 120 |
| 500 -600 C | 1198.9 | 0.04 | 4.47 | 100 |
| 600 - 700 C | 1199 | 0.02 | 2.93 | 100 |
| 700 -800 C | 1199.1 | 0.02 | 1.93 | 100 |
| 800 - 850 C | 605.2 | 0.01 | 0.84 | 50 |
| 850 C hold | 1025.6 | 0.01 | 1.48 | 0 |

*Table 2.5 Mass balance for Jarrah @ 5 K/min H.R; 106-150 μm ps, 1 mg sample*

|  | Δt (sec) | Δm (mg) | % mass loss | ΔT (°K) |
|---|---|---|---|---|
| RT-100 hold | 687 | 0.06 | 5.92135036 | 63.87 |
| 100 - 200 C | 228.5 | 0.00 | 0 | 100.4 |
| 200 - 250 C | 10.9 | 0.07 | 6.87 | 49.7 |
| 250 - 300 C | 10.6 | 0.13 | 13.93 | 50 |
| 300 - 380 C | 17.1 | 0.26 | 26.88 | 80.2 |
| 380 - 500 C | 26.5 | 0.17 | 17.04 | 120 |
| 500 -600 C | 22.7 | 0.03 | 3.51 | 100 |
| 600 - 700 C | 23.1 | 0.02 | 1.86 | 100 |
| 700 -800 C | 23.2 | 0.03 | 2.75 | 100 |
| 800 - 850 C | 18.2 | 0.03 | 3.35 | 50 |

| | | | | |
|---|---|---|---|---|
| 850 C hold | 987 | 0.15 | 14.82 | 0 |

*Table 2.6 Mass balance for Pine needle @ 250 K/min H.R; 106-150 µm ps, 1 mg sample*

| | Δt (sec) | Δm (mg) | % mass loss | ΔT (°K) |
|---|---|---|---|---|
| RT-100 hold | 687.1 | 0.05 | 5.93 | 63.8 |
| 100 - 200 C | 1405.5 | 0.02 | 2.52 | 100 |
| 200 - 250 C | 598.1 | 0.08 | 8.91 | 50 |
| 250 - 300 C | 598.4 | 0.13 | 15.14 | 50 |
| 300 - 380 C | 957.7 | 0.24 | 27.84 | 80 |
| 380 - 500 C | 1437.9 | 0.1 | 11.27 | 120 |
| 500 -600 C | 1198.7 | 0.03 | 3.51 | 100 |
| 600 - 700 C | 1199.1 | 0.03 | 3.65 | 100 |
| 700 -800 C | 1199.1 | 0.08 | 9.00 | 100 |
| 800 - 850 C | 604.7 | 0.06 | 6.61 | 50 |
| 850 C hold | 1185.1 | 0.02 | 2.83 | 0 |

*Table 2.7 Mass balance for Pine needle @ 5 K/min H.R; 106-150 µm ps, 1 mg sample*

| | Δt (sec) | Δm (mg) | % mass loss | ΔT (°K) |
|---|---|---|---|---|
| RT-100 hold | 684 | 0.06 | 6.62 | 63.9 |
| 100 - 200 C | 231.6 | 0 | 0 | 100 |
| 200 - 250 C | 10.9 | 0.01 | 1.71 | 50 |
| 250 - 300 C | 10.6 | 0.06 | 6.27 | 50 |
| 300 - 380 C | 17.1 | 0.29 | 31.60 | 80 |
| 380 - 500 C | 26.5 | 0.34 | 37.78 | 120 |
| 500 -600 C | 22.7 | 0.02 | 2.19 | 100 |
| 600 - 700 C | 23.1 | 0.01 | 1.47 | 100 |
| 700 -800 C | 23.2 | 0.01 | 0.87 | 100 |
| 800 - 850 C | 18 | 0.01 | 0.79 | 50 |
| 850 C hold | 422.9 | 0.10 | 11.54 | 0 |

*Table 2-8 Mass balance for Pine wood @ 250 K/min H.R; 106-150 µm ps, 1 mg sample*

| | Δt (sec) | Δm (mg) | % mass loss | ΔT (°K) |
|---|---|---|---|---|
| RT-100 hold | 683.9 | 0.06 | 6.97 | 64 |
| 100 - 200 C | 1408.9 | 0.00 | -0.02 | 100 |
| 200 - 250 C | 598.1 | 0.02 | 2.50 | 50 |
| 250 - 300 C | 598.2 | 0.12 | 13.42 | 50 |
| 300 - 380 C | 957.7 | 0.48 | 53.89 | 80 |
| 380 - 500 C | 1437.9 | 0.05 | 5.40 | 120 |
| 500 -600 C | 1198.9 | 0.03 | 2.93 | 100 |

| | | | | |
|---|---|---|---|---|
| 600 - 700 C | 1199 | 0.02 | 2.28 | 100 |
| 700 -800 C | 1199.1 | 0.01 | 1.66 | 100 |
| 800 - 850 C | 605.1 | 0.01 | 1.01 | 50 |
| 850 C hold | 800.1 | 0.01 | 1.66 | 0 |

Table 2.9 Mass balance for Pine wood @ 5 K/min H.R; 106-150 μm ps, 1 mg sample

| | Δt (sec) | Δm (mg) | % mass loss | ΔT (°K) |
|---|---|---|---|---|
| RT-100 hold | 739.5 | 0.06 | 6.58 | 63.8 |
| 100 - 200 C | 177.2 | -0.02 | -2.09 | 100 |
| 200 - 250 C | 11.4 | 0.02 | 2.41 | 50 |
| 250 - 300 C | 10.9 | 0.09 | 9.11 | 50 |
| 300 - 380 C | 17.2 | 0.34 | 34.45 | 80 |
| 380 - 500 C | 26.6 | 0.2 | 20.28 | 120 |
| 500 -600 C | 22.6 | 0.03 | 3.34 | 100 |
| 600 - 700 C | 23 | 0.02 | 2.52 | 100 |
| 700 -800 C | 23.2 | 0.02 | 1.65 | 100 |
| 800 - 850 C | 109.2 | 0.03 | 2.96 | 50 |
| 850 C hold | 864 | 0.18 | 18.21 | 0 |

Table 2-10 Mass balance for Merbau @ 250 K/min H.R; 106-150 μm ps, 1 mg sample

| | Δt (sec) | Δm (mg) | % mass loss | ΔT (°K) |
|---|---|---|---|---|
| RT-100 hold | 739.4 | 0.06 | 6.66 | 63.65 |
| 100 - 200 C | 1353.2 | 0.00 | 0.15 | 100 |
| 200 - 250 C | 598.2 | 0.03 | 3.34 | 50 |
| 250 - 300 C | 598.2 | 0.12 | 13.33 | 50 |
| 300 - 380 C | 957.8 | 0.33 | 36.66 | 80 |
| 380 - 500 C | 1437.9 | 0.06 | 6.88 | 120 |
| 500 -600 C | 1198.7 | 0.04 | 4.33 | 100 |
| 600 - 700 C | 1199.1 | 0.02 | 2.5 | 100 |
| 700 -800 C | 1199.1 | 0.02 | 2.5 | 100 |
| 800 - 850 C | 604.6 | 0.02 | 2.23 | 50 |
| 850 C hold | 786.5 | 0.03 | 3.42 | 0 |

Table 2-11 Mass balance for Merbau @ 5 K/min H.R; 106-150 μm ps, 1 mg sample

## Results and discussions

The elemental analysis of biomass pyrolysis points towards some of the inherent limitations associated with pyrolysis crude oil quality. The amount of elemental oxygen present in woody samples is quite high ~45 wt%. The presence of high elemental oxygen leads to formation of bio-oil with high cross linking and is marked by presence of large quantities of polyaromatic hydrocarbons.[44–46] These highly crosslinked compounds and PAHs affect the combustion

quality of fuel negatively. In-situ or ex-situ catalytic treatment for deoxygenation to improve the quality of product has been prescribed in literature to deal with the said issue.[47–50]

The structural carbohydrates present in biomass samples is shown in table 2.2 and table 2.3. The role of these structural carbohydrates in determination of reaction mechanism and pyrolysis product distribution is relatively less explored. Cellulose, hemicellulose and lignin are three main structural carbohydrates of biomass samples. The variable devolatilization profiles of these components is one of the reasons for inability to get an accurate dynamic control of biomass fast pyrolysis processes. The samples chosen for this study have a relatively well grouped cluster of Cellulose : Hemicellulose : Lignin distribution. This will ensure specific limits to model prediction. The samples are majorly woody samples along with pure cellulose, hemicellulose and lignin.

The effects of particle size and sample size on the rate of reaction are measured over time-scale and temperature scale. Time-scale measurements reveal variations along the x-axis as well as the y-axis. Temperature scale measurements reveal that rate of reaction has no significant variations with respect to temperature along the x-axis. The particle size selected for TGA runs ensure that the reaction occurs predominantly in kinetically controlled regime. As the particle size is reduced, a slight reduction in maximum rate of reaction is observed in the regime dominated by cellulose decomposition. Rate of reaction dominated by hemicellulose breakdown is relatively less affected by particle and sample size. Sample size of 1 mg and particle size of 250-300 μm show the maximum rate of reaction. Similar trends are shown by mallewood, jarrah and pinewood samples. The effect of particle size is most clear with pineneedle and pinewood samples. A minor lateral shift along with a significant vertical shift is observed in rate of reaction profiles for pinewood samples. Catalytic effects are known to contribute to either promotion or inhibition of reaction rates.

At lower heating rates, conversion occurs slowly and proceeds to maximum conversion at a lower final temperature. At faster heating rates, the conversion occurs rapidly and is completed at a higher final temperature. This points to the effect of (high) specific heat capacity of biomass constituents during the reaction. The effect of heating rate on rate of reaction for biomass pyrolysis is studied over a temperature scale and time scale. Comparing rate of reactions at different heating rates over time and temperature scales reveals that as the heating rate is decreased, the reaction becomes progressively more lumped and vice-versa. At faster heating rates, the reaction can be observed in two discrete and distinct regions; whereas at slower heating rates, the reaction is revealed to be highly lumped with no discrete and distinct reaction regimes.

Further, comparing reaction profiles of different biomass samples at same heating rates and particle size reveals that compositional heterogeneity is also a factor influencing progress of biomass pyrolysis reaction.

Studies until now have majorly focussed on deriving kinetic parameters for closely grouped slow heating rate conditions at fixed or variable particle sizes. To the best of authors'

knowledge no significant work has reported incorporation of compositional heterogeneity into reaction kinetic model for biomass pyrolysis. Also, there is a lack of significant literature on models that can be applicable over slow to fast (wide range of) heating rates. The current work incorporates compositional heterogeneity of biomass for predictive kinetic modelling. Further, the said predictive kinetic model can be extended to heating rates ranging from slow pyrolysis conditions (~1-5 C/min) to faster pyrolysis conditions (~250-300 C/min).

## Conclusion

It is in this chapter that we first observe that the mass loss curve function for the same sample of biomass changes from slow pyrolysis conditions to fast pyrolysis conditions. At slow pyrolysis conditions the mass loss function could be assumed to be a straight line since the reactions are lumped together. At slow pyrolysis conditions, for the complete conversion of biomass sample, $\Delta T/\Delta t$ is $\ll$ than $\Delta T/\Delta t$ at fast pyrolysis conditions.

# References

(1)  Cano-Díaz, G. S.; Rosas-Aburto, A.; Vivaldo-Lima, E.; Flores-Santos, L.; Vega-Hernández, M. A.; Hernández-Luna, M. G.; Martinez, A. Determination of the Composition of Lignocellulosic Biomasses from Combined Analyses of Thermal, Spectroscopic, and Wet Chemical Methods. *Ind. Eng. Chem. Res.* **2021**, *60* (9), 3502–3515. https://doi.org/10.1021/acs.iecr.0c05243.

(2)  AU  - Foster, C. E.; AU  - Martin, T. M.; AU  - Pauly, M. Comprehensive Compositional Analysis of Plant Cell Walls (Lignocellulosic Biomass) Part II: Carbohydrates. *J. Vis. Exp.* **2010**, No. 37, e1837. https://doi.org/10.3791/1837.

(3)  AU  - Foster, C. E.; AU  - Martin, T. M.; AU  - Pauly, M. Comprehensive Compositional Analysis of Plant Cell Walls (Lignocellulosic Biomass) Part I: Lignin. *J. Vis. Exp.* **2010**, No. 37, e1745. https://doi.org/10.3791/1745.

(4)  Cai, J.; He, Y.; Yu, X.; Banks, S. W.; Yang, Y.; Zhang, X.; Yu, Y.; Liu, R.; Bridgwater, A. V. Review of Physicochemical Properties and Analytical Characterization of Lignocellulosic Biomass. *Renew. Sustain. Energy Rev.* **2017**, *76*, 309–322. https://doi.org/10.1016/j.rser.2017.03.072.

(5)  Hames, B.; Ruiz, R.; Scarlata, C.; Sluiter, A.; Sluiter, J.; Templeton, D. Preparation of Samples for Compositional Analysis: Laboratory Analytical Procedure (LAP); Issue Date 08/08/2008. *Tech. Rep.* **2008**.

(6)  Sluiter, A. Determination of Sugars, Byproducts, and Degradation Products in Liquid Fraction Process Samples: Laboratory Analytical Procedure (LAP); Issue Date: 12/08/2006. *Tech. Rep.* **2008**.

(7)  Sluiter, A. Determination of Ash in Biomass: Laboratory Analytical Procedure (LAP); Issue Date: 7/17/2005. *Tech. Rep.* **2008**.

(8)  Sluiter, A. Determination of Extractives in Biomass: Laboratory Analytical Procedure (LAP); Issue Date 7/17/2005. *Tech. Rep.* **2008**.

(9)  Sluiter, A. Determination of Insoluble Solids in Pretreated Biomass Material: Laboratory Analytical Procedure (LAP). *Tech. Rep.* **2008**.

(10) Sluiter, A. Determination of Total Solids in Biomass and Total Dissolved Solids in Liquid Process Samples: Laboratory Analytical Procedure (LAP). *Tech. Rep.* **2008**.

(11) Seo, D. K.; Park, S. S.; Hwang, J.; Yu, T.-U. Study of the Pyrolysis of Biomass Using Thermo-Gravimetric Analysis (TGA) and Concentration Measurements of the Evolved Species. *J. Anal. Appl. Pyrolysis* **2010**, *89* (1), 66–73. https://doi.org/10.1016/j.jaap.2010.05.008.

(12) Anca-Couce, A.; Tsekos, C.; Retschitzegger, S.; Zimbardi, F.; Funke, A.; Banks, S.; Kraia, T.; Marques, P.; Scharler, R.; de Jong, W.; Kienzl, N. Biomass Pyrolysis TGA Assessment with an International Round Robin. *Fuel* **2020**, *276*, 118002. https://doi.org/10.1016/j.fuel.2020.118002.

(13) Xiao, R.; Yang, W.; Cong, X.; Dong, K.; Xu, J.; Wang, D.; Yang, X. Thermogravimetric Analysis and Reaction Kinetics of Lignocellulosic Biomass Pyrolysis. *Energy* **2020**, *201*, 117537. https://doi.org/10.1016/j.energy.2020.117537.

(14) Ren, S.; Lei, H.; Wang, L.; Bu, Q.; Chen, S.; Wu, J. Thermal Behaviour and Kinetic Study for Woody Biomass Torrefaction and Torrefied Biomass Pyrolysis by TGA. *Biosyst. Eng.* **2013**, *116* (4), 420–426. https://doi.org/10.1016/j.biosystemseng.2013.10.003.

(15) Stenseng, M.; Jensen, A.; Dam-Johansen, K. Investigation of Biomass Pyrolysis by Thermogravimetric Analysis and Differential Scanning Calorimetry. *J. Anal. Appl. Pyrolysis* **2001**, *58–59*, 765–780. https://doi.org/10.1016/S0165-2370(00)00200-X.

(16) Quan, C.; Gao, N.; Song, Q. Pyrolysis of Biomass Components in a TGA and a Fixed-Bed Reactor: Thermochemical Behaviors, Kinetics, and Product Characterization. *J. Anal. Appl. Pyrolysis* **2016**, *121*, 84–92. https://doi.org/10.1016/j.jaap.2016.07.005.

(17) Brillard, A.; Brilhac, J.-F. Improved Relationships between Kinetic Parameters Associated with Biomass Pyrolysis or Combustion. *Bioresour. Technol.* **2021**, *342*, 126053. https://doi.org/10.1016/j.biortech.2021.126053.

(18) Slopiecka, K.; Bartocci, P.; Fantozzi, F. Thermogravimetric Analysis and Kinetic Study of Poplar Wood Pyrolysis. *Energy Solut. Sustain. World - Proc. Third Int. Conf. Appl. Energy May 16-18 2011 - Perugia Italy* **2012**, *97*, 491–497. https://doi.org/10.1016/j.apenergy.2011.12.056.

(19) Saldarriaga, J. F.; Aguado, R.; Pablos, A.; Amutio, M.; Olazar, M.; Bilbao, J. Fast Characterization of Biomass Fuels by Thermogravimetric Analysis (TGA). *Fuel* **2015**, *140*, 744–751. https://doi.org/10.1016/j.fuel.2014.10.024.

(20) Szabó, Z. G.; Bérces, T. The Transition State and the Arrhenius' Parameters. **1968**, *57* (3_6), 113–122. https://doi.org/10.1524/zpch.1968.57.3_6.113.

(21) Galwey, A. K.; Brown, M. E. Application of the Arrhenius Equation to Solid State Kinetics: Can This Be Justified? *Thermochim. Acta* **2002**, *386* (1), 91–98. https://doi.org/10.1016/S0040-6031(01)00769-9.

(22) Pilling, M. J.; Seakins, P. W. *Reaction Kinetics*; Oxford University Press: Oxford [England] ;, 1995.

(23) Anca-Couce, A.; Berger, A.; Zobel, N. How to Determine Consistent Biomass Pyrolysis Kinetics in a Parallel Reaction Scheme. *Fuel* **2014**, *123*, 230–240. https://doi.org/10.1016/j.fuel.2014.01.014.

(24) Ding, Y.; Zhang, J.; He, Q.; Huang, B.; Mao, S. The Application and Validity of Various Reaction Kinetic Models on Woody Biomass Pyrolysis. *Energy* **2019**, *179*, 784–791. https://doi.org/10.1016/j.energy.2019.05.021.

(25) Agarwal, R. K. On the Use of the Arrhenius Equation to Describe Cellulose and Wood Pyrolysis. *Thermochim. Acta* **1985**, *91*, 343–349. https://doi.org/10.1016/0040-6031(85)85227-8.

(26) Mandapati, R. N.; Ghodke, P. K. Kinetics of Pyrolysis of Cotton Stalk Using Model-Fitting and Model-Free Methods. *Fuel* **2021**, *303*, 121285. https://doi.org/10.1016/j.fuel.2021.121285.

(27) Dhyani, V.; Bhaskar, T. Kinetic Analysis of Biomass Pyrolysis. In *Waste Biorefinery*; Elsevier, 2018; pp 39–83. https://doi.org/10.1016/B978-0-444-63992-9.00002-1.

(28) Phuakpunk, K.; Chalermsinsuwan, B.; Assabumrungrat, S. Pyrolysis Kinetic Parameters Investigation of Single and Tri-Component Biomass: Models Fitting via Comparative Model-Free Methods. *Renew. Energy* **2022**, *182*, 494–507. https://doi.org/10.1016/j.renene.2021.10.011.

(29) Mishra, G.; Bhaskar, T. Non Isothermal Model Free Kinetics for Pyrolysis of Rice Straw. *Bioresour. Technol.* **2014**, *169*, 614–621. https://doi.org/10.1016/j.biortech.2014.07.045.

(30) Baroni, É. de G.; Tannous, K.; Rueda-Ordóñez, Y. J.; Tinoco-Navarro, L. K. The Applicability of Isoconversional Models in Estimating the Kinetic Parameters of Biomass Pyrolysis. *J. Therm. Anal. Calorim.* **2016**, *123* (2), 909–917. https://doi.org/10.1007/s10973-015-4707-9.

(31) Vyazovkin, S. *Isoconversional Kinetics of Thermally Stimulated Processes*; Springer International Publishing: Cham, 2015. https://doi.org/10.1007/978-3-319-14175-6.

(32) Trache, D.; Abdelaziz, A.; Siouani, B. A Simple and Linear Isoconversional Method to Determine the Pre-Exponential Factors and the Mathematical Reaction Mechanism Functions. *J. Therm. Anal. Calorim.* **2017**, *128* (1), 335–348. https://doi.org/10.1007/s10973-016-5962-0.

(33) Jagtap, A.; Kalbande, S. R. Investigation on Pyrolysis Kinetics and Thermodynamic Parameters of Soybean Straw: A Comparative Study Using Model-Free Methods. *Biomass Convers. Biorefinery* **2022**. https://doi.org/10.1007/s13399-021-02228-9.

(34) Burra, K. R. G.; Gupta, A. K. Modeling of Biomass Pyrolysis Kinetics Using Sequential Multi-Step Reaction Model. *Fuel* **2019**, *237*, 1057–1067. https://doi.org/10.1016/j.fuel.2018.09.097.

(35) Huang, Y. F.; Kuan, W. H.; Chiueh, P. T.; Lo, S. L. A Sequential Method to Analyze the Kinetics of Biomass Pyrolysis. *Bioresour. Technol.* **2011**, *102* (19), 9241–9246. https://doi.org/10.1016/j.biortech.2011.07.015.

(36) Wang, S.; Lin, H.; Ru, B.; Dai, G.; Wang, X.; Xiao, G.; Luo, Z. Kinetic Modeling of Biomass Components Pyrolysis Using a Sequential and Coupling Method. *Fuel* **2016**, *185*, 763–771. https://doi.org/10.1016/j.fuel.2016.08.037.

(37) Emiola-Sadiq, T.; Zhang, L.; Dalai, A. K. Thermal and Kinetic Studies on Biomass Degradation via Thermogravimetric Analysis: A Combination of Model-Fitting and Model-Free Approach. *ACS Omega* **2021**, *6* (34), 22233–22247. https://doi.org/10.1021/acsomega.1c02937.

(38) Vikram, S.; Rosha, P.; Kumar, S. Recent Modeling Approaches to Biomass Pyrolysis: A Review. *Energy Fuels* **2021**, *35* (9), 7406–7433. https://doi.org/10.1021/acs.energyfuels.1c00251.

(39) Papari, S.; Hawboldt, K. A Review on the Pyrolysis of Woody Biomass to Bio-Oil: Focus on Kinetic Models. *Renew. Sustain. Energy Rev.* **2015**, *52*, 1580–1595. https://doi.org/10.1016/j.rser.2015.07.191.

(40) White, J. E.; Catallo, W. J.; Legendre, B. L. Biomass Pyrolysis Kinetics: A Comparative Critical Review with Relevant Agricultural Residue Case Studies. *J. Anal. Appl. Pyrolysis* **2011**, *91* (1), 1–33. https://doi.org/10.1016/j.jaap.2011.01.004.

(41) Koga, N.; Vyazovkin, S.; Burnham, A. K.; Favergeon, L.; Muravyev, N. V.; Pérez-Maqueda, L. A.; Saggese, C.; Sánchez-Jiménez, P. E. ICTAC Kinetics Committee Recommendations for Analysis of Thermal Decomposition Kinetics. *Thermochim. Acta* **2023**, *719*, 179384. https://doi.org/10.1016/j.tca.2022.179384.

(42) Vyazovkin, S.; Burnham, A. K.; Criado, J. M.; Pérez-Maqueda, L. A.; Popescu, C.; Sbirrazzuoli, N. ICTAC Kinetics Committee Recommendations for Performing Kinetic Computations on Thermal Analysis Data. *Thermochim. Acta* **2011**, *520* (1), 1–19. https://doi.org/10.1016/j.tca.2011.03.034.

(43) Vyazovkin, S.; Burnham, A. K.; Favergeon, L.; Koga, N.; Moukhina, E.; Pérez-Maqueda, L. A.; Sbirrazzuoli, N. ICTAC Kinetics Committee Recommendations for Analysis of Multi-Step Kinetics. *Thermochim. Acta* **2020**, *689*, 178597. https://doi.org/10.1016/j.tca.2020.178597.

(44) Atkins, A.; Bignal, K. L.; Zhou, J. L.; Cazier, F. Profiles of Polycyclic Aromatic Hydrocarbons and Polychlorinated Biphenyls from the Combustion of Biomass Pellets. *Chemosphere* **2010**, *78* (11), 1385–1392. https://doi.org/10.1016/j.chemosphere.2009.12.065.

(45) Zhang, H.; Zhang, X.; Wang, Y.; Bai, P.; Hayakawa, K.; Zhang, L.; Tang, N. Characteristics and Influencing Factors of Polycyclic Aromatic Hydrocarbons Emitted from Open Burning and Stove Burning of Biomass: A Brief Review. *Int. J. Environ. Res. Public. Health* **2022**, *19* (7). https://doi.org/10.3390/ijerph19073944.

(46) Zhou, H.; Wu, C.; Meng, A.; Zhang, Y.; Williams, P. T. Effect of Interactions of Biomass Constituents on Polycyclic Aromatic Hydrocarbons (PAH) Formation during Fast Pyrolysis. *J. Anal. Appl. Pyrolysis* **2014**, *110*, 264–269. https://doi.org/10.1016/j.jaap.2014.09.007.

(47) Vispute, T. P.; Zhang, H.; Sanna, A.; Xiao, R.; Huber, G. W. Renewable Chemical Commodity Feedstocks from Integrated Catalytic Processing of Pyrolysis Oils. *Science* **2010**, *330* (6008), 1222–1227. https://doi.org/10.1126/science.1194218.

(48) De, S.; Saha, B.; Luque, R. Hydrodeoxygenation Processes: Advances on Catalytic Transformations of Biomass-Derived Platform Chemicals into Hydrocarbon Fuels. *Bioresour. Technol.* **2015**, *178*, 108–118. https://doi.org/10.1016/j.biortech.2014.09.065.

(49) Gea, S.; Hutapea, Y. A.; Piliang, A. F. R.; Pulungan, A. N.; Rahayu, R.; Layla, J.; Tikoalu, A. D.; Wijaya, K.; Saputri, W. D. A Comprehensive Review of Experimental Parameters in Bio-Oil Upgrading from Pyrolysis of Biomass to Biofuel Through Catalytic Hydrodeoxygenation. *BioEnergy Res.* **2023**, *16* (1), 325–347. https://doi.org/10.1007/s12155-022-10438-w.

(50) Naqvi, S. R.; Khoja, A. H.; Ali, I.; Naqvi, M.; Noor, T.; Ahmad, A.; Luque, R.; Amin, N. A. S. Recent Progress in Catalytic Deoxygenation of Biomass Pyrolysis Oil Using Microporous Zeolites for Green Fuels Production. *Fuel* **2023**, *333*, 126268. https://doi.org/10.1016/j.fuel.2022.126268.

# Chapter 3 Reaction kinetics of biomass pyrolysis

*In this chapter, the difference in nature of reaction phenomena at slow heating rates (slow pyrolysis condition) and faster heating rates (approaching fast pyrolysis conditions) is expound upon. The effect of heterogeneity inherent in composition of biomass and the effect it has on reactor-process design considerations and product yield prediction is then discussed. The existing approaches used for determining kinetic parameters, their historical development, philosophies, applicability, and limitations for biomass pyrolysis are then critically reviewed. Model-free approach has been used to gain some insights into nature of pyrolysis reaction. We show how they fail to capture both the compositional heterogeneity and difference in nature of slow and fast pyrolysis which might lead to critical errors in modelling and designing fast pyrolysis reactor-process.*

Study of reaction kinetics is the study of rate of reaction and its parameterization.[1] The rate of reaction is usually the measure of rate of mass change or concentration change and the parameterization is terms of activation energy, frequency factor and order of reaction related by Arrhenius form. Fair amount of literature and consensus is available on slow pyrolysis [2–7], whereas fast pyrolysis remains relatively less explored.[8–13]

Once temperature dependence is established through a series of different linear heating rates then isoconversional rate (linear/constant heating rate) can be determined by parameterization and combination of equations 2.1 and 2.2, [1]

$$\ln\left(\frac{d\alpha}{dt}\right)_{\alpha,i} = \ln[A_\alpha f(\alpha)] - \frac{E_a}{RT_{\alpha,i}}$$

3.1

Equation 3.1 is the base equation for Friedman method[14]

Equation 3.1 can be used to check whether $E_a$ varies significantly with respect to conversion($\alpha$). If it doesn't – it's a single step reaction. If $E_a$ varies significantly then it is reaction having two or more steps with different activation energies. Looking at results (refer figures 3.1 – 3.6) for biomass pyrolysis a high variability is observed, suggesting multitude of reactions with varying activation energies. What is meaning of variable activation energy? What is its physical significance? These questions do not have satisfactory explanations within the classical schema of transition state theory and Arrhenius parameters for rate estimation. Nevertheless, occurrence of multistep processes hasn't inhibited authors from using fair approximations at slow heating rates within close range to describe lumped reaction kinetics using multiple single step kinetic equations. When the heating rate range is low and the difference between multiple heating rates is low, straight line lumped assumptions can be

valid. However, when the heating range is wide and the difference between heating rates is high (extrapolating slow pyrolysis kinetics to fast pyrolysis condition), the linearity is absent and such assumptions do not hold true.Another approach that is sometimes suggested is when the number of steps is known and inter relation between them i.e. the mechanism is known, then multi-step model fitting would certainly secure best possible solution[15]. However, for biomass fast pyrolysis this mechanism and the number of steps is not completely known, although work has been performed in this regard by some groups.[16–18]

The first use of iso-conversional method was in 1925 by[19,20]. Mass loss data was fitted to an empirical equation under isothermal conditions.

$$\log t = \frac{Q}{T} - F(w)$$

3.2

$$w \rightarrow mass\ loss\ in\ \%\ of\ the\ initial\ value;\ t$$
$$\rightarrow time\ to\ reach\ the\ extent\ of\ w\ conversion;\ Q$$
$$\rightarrow material\ constant\ which\ is\ temperature\ dependent$$

The slope of log t v/s $T^{-1}$ is expected to be a straight line

The basic kinetic equation can be written as,

$$\frac{d\alpha}{dt} = A \times exp^{\left[\frac{-E_a}{RT}\right]} \times f(\alpha)$$

3.3

Integrating equation 3.3 for isothermal conditions,

$$g(\alpha) \equiv \int_0^\alpha \frac{d\alpha}{f(\alpha)} = A \times exp^{\left[\frac{-E_a}{RT}\right]} \times t$$

3.4

$$g(\alpha)\ is\ the\ integral\ form\ of\ reaction\ mdoel$$

Solving equation 3.4 for 't' and taking decimal log gives,

$$\log t = \frac{E}{2.303RT} - \log\left[\frac{g(\alpha)}{A}\right]$$

3.5

For any constant value of α, the log term in equation 3.5 will be a constant. Therefore, $E_a$ can be determined from the slope of log t vs $T^{-1}$ without identifying the form of reaction model. An assumption here is that, so long as the total mass loss in percentage is independent of temperature, a constant value of 'w' is equivalent to a constant value of α. In case of biomass

pyrolysis, the rate of mass loss is a function of conversion α. The dα/dt values are different at different temperatures and vary over temperature ranges. This is exemplified in particular by the fact that at slower heating rate, the deviations are not as significant for isoconversional predictions as they are in case of higher heating rates. In the case when temperature is low and the heating rate is very gradual/slow, i.e. ΔT is low and Δt is high, then the assumption that mass loss in percentage is independent of temperature can be considered sensible. This assumption is held throughout isoconversional methods including FWO approach and perhaps foreshadows the pitfalls of extending isoconversional principle over wide heating rate ranges (slow to fast). Another assumption common to all Isoconversional methods is that at a specific (α,t) point, the rate of reaction is a function of temperature only. We see later on, how extending this assumption to biomass fast pyrolysis can lead to erroneous results as biomass fast pyrolysis reaction is function of its composition as well.}[21]

Comparing equations 3.2 and 3.5, it can be suggested that $Q = \frac{E}{2.303}$ $and$ $f(w) = \log\left[\frac{g(\alpha)}{A}\right]$

It is of significance to note that Kujirai and Akahira (1925), later rediscovered by Dakin (1948), both bypassed the need for models in kinetic calculations as they were both dealing with decomposition of complex materials, i.e. materials that are nearly impossible to represent adequately using models.[1]

Earlier works shows that isocoversional methods were used also for isothermal kinetics, albeit with approximations[22,23]. Isothermal kinetics have been mostly dealt with using model-fitting approach. Development and proliferation of high accuracy and high fidelity TGA machines led to generation of non-isothermal data with linear heating rates. Isocoversional methods were rediscovered in a way to gain insights into non-isothermal kinetics from TGA data. [24]

The first isoconversional methods proposed for treatment of non-isothermal kinetics was in 1960s by Friedman[14] (equation 3.1) (differential method) and integral methods of Ozawa Flynn and Wall[25].

From equation 3.1, for any value of α, Eα is estimated from slope of a plot of

$$\ln\left(\frac{d\alpha}{dt}\right)_{\alpha,i} v/s \frac{1}{T_{\alpha,i}}$$

For integral isoconversional methods, integrating equation 3.3 yields,

$$g(\alpha) = A \int_0^t \left(e^{\left(\frac{-Ea}{RT}\right)}\right) dt$$

3.6

Raising temperature at constant heating rate,

$$T = T_0 + \beta \times t$$

3.7

Replacing integration over time with integration over temperature,,

$$g(\alpha) = \frac{A}{\beta} \int_{T_0}^{T} \left( e^{\left( \frac{-E}{RT} \right)} \right) dT \equiv \frac{A}{\beta} I[E, T]$$

3.8

The temperature integral here has no analytical solution.[15] Various optimization methods can be found in literature to obtain the best approximation of the temperature integral.[26,27] However, that is a mathematical rigorous process which does not greatly contribute to the understanding of pyrolysis mechanism or for obtaining kinetics results suitable for reactor design and process control. As such the optimization techniques won't be discussed in this thesis.

Some of the earlier applications of isoconversional or model free approaches are found in the works of Kissinger, Akahira, Sunose, Doyle, Flynn, Wall, Ozawa and others.[28–32] A review of these papers brings forth some of the latent aspects and assumptions embedded in these model-free approaches. They are discussed below.

Kissinger (1957)[31] studied the relationship between differential temperature and reaction rate. The heating rates were constant and the materials used to study were magnesite, calcite and brucite. A major takeaway from this work, relevant for us in current times with the purpose of gaining kinetic insights into reaction for the sake of designing reactors is the assumption that 'the temperature of maximum deflection in differential thermal analysis is also the temperature at which the reaction rate is maximum'. A detailed discussion of the validity of this assumption is given the paper. This assumption for our case, gives us the time and temperature at which maximum rate of reaction for biomass pyrolysis is achieved. For achieving fast pyrolysis conditions, this is important; and its implications in reactor design are discussed in chapter 5.

Doyle (1961, 1962)[22,23] carried out studies to check the potential of Thermogravimetric analyser in studying thermal decomposition of octamethylcyclotetrasiloxane (1961, organosilicon compound) and polytertrafluoroethylene (1962, similar to Teflon). Useful takeaway from the work were to ensure that sample temperature is considered for kinetic calculations rather than reactor temperature and to ensure enough dwell time (or rapid data point extraction) at each temperature. The inaccuracies associated with using isoconversional methods to calculate kinetic data over wide heating rate range is touched upon in this paper. The works were however carried out at single heating rate of 3°C/min which is really slow compared to fast pyrolysis of biomass case.

Friedman (1964)[14] studied the thermal degradation of glass reinforced phenol-formaldehyde (phenolic resin) at multiple slow heating rates (50, 100, 180 and 360 °C/hr). We see that the early use of model-free approach arose from studying large samples of complex cross-linked polymers over long time scales. Over such long time scales and slow heating rates, the assumption of 'w' being independent of T temperature perhaps holds true, at least for the sake of mathematical treatment. An important observation made in this work is the tendency of curves being displaced to higher temperatures with increased heating rate, as would be predicted theory. We see this in our multiple heating rate isoconversional graphs for biomass samples. It is important to note that the polymer being studied was still homogenous (unlike biomass which is heterogeneous – composed of different cross-linked polymers) and yet showed a fifth-order dependence, which the author attributed to the reaction complexity rather than any real physical significance. The triviality of kinetic parameters from this approach for Arrhenius type kinetic interpretation was underlined in some of these early papers. The advantage of this approach is the possibility of activation energy calculation for the main lumped degradation process without any knowledge of the form of the kinetic equation. It is also useful for deriving semi-empirical rate law.

Coats and Redfern (1964)[33] approach is based on assuming the order of reaction and performing best fit calculations. Summarizing briefly, for a reaction expressed as

$$\frac{d\alpha}{dt} = k(1 - \alpha)^n$$

3.9

Where α: fraction of reactant decomposed at time t; *n*: order of reaction and *k*: rate constant of the reaction.

The plot of either $\log_{10}\left[\frac{1-(1-\alpha)^{1-n}}{T^2(1-n)}\right]$ against $\frac{1}{T}$

Or, where n= 1, $\log_{10}\left[\frac{-\log_{10}(1-\alpha)}{T^2}\right]$ against $\frac{1}{T}$

Should result in a straight line of slope –E/2.3R for the correct value of n. A priori knowledge about the order of reaction could make this approach useful. However, despite being used for determining kinetic parameters, this approach has been rightly critiqued by other authors for producing erroneous results.[15] Its validity for biomass pyrolysis relies on a priori knowledge of order of reaction which is absent for the biomass pyrolysis reaction.

[4

Ozawa (1965)[21] delineated the differential approach and integral approach in processing TGA data for calculating kinetic parameters. An approximate integral method was presented to study the decomposition of calcium-oxate into calcium carbonate and carbon monoxide, and

---

[4] The term 'rate constant' is used here instead of 'rate coefficient'. For biomass pyrolysis, the value of K is largely variable over reaction regime and as such the term rate coefficient for 'k' would be more appropriate.

the degradation of nylon-6. The integral method was applied over slow heating hates and long-time scales to perform straight line fits for determining activation energy as is characteristic of model free methods. The most important contribution for biomass pyrolysis would be the limitation of this approach articulated - *"However, if the weight changes in the manner of parallel reactions or consecutive reactions (in other words, if the weight-change is governed by two or more activation energies), the curves of the weight versus the reciprocal absolute temperature at different heating rates cannot be superposed, and the analysis mentioned cannot be applied. This is also the case for the other methods analysing thermogravimetric data."*

This makes it clear that the kinetic parameters data obtained from model-free methods must be treated with caution. This becomes rather exemplified when the calculations are going to be used for training machine learning algorithms or for designing reactors and will have real life consequences. The limitations of model-fitting approach are discussed elsewhere[34,35]

Flynn and Wall (1966)[28] reiterated the need to use several heating rates rather than using a single rate and fitting it based on an often spuriously assumed reaction order. They introduced their model as an alternative to the noise amplified in differential method. Their approach is based on the assumption that A, $f(\alpha)$, and E are independent of T and that A and E are independent of $\alpha$. Use of Doyle's approximation was used in calculations.

J Sestak discussed the thermodynamic aspects and links to kinetic aspects in thermos-physical experiments.[36] He also addressed certain unresolved aspects about non-isothermal kinetics and the consequences of dynamic experiments. The classical kinetic procedures do not satisfactorily describe the reality of heterogeneous reactions. The interdependence of kinetic parameters and ways to resolve them in a manner in order to get meaningful insights into heterogeneous reactions is discussed.[37]

Vyazovkin (1997)[38] justifies the use of Arrhenius equation not only in terms of a rational parametrization, but also its use and physical interpretation, since they are supported by a sound theoretical foundation. Model fitting method produces highly variable kinetic parameters with little reliability or consistency. Also, for a particular reaction, more than one model could satisfy the fit leading to multiple kinetic parameters for same conditions which is highly problematic. As such, Vyazovkin makes the case for model-free method since these methods are not based on an assumption of a reaction model. However, Vyazovkin reiterates the basic assumption of isoconversional methods – the reaction model is not dependent on temperature or heating rate.

It is in this assumption that roots of inapplicability or limitations of isoconversional methods for biomass fast pyrolysis.

As such, we have presented a novel kinetic approach in chapter 4 of the thesis.

## Results and discussion
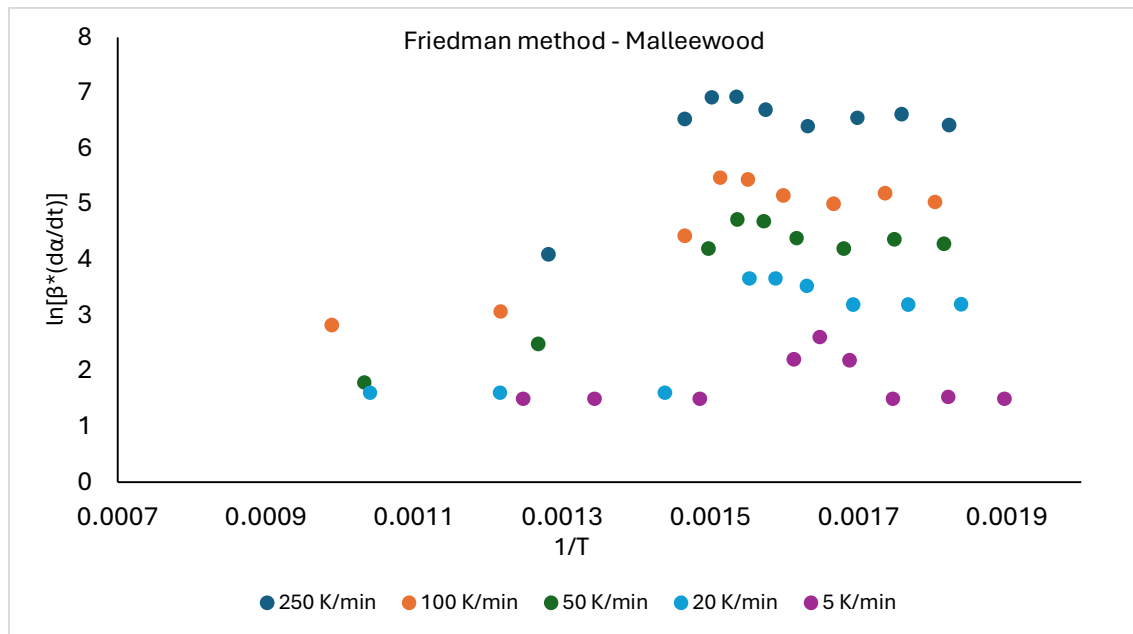


*Figure 3 Representative activation energy distribution for malleewood using Friedman method*
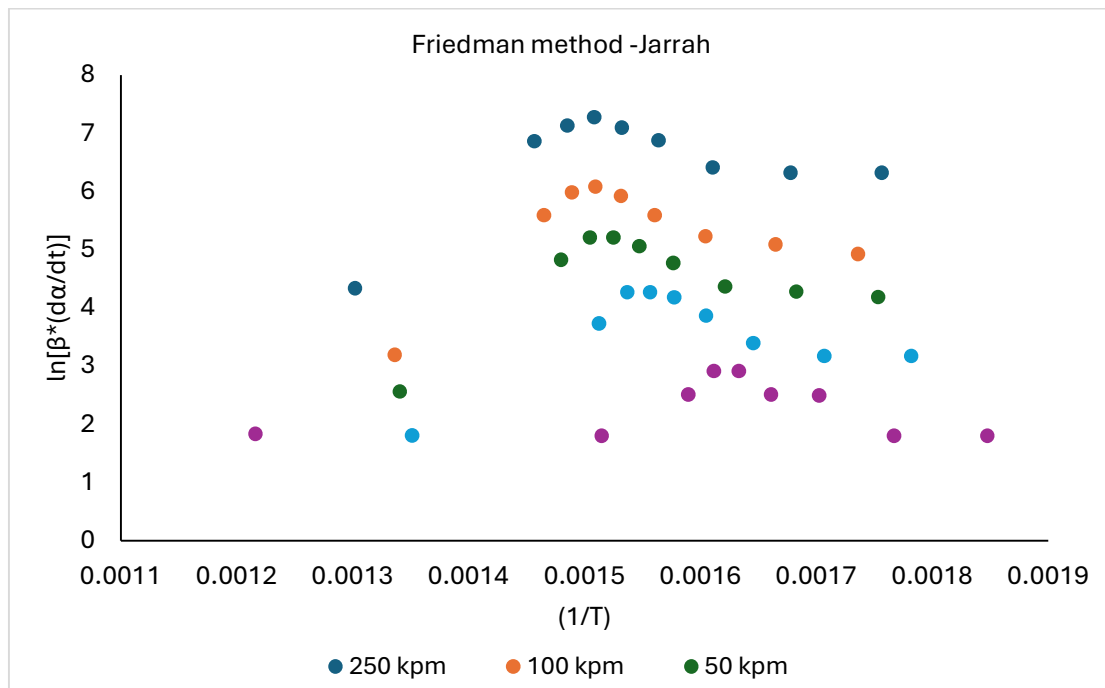


*Figure 4 Activation energy distribution for jarrah using Friedman method*
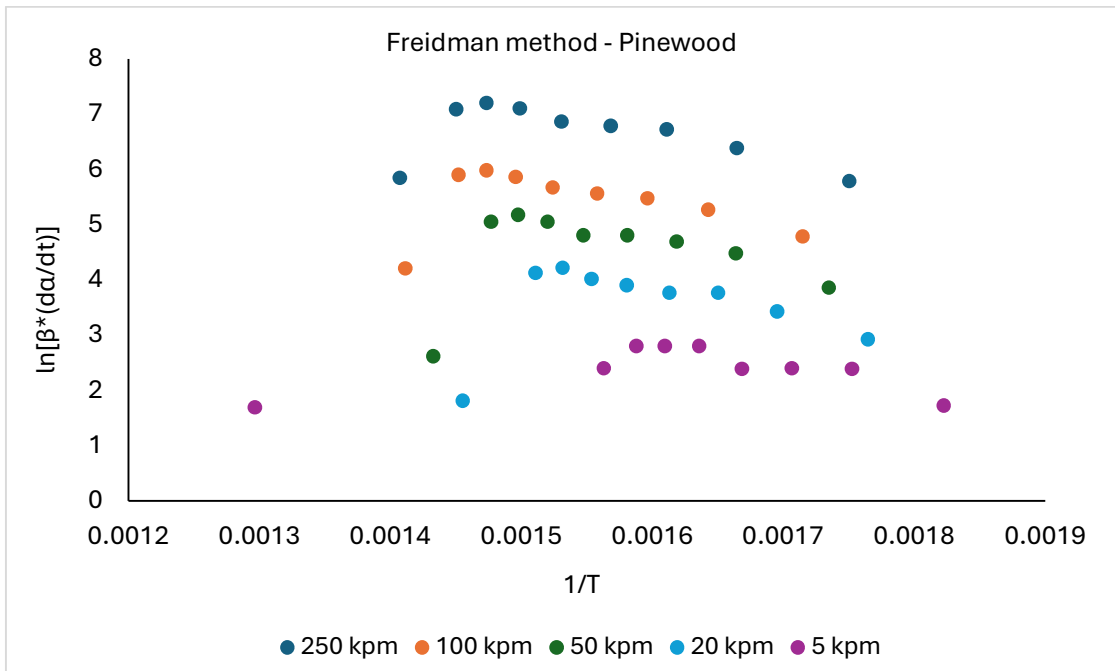
*Figure 5  Activation energy distribution for pinewood using Friedman method*
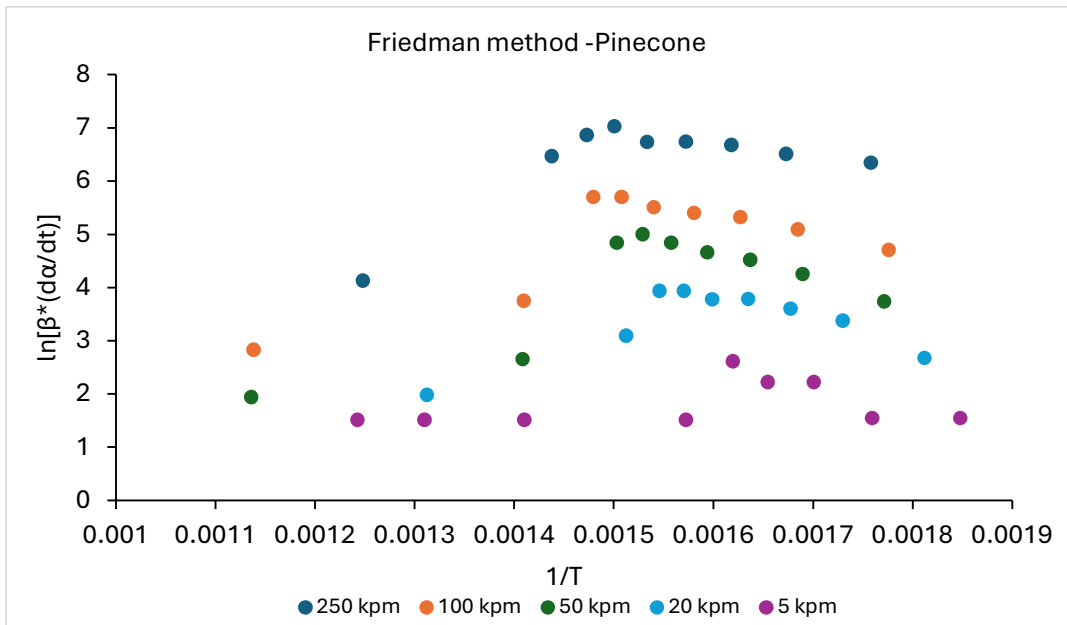


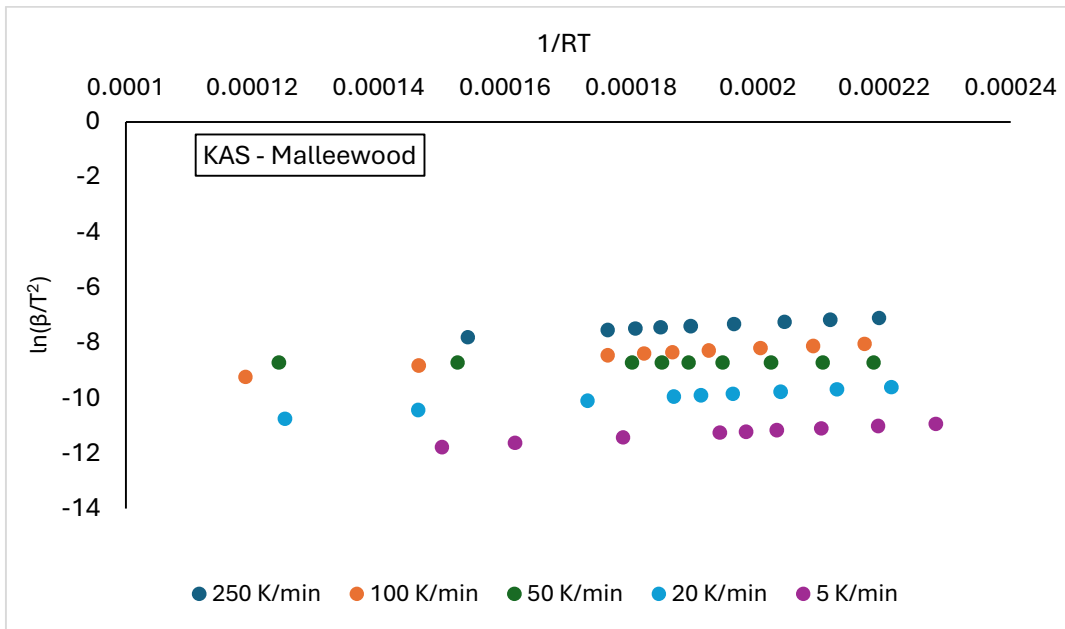*Figure 6 Activation energy distribution for pinecone using Friedman method*

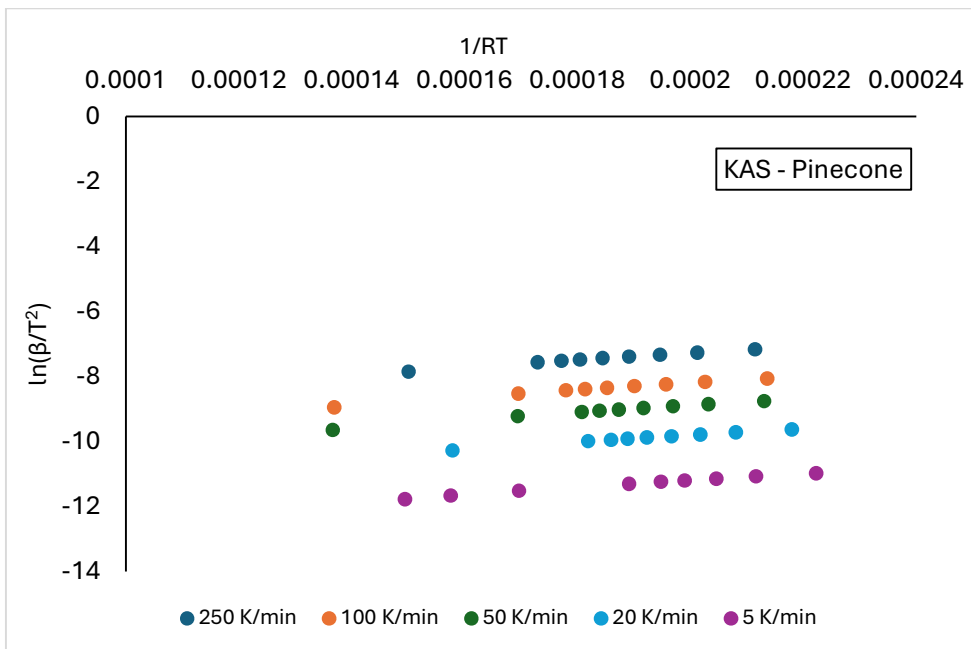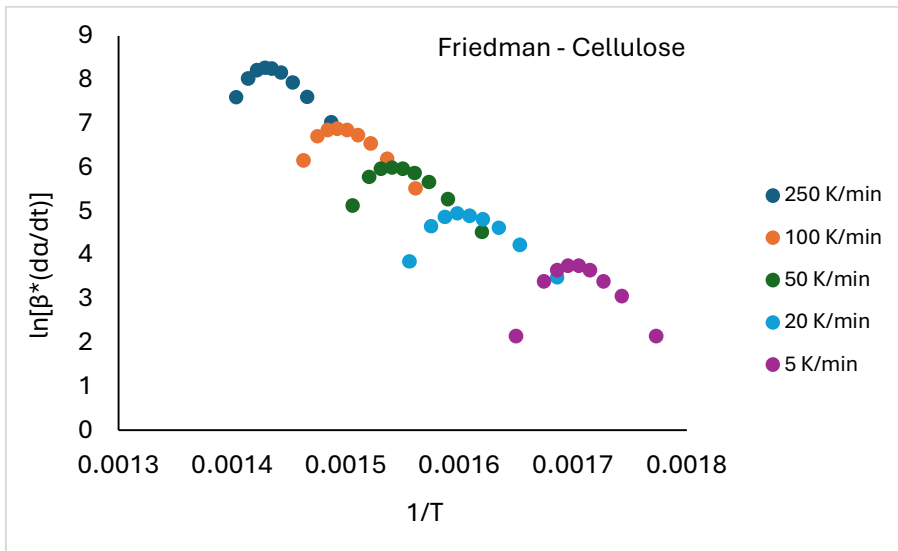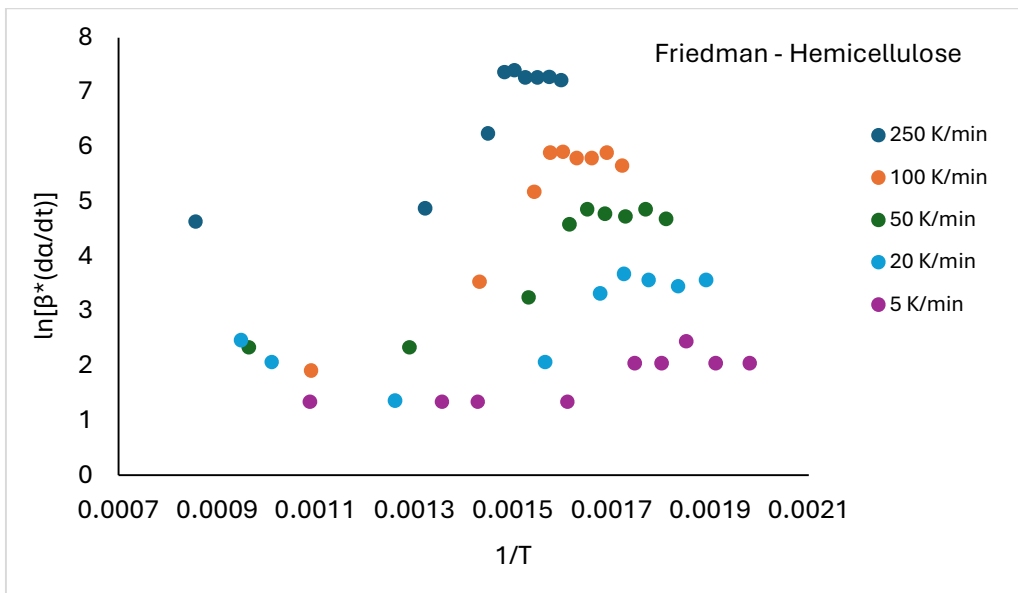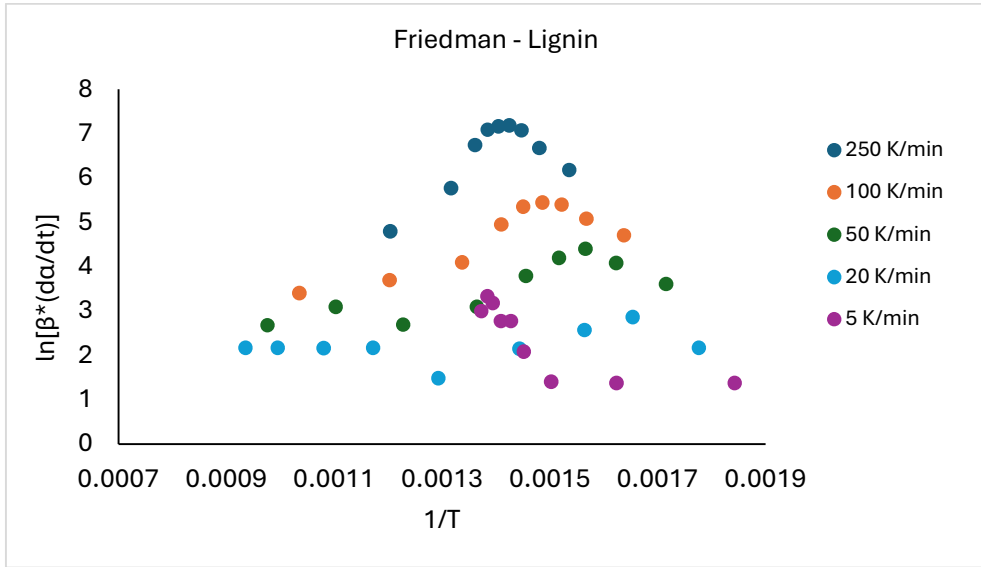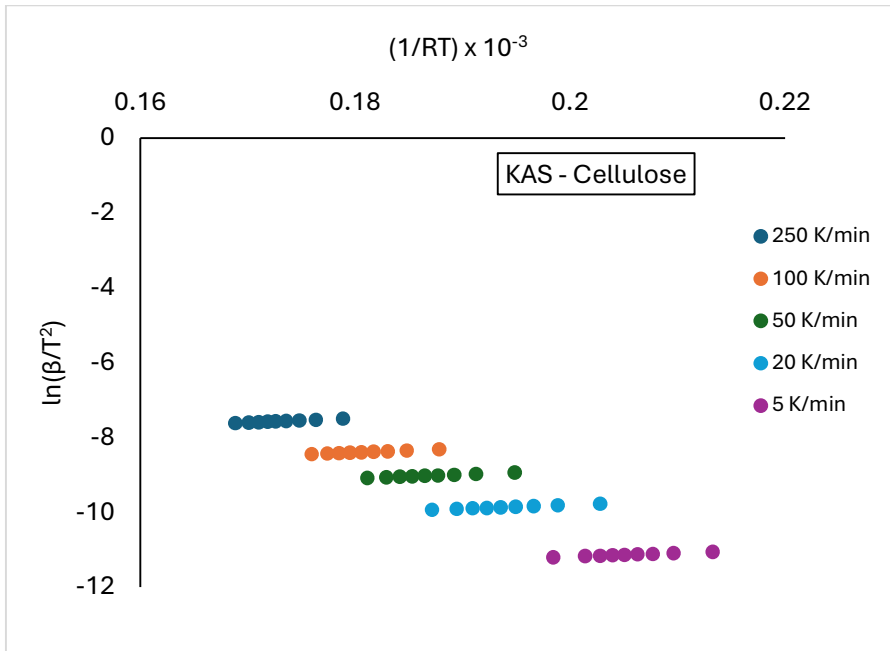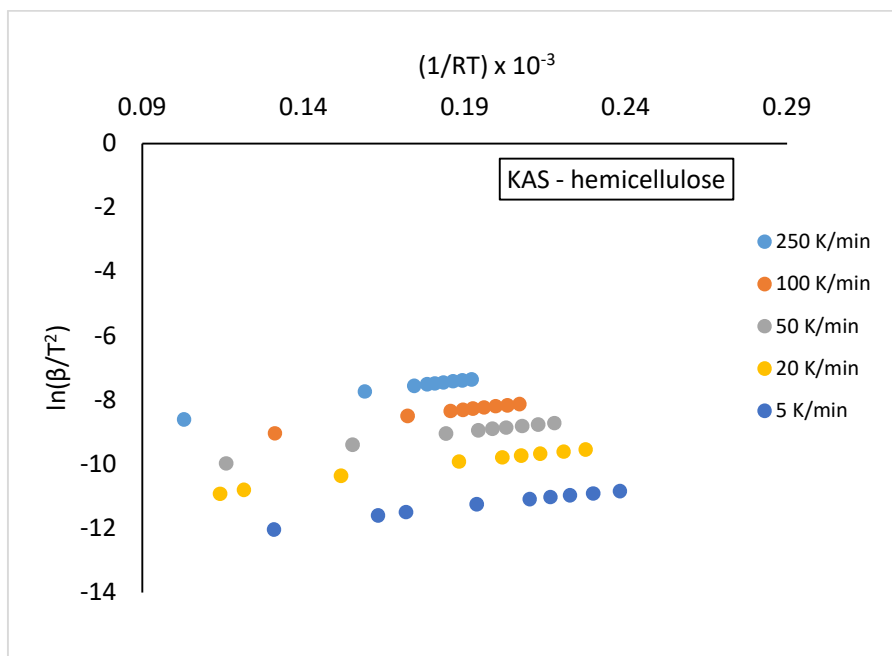*Figure 7 Activation energy distribution for malleewood using Kissinger Akahira Sunose (KAS) method*



*Figure 8 Activation energy distribution for pinecone using (KAS) method*

*Figure 9 Activation energy distribution for cellulose using Friedman method*



*Figure 10 Activation energy distribution for hemicellulose using Friedman method*

*Figure 3.9 Activation energy distribution for lignin using Friedman method*



*Figure 3.10 Activation energy distribution for cellulose using KAS method*

*Figure 3.11 Activation energy distribution for hemicellulose using KAS method*
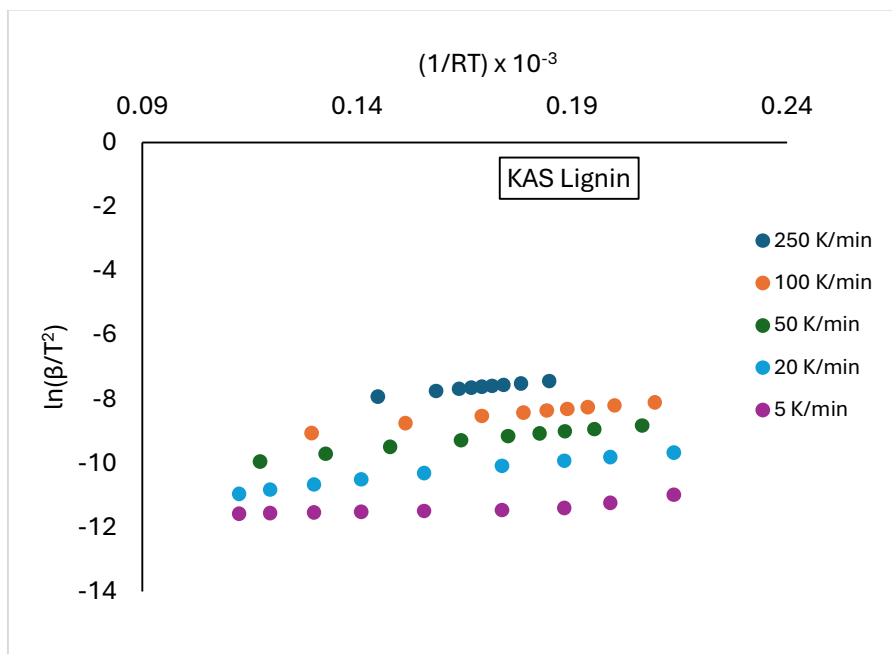


*Figure 3.12 Activation energy distribution for lignin using KAS method*

**Jarrah_1_106_1_ConversionPREDplotKAS**
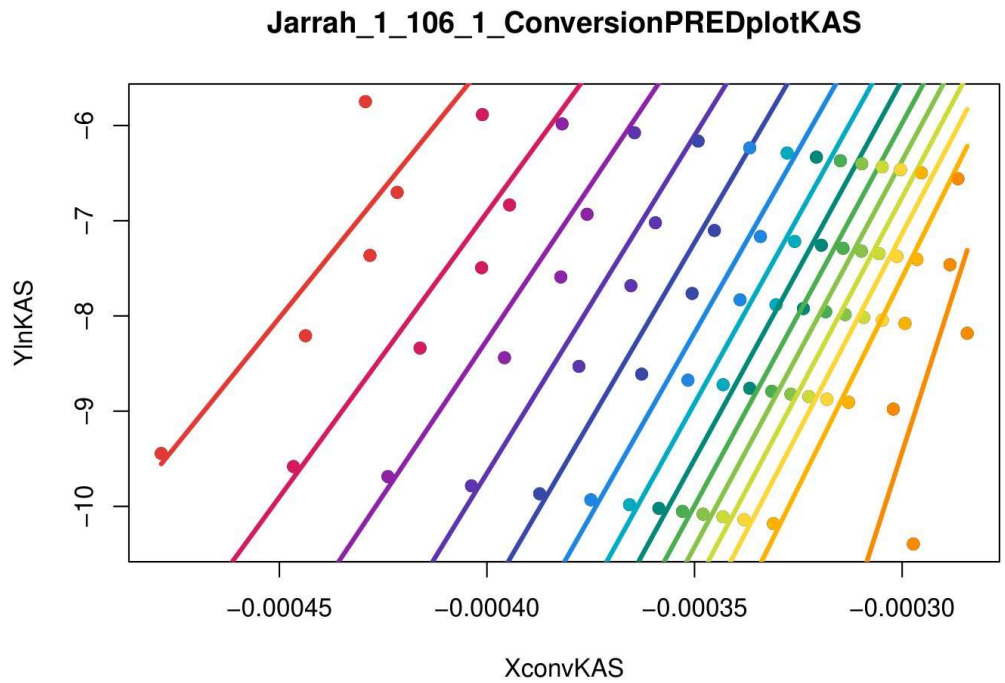
*Figure 3.13 Representative linear fit for slope determination at various conversions using KAS method for Jarrah; particle size 106-150 µm and 1 mg sample size*
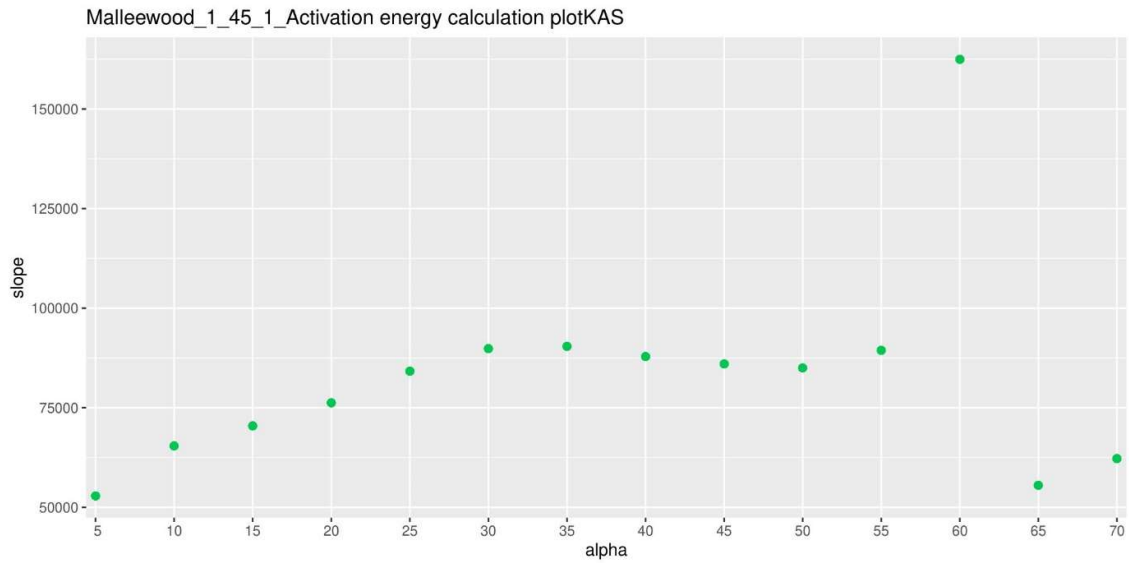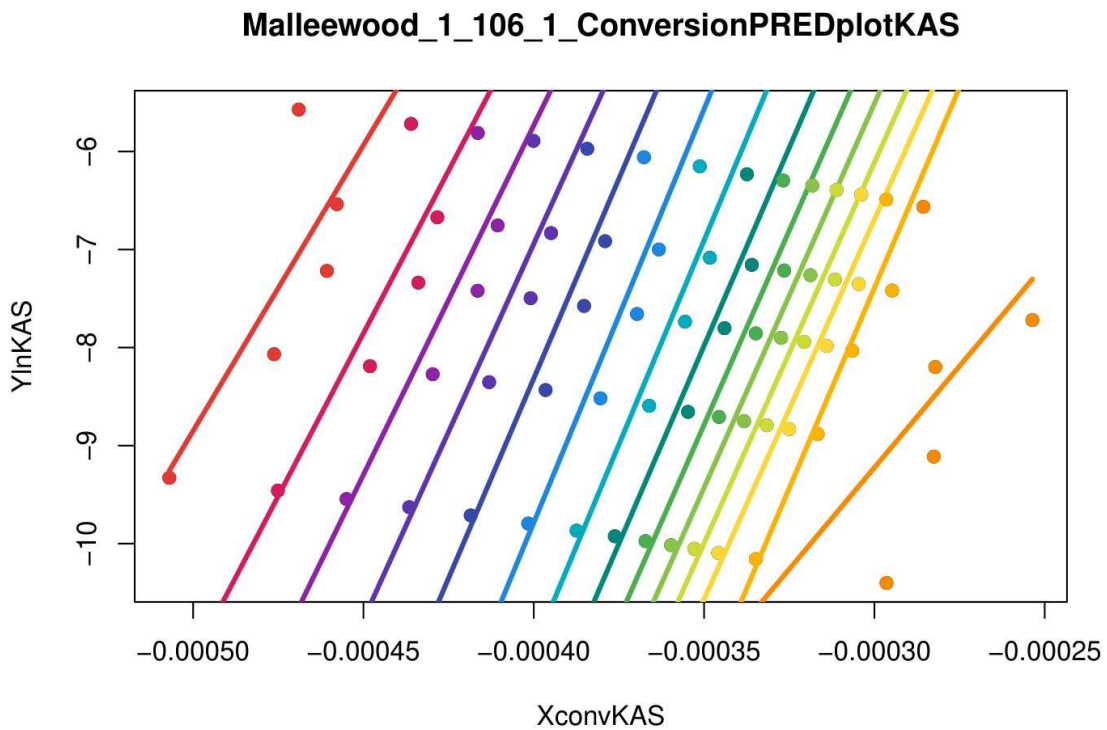


Jarrah_1_106_1_Activation energy calculation plotKAS
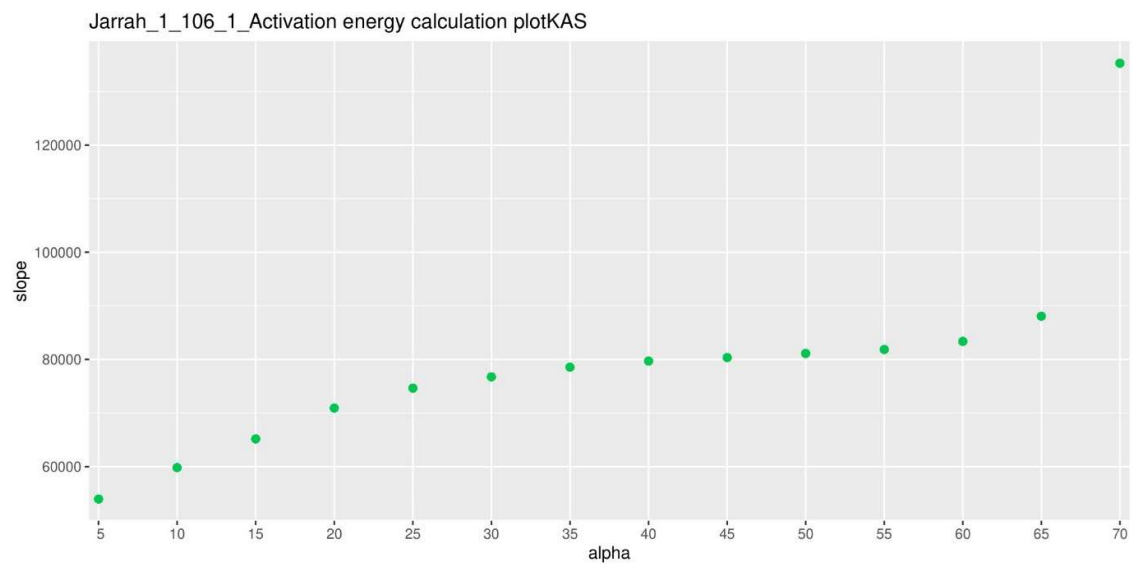
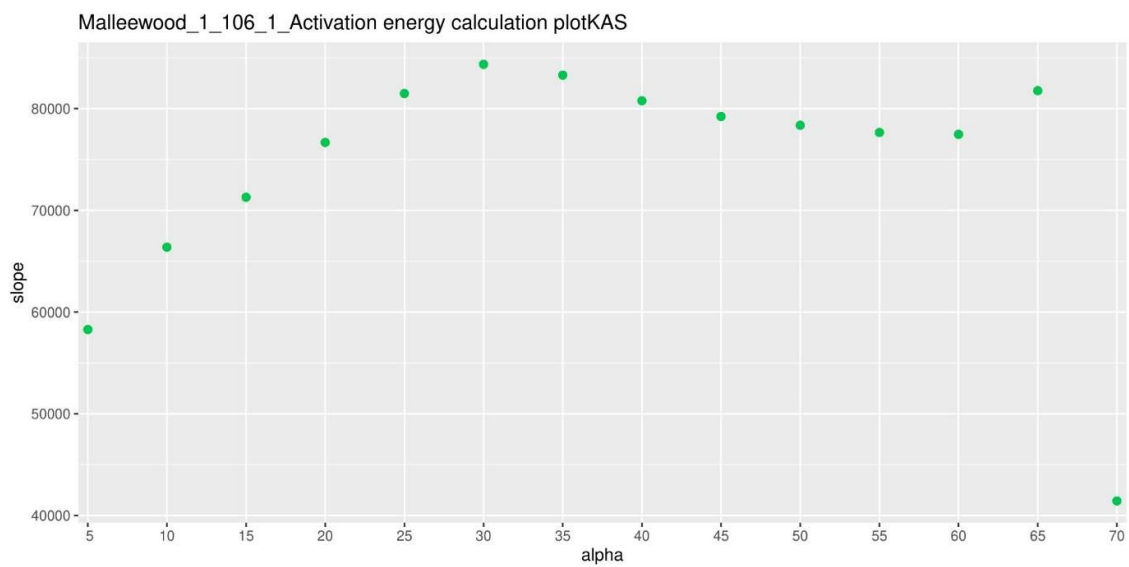*Figure 3.14 Representative activation energy distribution at various conversions using KAS method for Jarrah; particle size 106-150 µm and 1 mg sample size*
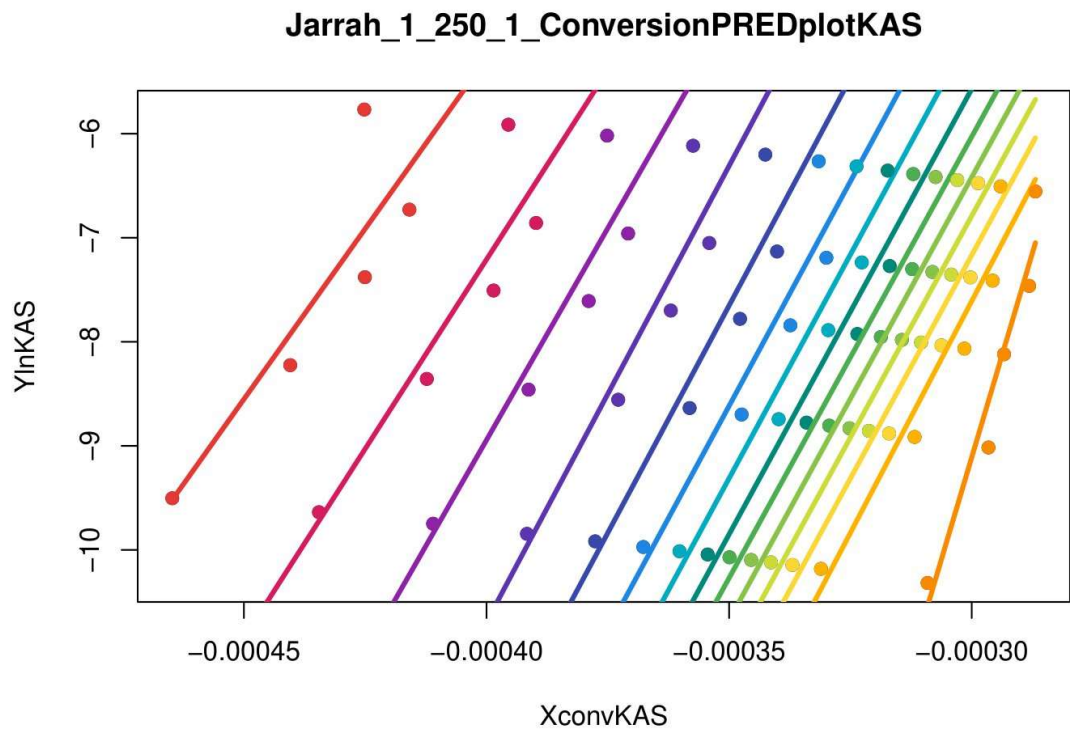
*Figure 3.15 Representative linear fit for slope determination at various conversions using KAS method for Jarrah; particle size 250-300 μm and 1 mg sample size*
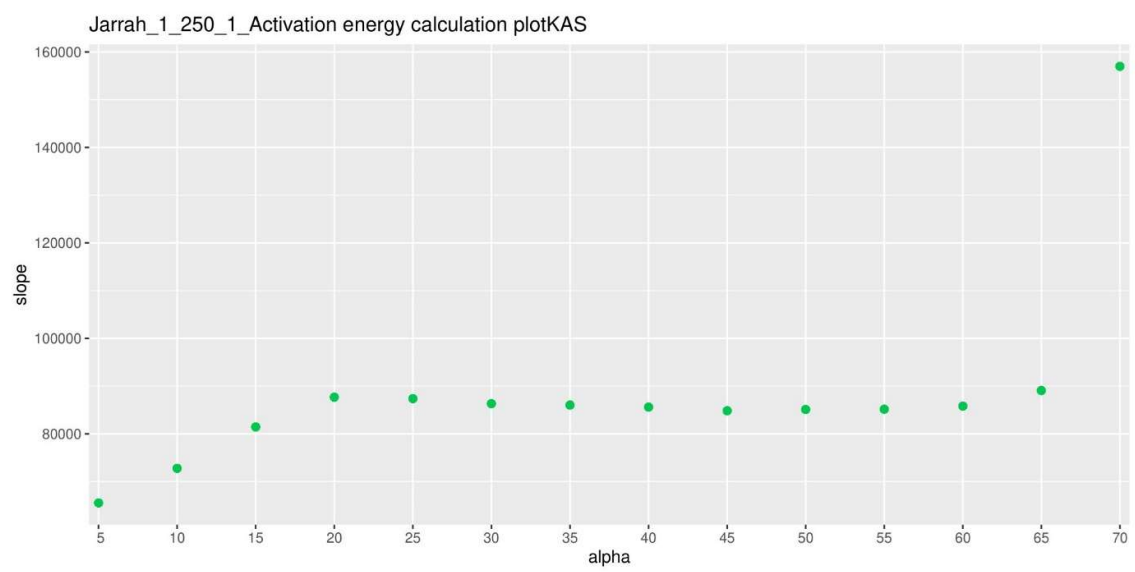


*Figure 3.16 Representative activation energy distribution at various conversions using KAS method for Jarrah; particle size 250-300 μm and 1 mg sample size*
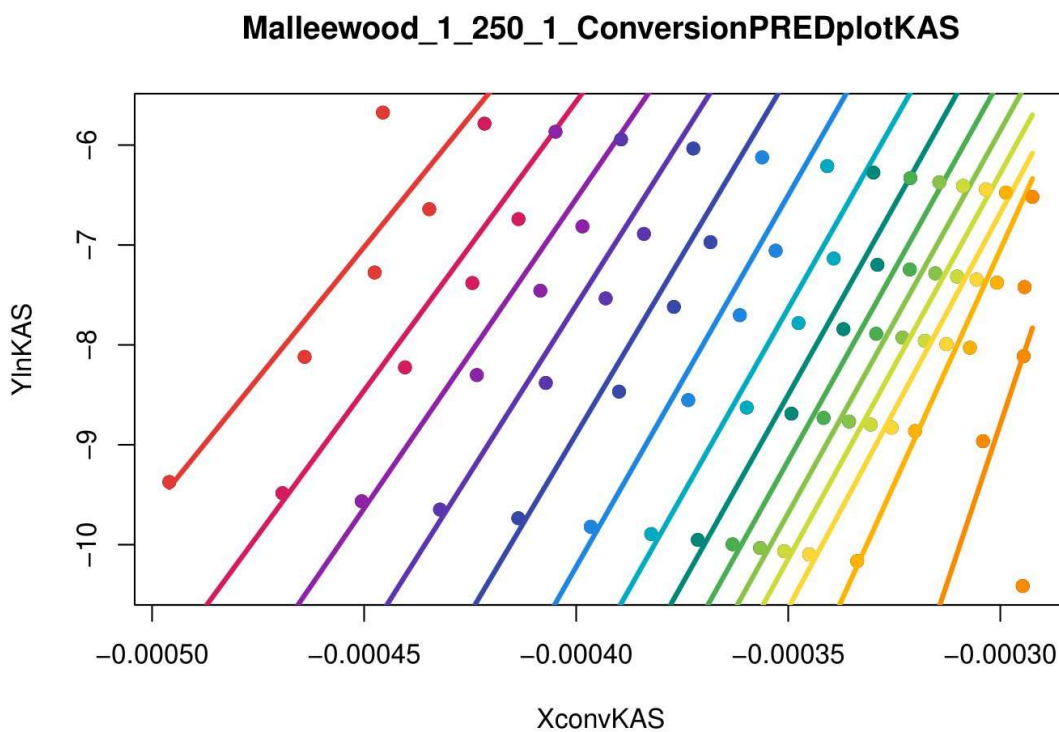
**Malleewood_1_45_1_ConversionPREDplotKAS**
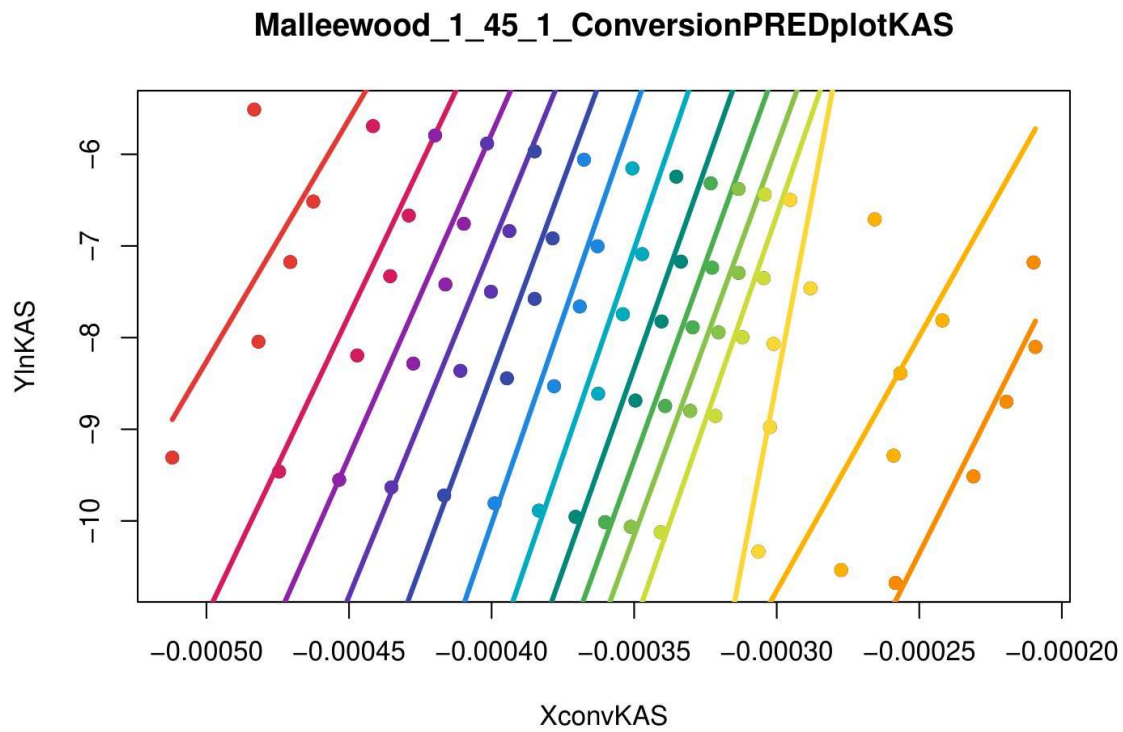


*Figure 3.17 Representative linear fit for slope determination at various conversions using KAS method for malleewood; particle size <45 μm and 1 mg sample size*

Figure 3.18 Representative activation energy distribution at various conversions using KAS method
for malleewood; particle size <45 μm and 1 mg sample size



Figure 3.19 Representative linear fit for slope determination at various conversions using KAS method
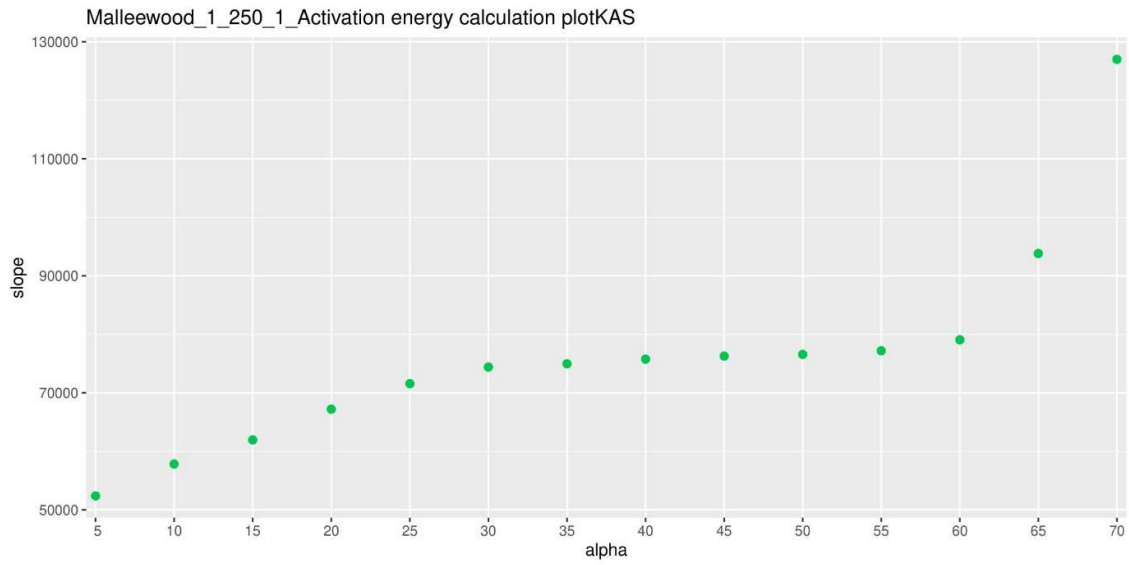for malleewood; particle size 106-150 μm and 1 mg sample size

Malleewood_1_106_1_Activation energy calculation plotKAS

*Figure 3.20 Representative activation energy distribution at various conversions using KAS method for malleewood; particle size 106-150 μm and 1 mg sample size*



**Malleewood_1_250_1_ConversionPREDplotKAS**

*Figure 3.21 Representative linear fit for slope determination at various conversions using KAS method for malleewood; particle size 250-300 μm and 1 mg sample size*

*Figure 3.22 Representative activation energy distribution at various conversions using KAS method for malleewood; particle size 250-300 μm and 1 mg sample size*
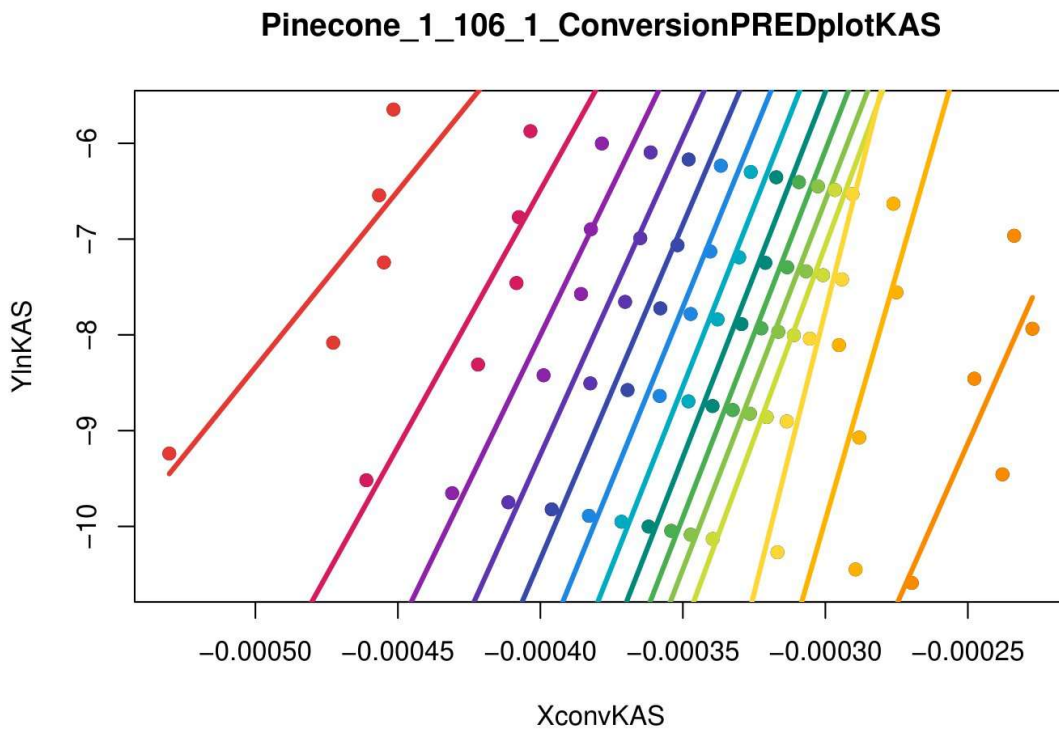


*Figure 3.23 Representative linear fit for slope determination at various conversions using KAS method for pinecone; particle size 106-150 μm and 1 mg sample size*
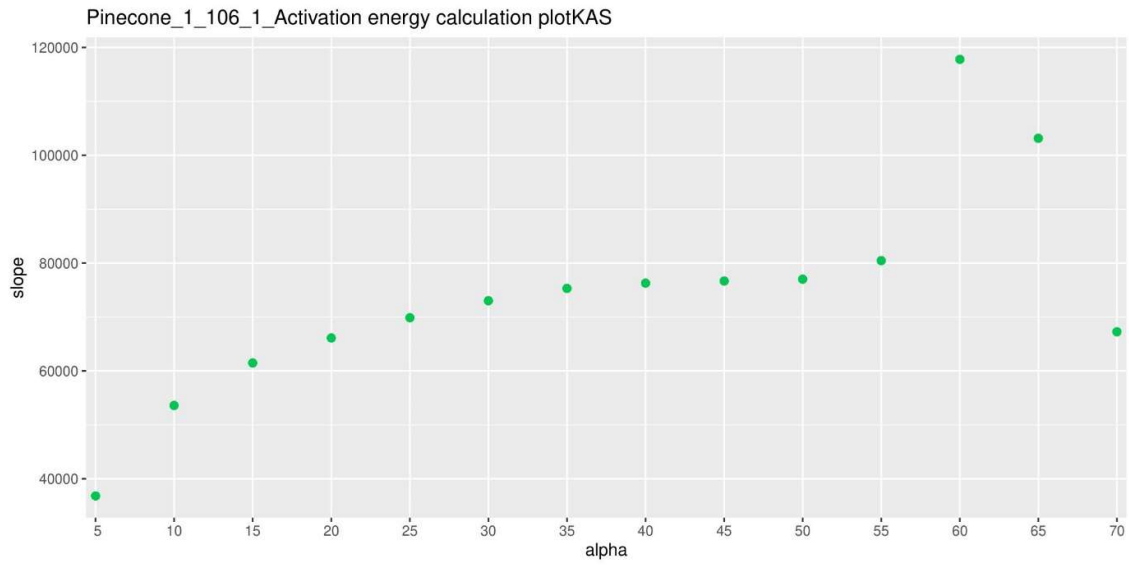
*Figure 3.24 Representative activation energy distribution at various conversions using KAS method for pinecone; particle size 106-150 μm and 1 mg sample size*
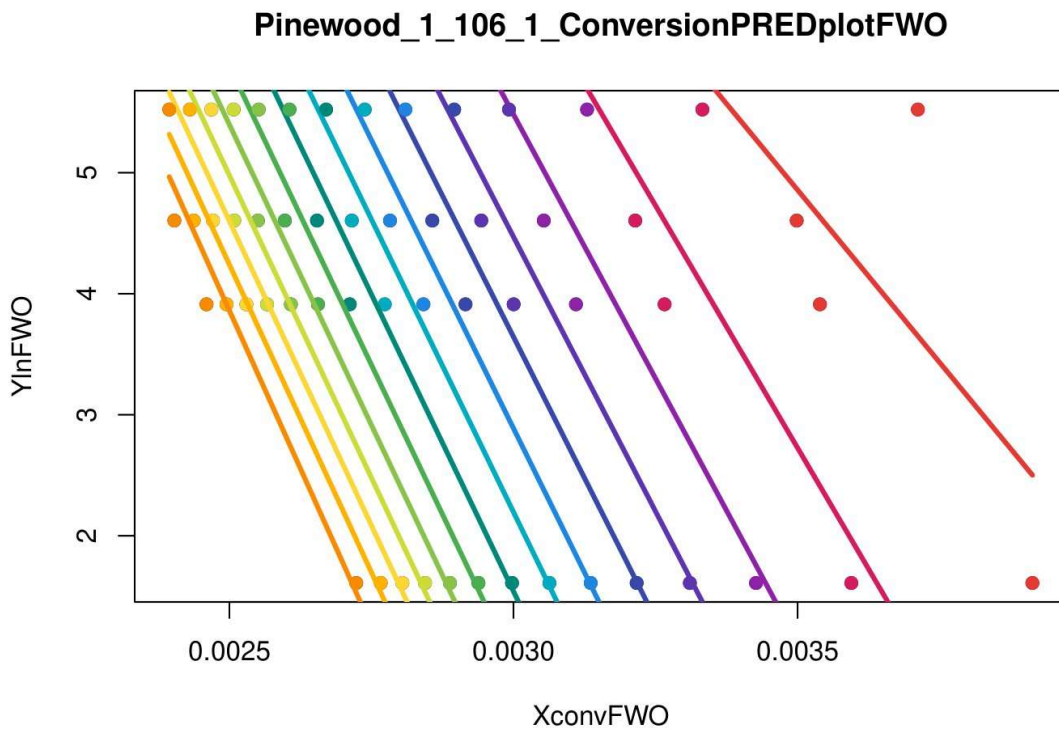


*Figure 3.25 Representative linear fit for slope determination at various conversions using FWO method for pinewood; particle size 106-150 μm and 1 mg sample size*
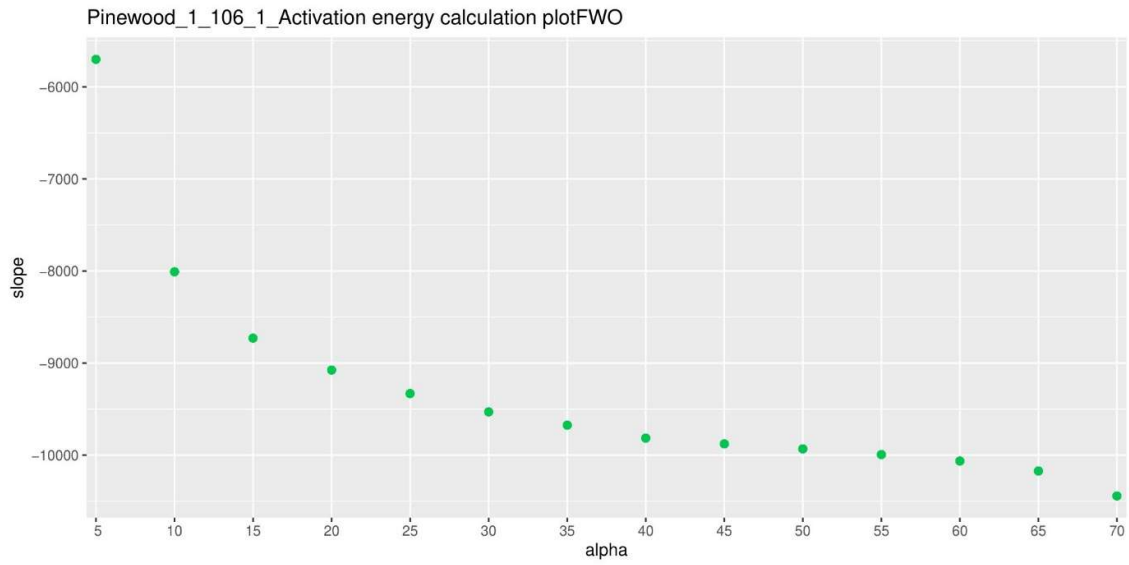
*Figure 3.26 Representative activation energy distribution at various conversions using FWO method for pinewood; particle size 106-150 μm and 1 mg sample size*
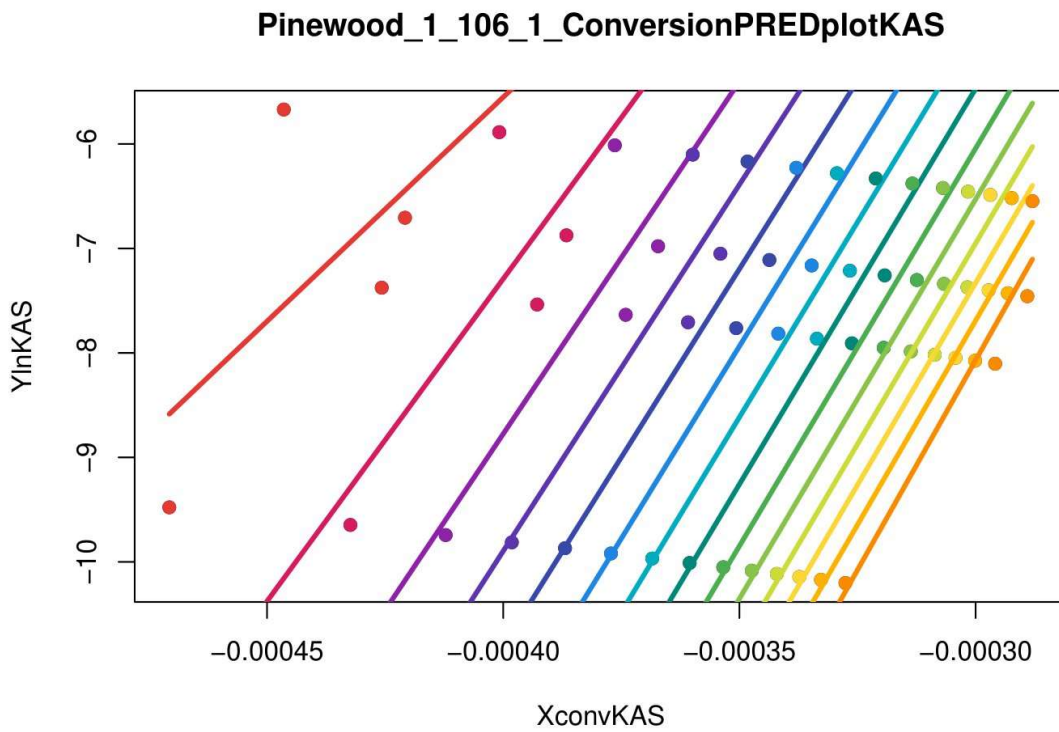


*Figure 3.27 Representative linear fit for slope determination at various conversions using KAS method for pinewood; particle size 106-150 μm and 1 mg sample size*
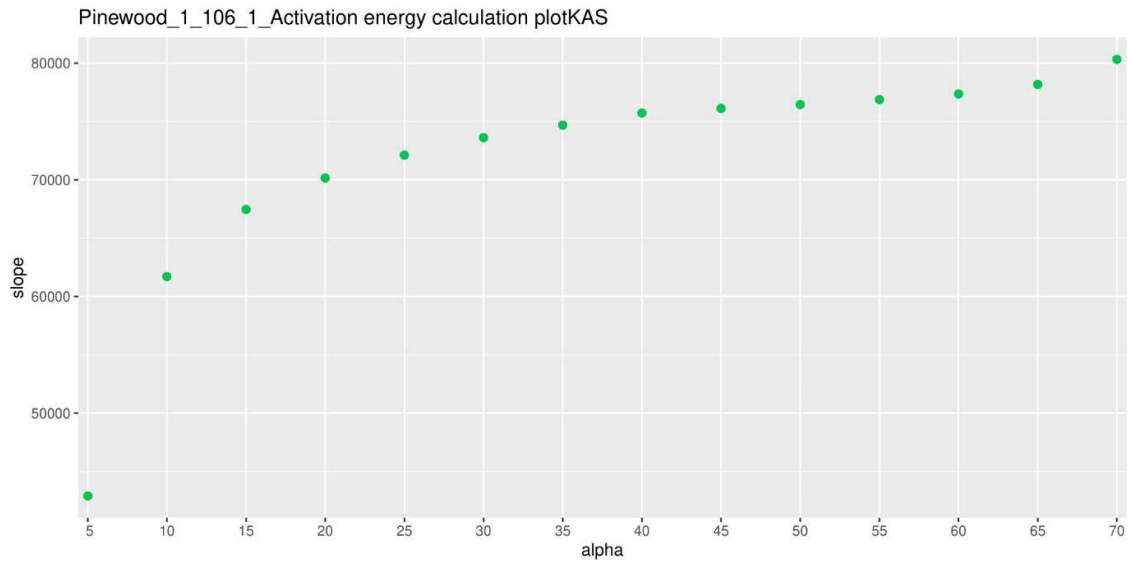
*Figure 3.28 Representative activation energy distribution at various conversions using KAS method for pinewood; particle size 106-150 µm and 1 mg sample size*
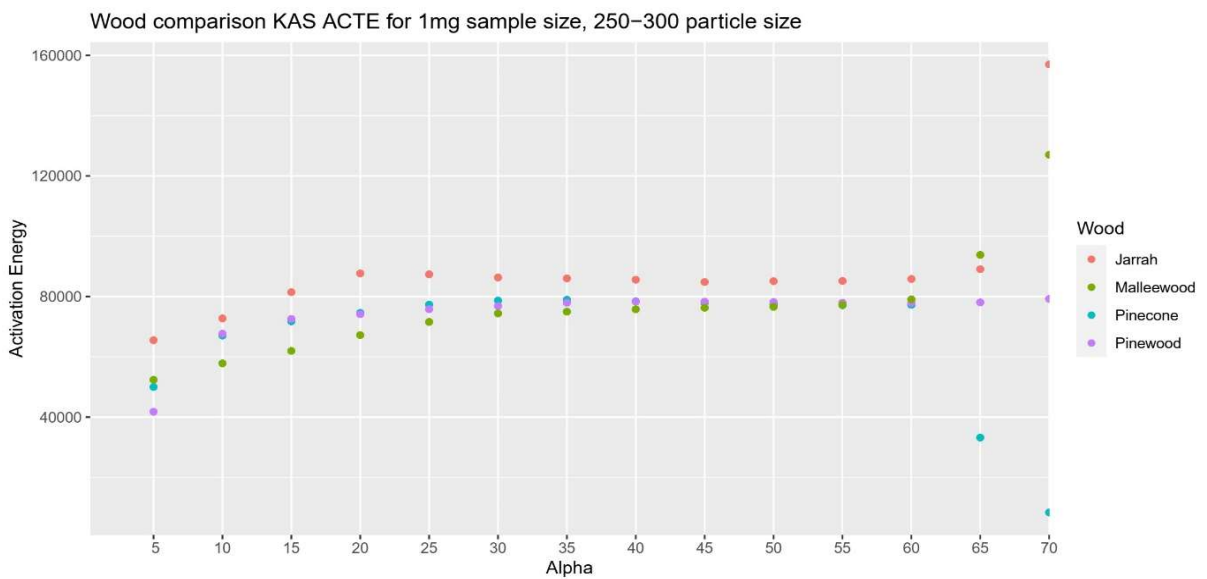


*Figure 3.29 Comparative activation energy distribution for jarrah, malleewood, pinecone, pinewood using KAS method at various conversions; 1 mg sample size and $250 - 300$ µm particle size*
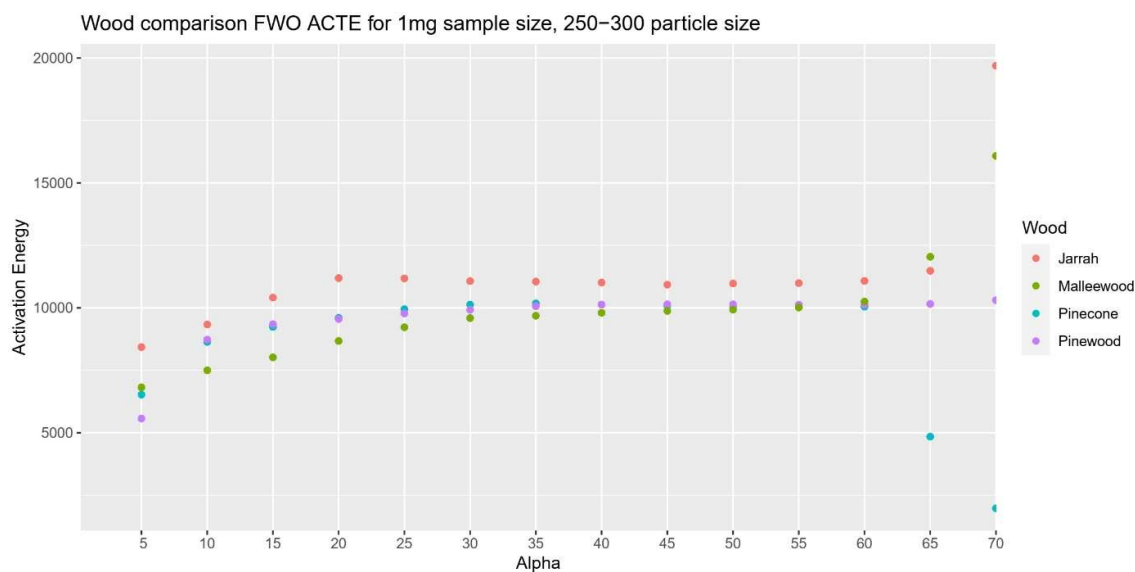
*Figure 3.30 Comparative activation energy distribution for jarrah, malleewood, pinecone, pinewood using FWO method at various conversions; 1 mg sample size and 250 − 300 μm particle size*

## Results and discussion

Application of model free or isoconversional methods to biomass pyrolysis helps to gain insights into nature of biomass pyrolysis. Using Friedman method for mallewood (Figure 3.1) there arises a possibility of two activation energies. A.E 1 as obtained from slope of line passing through 5 C/min alpha values and 250 C/min alpha values. A.E 2 as obtained from slope of line passing through 20 C/min, 50 C/min and 100 C/min. Alternatively, an arbitrary best fit slope could be assumed for generalization. However, this linearity is completely lost within the reaction regime conversion points. In the case of jarrah and pinewood using Friedman method (figure 3.2 and figure 3.3), there is a certain degree of approximate fit between conversion points 0.2 to 0.6. However, the problem of multiple activation energy persists, and between conversion points 0.6 - 0.9, the linearity is lost. The improbability of obtaining a sensible activation energy value via straight line fit (linear assumption) is seen clearly in case of pinecone (figure 3.6).

A closer cluster of heating rate points on Y-axis for α values is obtained in case of KAS method. However, the problem of possibility of multiple activation energies still persists. This can be seen in figure 3.5 and figure 3.6 for mallewood and pinecone respectively. This lack of linearity is especially observed in the reaction regime. The problems associated with Friedman method and KAS method are also observed when Flynn-Wall-Ozawa (FWO) method is used for activation energy determination as shown in figure 3.25 and figure 3.26. To further illustrate the uncertainty in obtaining stable activation energy values, distribution of activation energy values for various conversions can be compared using KAS and FWO method (Figure 3.22 -

3.26). KAS method predicts lower activation energies as compared to FWO method for same conversion values and same process conditions. This variance in activation energy values based on the method used has been addressed in previous published works.

Activation energy is a theoretical concept which can be applied to practical process only when the requisite conditions are met. In case of feedstock with low degree of cross-linking or when there are no competing and parallel reactions, a single activation energy value can represent the amount of energy needed for a reaction to occur. In case of complex reactions with multiple parallel and competitive reactions occurring simultaneously, a single activation energy value cannot satisfactorily describe the energy requirements of reaction progression. However, certain lumped assumptions can be made to obtain a distribution of activation energies over the course of reaction. This approach can perhaps give some sensible insights into nature of reaction and its energetics if the feedstock is homogenous. Biomass is a heterogeneous feedstock whose major constituents are highly crosslinked polymers and varying degrees of further heterogeneity (primarily lignin).

Cellulose is a crystalline polymer with d-glucopyranose (glucose) monomer units. Despite the high degree of polymerization (10,000-15,000 units), cellulose is homogenous. Using Friedman method (figure 3.7 ) and KAS method (figure 3.10 ) a distribution of activation energies with good straight fit over wide heating rates is observed. However, in case of hemicellulose, using Friedman method (figure 3.8 ) certain degree of linearity is maintained until $\alpha = 0.5$. For $\alpha = 0.6\text{-}0.9$ any semblance of linearity is lost. The same is observed when KAS method is employed for hemicellulose (figure 3.11 ). This can be ascribed to hemicellulose being more heterogenous than cellulose. Hemicellulose, despite having a low degree of polymerization (100-200 units) is composed of heterogenous sugar monomer repeating units such as xylose, arabinose, mannose, galactose and glucose. This heterogenous can be ascribed to lack of linearity over extended heating rates in case of hemicellulose. Lignin is a highly heterogenous three-dimensional amorphous polymer consisting of aliphatic and aromatic compounds with varying degree of cross-linking of lignols and phenyl propane units. Employing Friedman method (figure 3.9) and KAS method (figure 3.12) for lignin pyrolysis, the high degree of heterogeneity is revealed in the lack of linearity over the range of temperature scale conversion.

Biomass is physically and chemically constituted of these three polymers. As such, the pyrolytic breakdown characteristics of biomass are influenced and determined by the breakdown characteristics of the constituent polymers. Despite the issues associated with heterogeneity, isoconversional method have found ample application in calculating kinetic parameters for biomass pyrolysis. This is driven mainly by pyrolysis processes at extremely slow heating rates, including heating rates appropriate for torrefaction. In these cases, the reaction is over such a wide time scale, that assumption of a lumped approach becomes an efficient and time saving approach. Biomass pyrolysis process has been analysed over timescales of heat diffusion, heating rate and reaction rate.[39] As seen in Chapter 2 over a wider

time scale the reaction appears highly lumped and a general approximate straight line assumption seems possible. At faster heating and shorter time scale Chapter 2 the reaction is discrete having two well defined reaction regimes with individual peaks (maximum rate of reaction). This phenomenon limits the applicability of isoconversional methods over wider heating rate ranges (from slow to fast).

The activation energy distribution for malleewood jarrah, pinecone and pinewood is shown in figure 3.29 and figure 3.30. The ambiguity associated with activation energy values for biomass using isoconversional methods coupled with the theoretical basis for activation energy values make it improbable to obtain a reliable value appropriate for rector design. The conventional approach to kinetic modelling includes calculation of kinetic triplet consisting of activation energy, frequency factor (pre-exponential factor) and order of reaction. These values and their comparative analysis help in gaining insights into the nature of reaction and its associated energetics. These values however, especially in case of biomass as feedstock, do not contribute greatly to the design of a fast pyrolysis reactor. Using TGA and conducting pyrolysis runs at faster heating rates reveals the presence of two discrete peaks, with a clear global maximum denoting the maximum rate of reaction (mass/time unit) over the course of reaction regime. With a controlled/known particle size or mass, it is possible to link the time and temperature necessary for fast pyrolysis (kinetically controlled) reaction. The length of reactor is then a function of residence time of feedstock in reactor. These aspects are dealt with in further detail in chapter 4 and chapter 5.

In conclusion, variable source and heterogenous nature of feedstock in case of biomass pyrolysis make it crucial that the reactor operating conditions can be controlled with increasing accuracy and response time. To optimize desired crude oil yield, it is important to improve the responsiveness of reactor and process conditions to incoming feedstock compositional variety. The existing approaches of model free and model fitting methods can prove to be cumbersome in tackling this problem. They are useful in gaining insight into the underlying reaction mechanism of process. However, for quicker process control and ability to handle heterogeneous feedstock over wider heating rate ranges a neural networks-based approach is presented in Chapter 4.

# References

(1) Vyazovkin, S. *Isoconversional Kinetics of Thermally Stimulated Processes*; Springer International Publishing: Cham, 2015. https://doi.org/10.1007/978-3-319-14175-6.

(2) Cong, H.; Meng, H.; Mašek, O.; Yao, Z.; Li, L.; Yu, B.; Qin, C.; Zhao, L. Comprehensive Analysis of Industrial-Scale Heating Plants Based on Different Biomass Slow Pyrolysis Technologies: Product Property, Energy Balance, and Ecological Impact. *Clean. Eng. Technol.* **2022**, *6*, 100391. https://doi.org/10.1016/j.clet.2021.100391.

(3) Di Blasi, C. Kinetic and Heat Transfer Control in the Slow and Flash Pyrolysis of Solids. *Ind. Eng. Chem. Res.* **1996**, *35* (1), 37–46. https://doi.org/10.1021/ie950243d.

(4) Doumer, M. E.; Arízaga, G. G. C.; Silva, D. A. da; Yamamoto, C. I.; Novotny, E. H.; Santos, J. M.; Santos, L. O. dos; Wisniewski, A.; Andrade, J. B. de; Mangrich, A. S. Slow Pyrolysis of Different Brazilian Waste Biomasses as Sources of Soil Conditioners and Energy, and for Environmental Protection. *J. Anal. Appl. Pyrolysis* **2015**, *113*, 434–443. https://doi.org/10.1016/j.jaap.2015.03.006.

(5) Hu, M.; Chen, Z.; Wang, S.; Guo, D.; Ma, C.; Zhou, Y.; Chen, J.; Laghari, M.; Fazal, S.; Xiao, B.; Zhang, B.; Ma, S. Thermogravimetric Kinetics of Lignocellulosic Biomass Slow Pyrolysis Using Distributed Activation Energy Model, Fraser–Suzuki Deconvolution, and Iso-Conversional Method. *Energy Convers. Manag.* **2016**, *118*, 1–11. https://doi.org/10.1016/j.enconman.2016.03.058.

(6) Manyà, J. J.; Azuara, M.; Manso, J. A. Biochar Production through Slow Pyrolysis of Different Biomass Materials: Seeking the Best Operating Conditions. *Biomass Bioenergy* **2018**, *117*, 115–123. https://doi.org/10.1016/j.biombioe.2018.07.019.

(7) Williams, P. T.; Besler, S. The Influence of Temperature and Heating Rate on the Slow Pyrolysis of Biomass. *Renew. Energy* **1996**, *7* (3), 233–250. https://doi.org/10.1016/0960-1481(96)00006-7.

(8) Bridgwater, A. V.; Meier, D.; Radlein, D. An Overview of Fast Pyrolysis of Biomass. *Org. Geochem.* **1999**, *30* (12), 1479–1493. https://doi.org/10.1016/S0146-6380(99)00120-5.

(9) Czernik, S.; Bridgwater, A. V. Overview of Applications of Biomass Fast Pyrolysis Oil. *Energy Fuels* **2004**, *18* (2), 590–598. https://doi.org/10.1021/ef034067u.

(10) Cai, W.; Luo, Z.; Zhou, J.; Wang, Q. A Review on the Selection of Raw Materials and Reactors for Biomass Fast Pyrolysis in China. *Fuel Process. Technol.* **2021**, *221*, 106919. https://doi.org/10.1016/j.fuproc.2021.106919.

(11) Chiaramonti, D.; Oasmaa, A.; Solantausta, Y. Fast Pyrolysis Oil for Power Generation. In *GT2006*; Volume 2: Aircraft Engine; Ceramics; Coal, Biomass and Alternative Fuels; Controls, Diagnostics and Instrumentation; Environmental and Regulatory Affairs, 2006; pp 325–332. https://doi.org/10.1115/GT2006-90245.

(12) Li, P.; Shi, X.; Wang, X.; Song, J.; Fang, S.; Bai, J.; Zhang, G.; Chang, C.; Pang, S. Bio-Oil from Biomass Fast Pyrolysis: Yields, Related Properties and Energy Consumption Analysis of the Pyrolysis System. *J. Clean. Prod.* **2021**, *328*, 129613. https://doi.org/10.1016/j.jclepro.2021.129613.

(13)     Kostetskyy, P.; Broadbelt, L. J. Progress in Modeling of Biomass Fast Pyrolysis: A
         Review. *Energy Fuels* **2020**, *34* (12), 15195–15216.
         https://doi.org/10.1021/acs.energyfuels.0c02295.

(14)     Friedman, H. L. Kinetics of Thermal Degradation of Char-Forming Plastics from
         Thermogravimetry. Application to a Phenolic Plastic. *J. Polym. Sci. Part C Polym. Symp.*
         **1964**, *6* (1), 183–195. https://doi.org/10.1002/polc.5070060121.

(15)     Dhyani, V.; Bhaskar, T. Chapter 2 - Kinetic Analysis of Biomass Pyrolysis. In *Waste
         Biorefinery*; Bhaskar, T., Pandey, A., Mohan, S. V., Lee, D.-J., Khanal, S. K., Eds.; Elsevier,
         2018; pp 39–83. https://doi.org/10.1016/B978-0-444-63992-9.00002-1.

(16)     Cano-Pleite, E.; Rubio-Rubio, M.; Riedel, U.; Soria-Verdugo, A. Evaluation of the
         Number of First-Order Reactions Required to Accurately Model Biomass Pyrolysis.
         *Chem. Eng. J.* **2021**, *408*, 127291. https://doi.org/10.1016/j.cej.2020.127291.

(17)     Ranzi, E.; Debiagi, P. E. A.; Frassoldati, A. Mathematical Modeling of Fast Biomass
         Pyrolysis and Bio-Oil Formation. Note I: Kinetic Mechanism of Biomass Pyrolysis. *ACS
         Sustain. Chem. Eng.* **2017**, *5* (4), 2867–2881.
         https://doi.org/10.1021/acssuschemeng.6b03096.

(18)     Branca, C.; Di Blasi, C. Multistep Mechanism for the Devolatilization of Biomass Fast
         Pyrolysis Oils. *Ind. Eng. Chem. Res.* **2006**, *45* (17), 5891–5899.
         https://doi.org/10.1021/ie060161x.

(19)     Kujirai, T.; Akahira, T. Effect of Temperature on the Deterioration of Fibrous
         Insulating Materials. *Sci Pap Inst Phys Chem Res* **1925**, *2*, 223–252.

(20)     Ozawa, T.; Sunose, T.; Kaneko, T. Historical Review on Research of Kinetics in
         Thermal Analysis and Thermal Endurance of Electrical Insulating Materials: I. Thermal
         Endurance Test and Isoconversion Methods. *J. Therm. Anal. Calorim.* **1995**, *44* (1), 205–
         216. https://doi.org/10.1007/bf02547149.

(21)     Ozawa, T. A New Method of Analyzing Thermogravimetric Data. *Bull. Chem. Soc. Jpn.*
         **1965**, *38* (11), 1881–1886. https://doi.org/10.1246/bcsj.38.1881.

(22)     Doyle, C. D. Kinetic Analysis of Thermogravimetric Data. *J. Appl. Polym. Sci.* **1961**, *5*
         (15), 285–292. https://doi.org/10.1002/app.1961.070051506.

(23)     Doyle, C. D. Estimating Isothermal Life from Thermogravimetric Data. *J. Appl. Polym.
         Sci.* **1962**, *6* (24), 639–642. https://doi.org/10.1002/app.1962.070062406.

(24)     Vyazovkin, S.; Burnham, A. K.; Favergeon, L.; Koga, N.; Moukhina, E.; Pérez-Maqueda,
         L. A.; Sbirrazzuoli, N. ICTAC Kinetics Committee Recommendations for Analysis of Multi-
         Step Kinetics. *Thermochim. Acta* **2020**, *689*, 178597.
         https://doi.org/10.1016/j.tca.2020.178597.

(25)     Flynn, J. H.; Wall, L. A. A Quick, Direct Method for the Determination of Activation
         Energy from Thermogravimetric Data. *J. Polym. Sci. [B]* **1966**, *4* (5), 323–328.
         https://doi.org/10.1002/pol.1966.110040504.

(26)     Ding, Y.; Zhang, W.; Yu, L.; Lu, K. The Accuracy and Efficiency of GA and PSO
         Optimization Schemes on Estimating Reaction Kinetic Parameters of Biomass Pyrolysis.
         *Energy* **2019**, *176*, 582–588. https://doi.org/10.1016/j.energy.2019.04.030.

(27)     Zhong, Y.; Ding, Y.; Lu, K.; Mao, S.; Li, C. Kinetic Parameters and Reaction Mechanism Study of Biomass Pyrolysis by Combined Kinetics Coupled with a Heuristic Optimization Algorithm. *Fuel* **2023**, *334*, 126622.

(28)     Flynn, J. H.; Wall, L. A. General Treatment of the Thermogravimetry of Polymers. *J. Res. Natl. Bur. Stand. Sect. Phys. Chem.* **1966**, *70A* (6), 487. https://doi.org/10.6028/jres.070A.043.

(29)     Flynn, J. H. The 'Temperature Integral' — Its Use and Abuse. *Thermochim. Acta* **1997**, *300* (1–2), 83–92. https://doi.org/10.1016/S0040-6031(97)00046-4.

(30)     Kissinger, H. E. Variation of Peak Temperature with Heating Rate in Differential Thermal Analysis. *J. Res. Natl. Bur. Stand.* **1956**, *57* (4), 217. https://doi.org/10.6028/jres.057.026.

(31)     Kissinger, H. E. Reaction Kinetics in Differential Thermal Analysis. *Anal. Chem.* **1957**, *29* (11), 1702–1706. https://doi.org/10.1021/ac60131a045.

(32)     Vyazovkin, S. Kissinger Method in Kinetics of Materials: Things to Beware and Be Aware Of. *Molecules* **2020**, *25* (12), 2813. https://doi.org/10.3390/molecules25122813.

(33)     Coats, A. W.; Redfern, J. Kinetic Parameters from Thermogravimetric Data. *Nature* **1964**, *201* (4914), 68–69.

(34)     Sánchez-Jiménez, P. E.; Pérez-Maqueda, L. A.; Perejón, A.; Criado, J. M. Limitations of Model-Fitting Methods for Kinetic Analysis: Polystyrene Thermal Degradation. *Resour. Conserv. Recycl.* **2013**, *74*, 75–81. https://doi.org/10.1016/j.resconrec.2013.02.014.

(35)     Fetisova, O. Yu.; Mikova, N. M.; Taran, O. P. Evaluation of the Validity of Model-Fitting and Model-Free Methods for Kinetic Analysis of Nonisothermal Pyrolysis of Siberian Fir Bark. *Kinet. Catal.* **2020**, *61* (6), 846–853. https://doi.org/10.1134/S0023158420050043.

(36)     Šesták, J.; Berggren, G. Study of the Kinetics of the Mechanism of Solid-State Reactions at Increasing Temperatures. *Thermochim. Acta* **1971**, *3* (1), 1–12. https://doi.org/10.1016/0040-6031(71)85051-7.

(37)     Šesták, J. Philosophy of Non-Isothermal Kinetics. *J. Therm. Anal. Calorim.* **1979**, *16* (2), 503–520. https://doi.org/10.1007/bf01910714.

(38)     Vyazovkin, S.; Wight, C. A. Isothermal and Nonisothermal Reaction Kinetics in Solids: In Search of Ways toward Consensus. *J. Phys. Chem. A* **1997**, *101* (44), 8279–8284. https://doi.org/10.1021/jp971889h.

(39)     Kardaś, D.; Hercel, P.; Polesek-Karczewska, S.; Wardach-Święcicka, I. A Novel Insight into Biomass Pyrolysis–The Process Analysis by Identifying Timescales of Heat Diffusion, Heating Rate and Reaction Rate. *Energy* **2019**, *189*, 116159.

# Chapter 4 Modelling approaches suitable for biomass pyrolysis

*In earlier chapters, we used the conventional kinetic approach to study the nature of biomass pyrolysis. While we saw that these methods are useful in gaining insight into the nature of biomass pyrolysis reaction, we also realized its limitations in obtaining kinetic models suitable for real world applications. The real-world problem of operating a continuous biomass pyrolysis plant for fast pyrolysis – crude oil maximizing condition could be characterized by a continuous heterogeneous feedstock and a lack of dynamic reactor control which takes this into account. (Apart from the associated techno-economics). In this chapter, we present an approach that is capable of accounting for this feedstock heterogeneity, and potentially for feedback control. To facilitate these requirements, we make use of artificial neural networks to predict mass loss profiles and kinetics of biomass samples having variable cellulose, hemicellulose, lignin compositions. The details of modelling work are presented in this chapter. Our approach shows promise in predictive modelling of biomass pyrolysis and enables the determination of consistent and relevant kinetics. A brief review of existing work related to predictive modelling of biomass pyrolysis, its shortcomings and promises has also been presented.*

## Background

For thermal processes, kinetics studies the rates of processes in order to accomplish two major objectives. The first is to parameterize the process rate as a function of state variables so that it can be predicted for any combination of these variables. The second is to obtain insights into the process mechanisms.[1] In classical approach, the rate of process is parameterized following Arrhenius relationship expressed in terms of activation energy, frequency factor and Temperature (as show in equation 3.1-3.) Theoretical underpinnings of Arrhenius relationship, transition state theory and link between kinetic approach and thermodynamic interpretation have been discussed in chapter 3. In this chapter we present a model which captures the inherent heterogeneity of biomass and define biomass pyrolysis as a function of its composition, along with time and temperature. We present first, a general modelling approach suitable for extended heating rates for biomass pyrolysis (approaching fast pyrolysis regime). Consequently, we train and test the fidelity of models developed using this approach. We also discuss the efficacy of this approach for designing fast pyrolysis reactors and achieving dynamic process control for selective product yield optimization. The details of modelling work are presented in this chapter. To the best of author's knowledge, such an approach has not been presented in published literature till date.

The issues associated with modelling as discussed in earlier chapters led us to develop a predictive kinetic model which incorporates the inherent heterogeneity of biomass and links

its mass loss conversion over time and temperature scales. Earlier approaches assumed biomass pyrolysis to be a function only of time (and time – temp linear assumption). The proposed model defines biomass pyrolysis as a function of composition along with temperature and time. It also has the capacity to incorporate newer dimensions, given sufficient training with enough experimental data. The earlier models were also limited in their predictive capabilities. They could be considered as static models. Incorporating neural networks to study kinetics enables the model to have dynamic properties as well as prediction capabilities.

In the current work, we develop a model which is applicable over wider heating range (from slow to fast pyrolysis rates) and incorporates the dependence of feedstock composition of biomass pyrolysis reaction kinetics. The model also has predictive capabilities and can predict conversion profiles (and reaction rate profiles) for unknown samples.

If dynamic control is to be achieved for real world applications of biomass fast pyrolysis it is pertinent to attain insight into the reaction process and extract information useful/valuable for design of suitable pyrolysis reactor (and the process). We have discussed in chapter 2 and chapter 3 the usefulness and limitations of existing approaches at kinetic modelling of biomass pyrolysis. The learning from that work prompted us to use neural networks to develop kinetic models suitable for biomass pyrolysis. The modelling work is presented in subsequent sections.
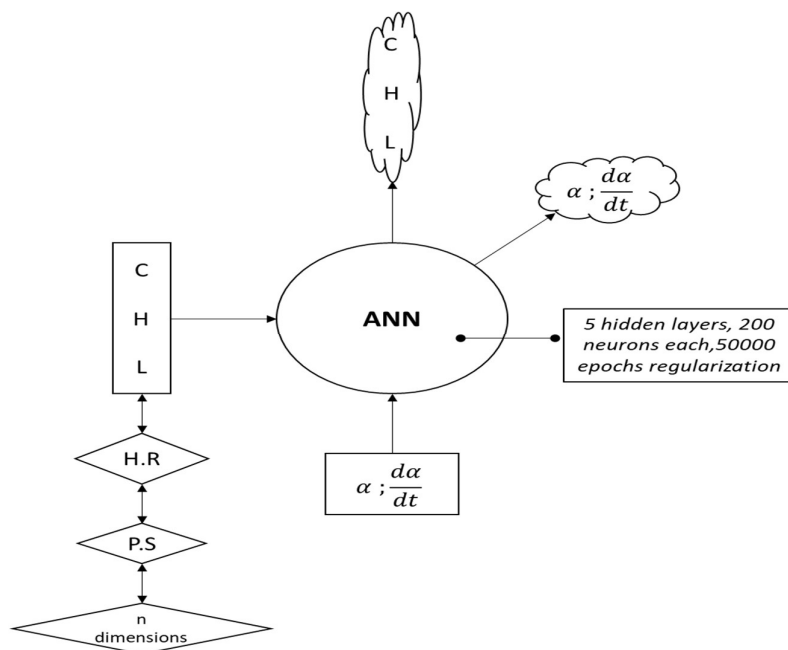


Figure 4.1 Overview of modelling approach and ANN knowledge cloud.

## What are Neural Networks?

Artificial neural networks are developed to mimic the neural activity of human brain. They make use of the universal approximation theorem to approximate complex functions and

correlations. As such artificial neural networks hold the potential to predict complex processes, which in our case is, biomass pyrolysis. Given sufficient data to establish a functional relationship between input and out parameters, an ANN model should be able to learn enough to predict the output values for an unknown input sample.

A computer program is said to learn from experience E with respect to some class of tasks T and performance measure P, if its performance at tasks in T, as measured by P, improves with experience E.[2] The performance of model's predictive capabilities are tested on unknown samples to evaluate its reliability. Therefore, in our work, we have evaluated the predictive capabilities/performance of the model using test data sets which are separate from the data used for training the machine system/ANN model.

A brief review of artificial neural networks application for biomass pyrolysis is presented here-

Artificial neural networks have been looked at for modelling thermal decompositions. [3]Artificial neural networks for thermochemical conversion of biomass was initially concerning biomass gasification. [4,5] ANN technique for biomass pyrolysis has mainly involved predicting kinetic parameters using ANN for different biomass samples. The problems discussed in chapter 3 get overlooked in such a machine learning approach. [6–11] Further, the range of model validity remains questionable, and no insight is obtained in the nature of biomass pyrolysis reaction. ANN has been used a framework for autonomously discovering biomass pyrolysis kinetic models from thermogravimetric analyzer (TGA) experimental data using the recently developed chemical reaction neural networks (CRNN).[12] Predictive PBM-DAEM model for biomass to char producing pyrolysis for thermally thick (Biot number, Bi>1 ) particle has also been presented.[13] Application of machine learning for hydrodynamics, transport and reactions in multiphase flows and reactor has been reviewed.[14] Minimum fluidization velocity for mixtures of biomass and inert solid particles have been predicted using artificial neural networks.[15] There are some efforts towards modelling waste pyrolysis[16,17] and gasification[18–20] along with co-pyrolysis of biomass and plastics[21] or coal[22,23]. It has been shown that using artificial neural networks and decision trees reduces computational expense of detailed kinetic models by four orders of magnitude making their application in comprehensive models possible.[24] ANN along with CFD has been used to link particle and reactor scale models.[25,26] There some works focussed on low heating rate operation for producing char and syngas via torrefaction and pyrolysis.[27–31] Utility of ANN for predicting higher heating value of biomass pyrolysis oil has been reviewed.[31] ANN has also shown promise in predicting lumped char, oil and gas yields for biomass pyrolysis.[32,33]

## ANN modelling for current work

The neural network model in current work is trained using experimentally procured data as described in chapter 2 section 2.1-2.3. The model is trained to predict the conversion profile for different biomass compositions described mass basis in terms of cellulose, hemicellulose, lignin for heating rate of 250 K.min$^{-1}$. The cellulose, hemicellulose and lignin weight percent values from *Chapter 2, Table 2* are used for training the models. Further a mix of 6 and then 3

more biomass samples were used to train the model. Particle size samples of 106 μm to 150 μm and of particle sizes 250 μm – 300 μm were used for all experiments. TGA mass loss data was used to calculate α vs t and alpha vs t which were then used for training and testing. Using real biomass samples and training and testing the ANN models with experimental data ensures that the model possess a higher degree of fidelity to reality (of biomass pyrolysis phenomena) as compared to models trained completely from simulation or literature data. The details of training, testing, data treatment and model validation are presented in subsequent sections.

## Structure

[initial 1 layer to layer 4 discuss] Initially the model is developed with four hidden layers with 50 neurons each to test the sensibility of this approach. Later, on realizing the validity of the approach, we redevelop the model with 5 hidden layers and 200 neurons each. [computational time trade off] The structure of model is shown in Figures 4.2 and 4.3.
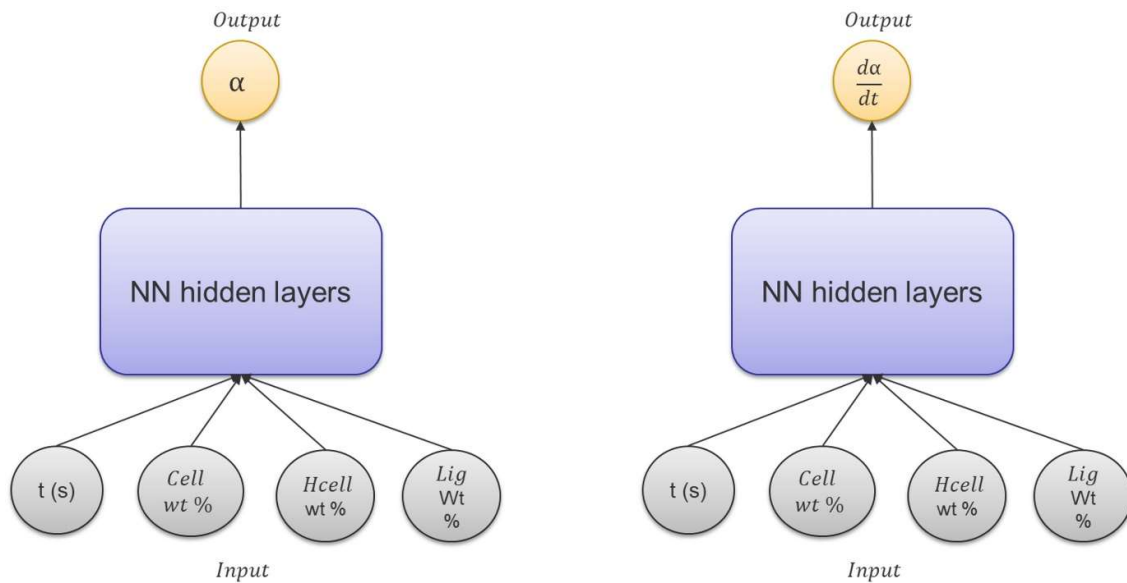


*Figure 4.2 ANN model overview*
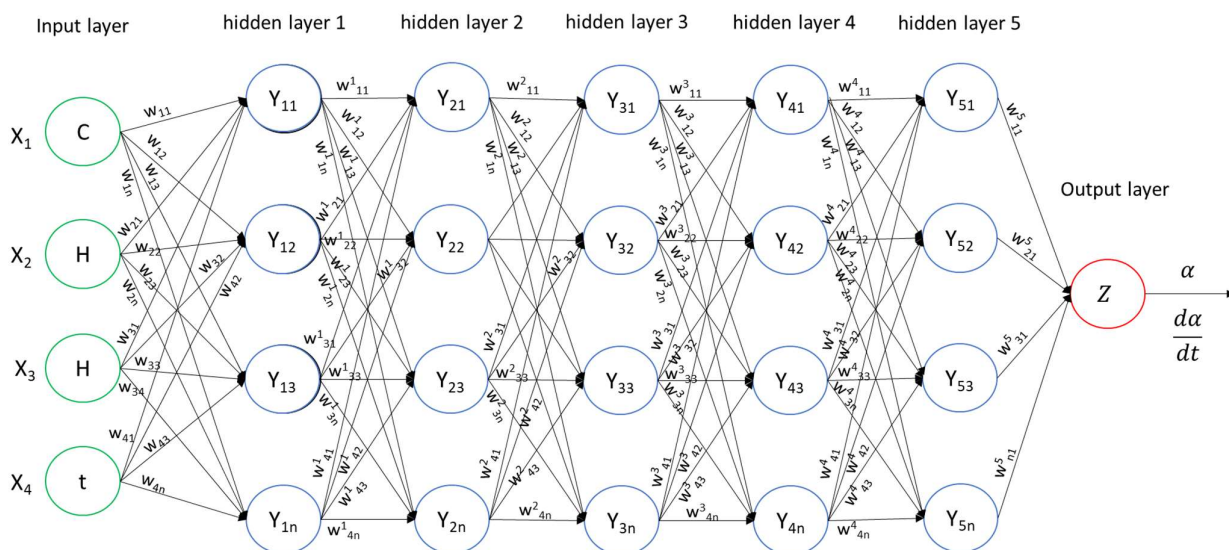
*Figure 4.3 Structure of ANN model*

## Model details

The models are normal feed forward neural networks with TGA experimental data as labelled data. Model 1-has 4 hidden layers and 50 neurons per layer. It is trained using 10 biomass samples. Model - 1a is trained to predict conversion α v/s time for unknown biomass sample. Model - 1b is trained to predict rate of conversion or rate of reaction $\frac{d\alpha}{dt}$ v/s time for unknown biomass sample. (Figures 4.4 – 4.7)

Two more versions, model - 1c and model - 1d are trained by adding a regularization term to the loss function (Figure 4.8 – 4.11). Regularization is in the form of Arrhenius equation. A second output is also included along with alpha to accommodate value of rate constant. Model 1-c is trained to predict conversion α v/s time with regularization using Arrhenius relationship. (Figure 4.10) Similarly, model 1-d is trained to predict rate of conversion or rate of reaction $\frac{d\alpha}{dt}$ v/s time for unknown biomass sample by trying to fit the predicted value using Arrhenius relationship between K and α (Figure 4.11). Regularisation technique is introduced to overcome possible generalization errors and to test the usefulness of Arrhenius correlation. Later, the model was modified to have 5 hidden layers with 200 neurons each and trained using additional cellulose, hemicellulose, lignin and newer particle size range. Model 2-a predicts conversion α v/s time. Model 2-b predicts rate of conversion or rate of reaction $\frac{d\alpha}{dt}$ v/s time. (Figures 4.12 & 4.13) The current models are trained and tested for 250 °K/min heating rate and for samples with particle size 106-150 μm and 250-300 μm.

Further, 6 new mixed biomass samples with varying cellulose, hemicellulose and lignin values were used to train and test the model 3a and 3-b. (Figure 4.14 & 4.15) This confirms the

dependence of predictive ability on the quanta and variation of compositional heterogeneity present in training data sets.

Lastly, to check the dependence of number of neurons on prediction results and to conclude the present work, the model with all biomass samples and pure cellulose, hemicellulose and lignin samples was retrained and retested with 100 neurons (model 4) and 500 neurons (model 5). The results are shown in table 4.1.

## Defining parameters

The loss function for non-regularized models can be given as:

$$\mathcal{L} = \sum_{i=1}^{N} (y - \hat{y})^2$$

4.1

The neural network is trained with Adam optimizer for 50000 epochs with Learning rate = $10e^{-4}$ and for another 50000 epochs with LR = $10e^{-5}$.

The loss function for regularized models can be given by:

$$\mathcal{L} = \sum_{i=1}^{N} (y - \hat{y})^2 + \sum_{j=1}^{N_C} \left(\frac{d\hat{y}_{1,j}}{dt} + \hat{y}_{2,j} \cdot \hat{y}_{1,j}^2\right)$$

4.2

$N_c$ is chosen as 5000 and these data points are randomly chosen from the entire data set to calculate regularization terms. Sigmoid activation function has been used since it shows the best result for current work.

$$S(x) = \frac{1}{1 + e^{-x}}$$

4.3

## Defining training and testing program

Inputs to the neural network are time, cellulose composition, hemicellulose composition and lignin composition. Output is either conversion or rate of conversion/reaction.

Sample of Jarrah, which is a part of training data is taken for validating the model and pinecone samples are taken for testing. The testing is also carried out for 2 additional unknown samples. TGA data for test case is not included in training data. So, tests carried on such experimental data are equivalent to prediction tests for unknown biomass sample.

Model is retrained for regularization approaches. Further, interchanging test and train data sets for models is done to ensure that fidelity of model. All models are tested on 3 unknown test samples to ensure reliability of this approach.

| Model Description | Test prediction MSE loss |
|---|---|
| Prediction of conversion function; 4 hidden layers, 50 neurons each; 9 training sets | 0.0067 |
| Prediction of conversion function; 5 hidden layers, 200 neurons each; 21 training sets | 0.0036 |
| Prediction of conversion function; 5 hidden layers, 200 neurons each; 27 training sets | 0.0021 |
| Prediction of conversion function; 5 hidden layers, 200 neurons each; 30 training sets | 0.0017 |
| Prediction of conversion function; 5 hidden layers, 200 neurons each; 30 training sets; regularization | 0.0016 |
| Prediction of conversion function; 5 hidden layers, 100 neurons each; 30 training sets; no regularization | 0.0018 |
| Prediction of conversion function; 5 hidden layers, 500 neurons each; 30 training sets; no regularization | 0.0016 |

*Table 4.1 Details of models presented in current work*

Results and discussion
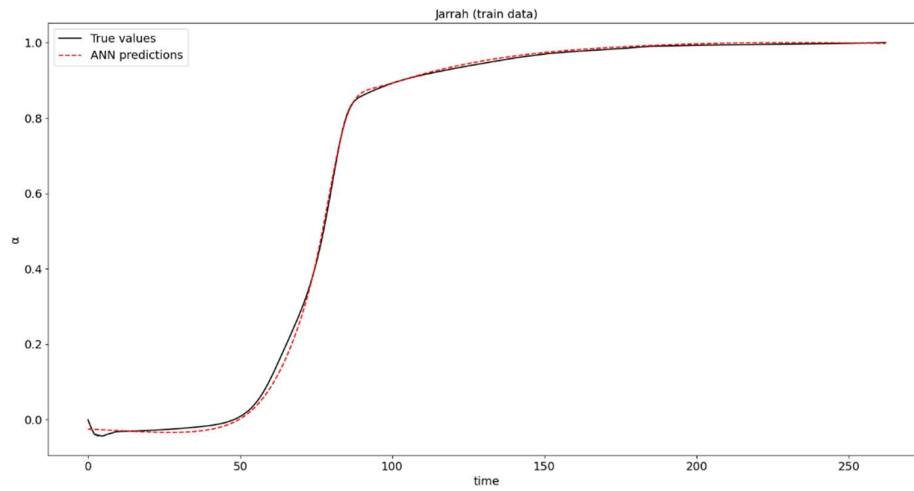


*Figure 4.4 Prediction of conversion for Jarrah (training data) using 9 samples*
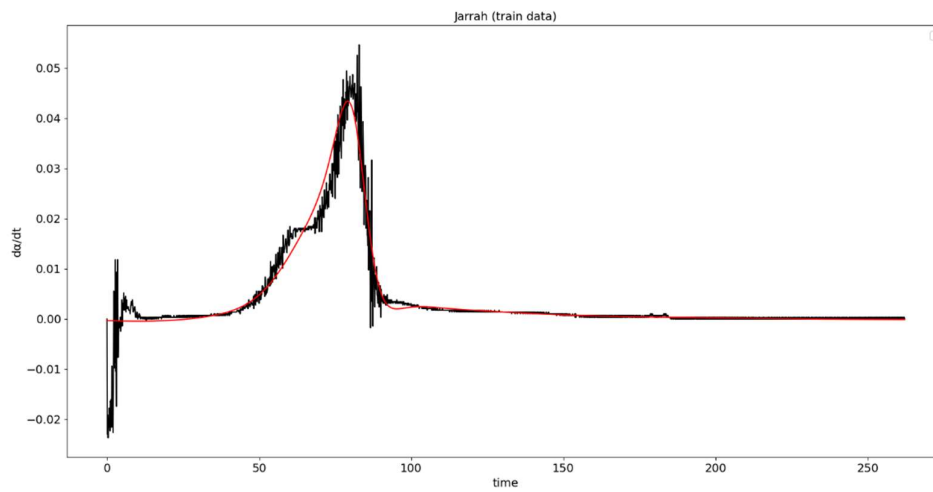


*Figure 4.5 Prediction of rate of conversion for Jarrah (training data) using 9 samples*
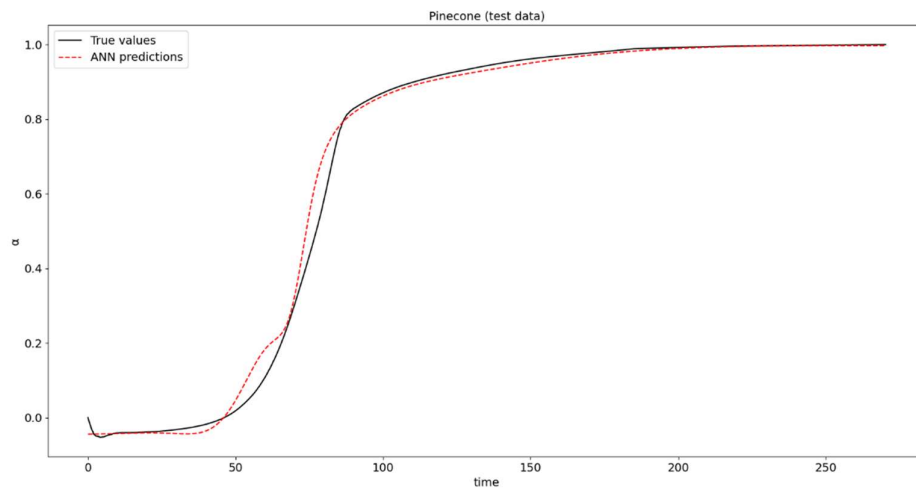
*Figure 4.6 Prediction of conversion for Pinecone (test data) using 9 samples*
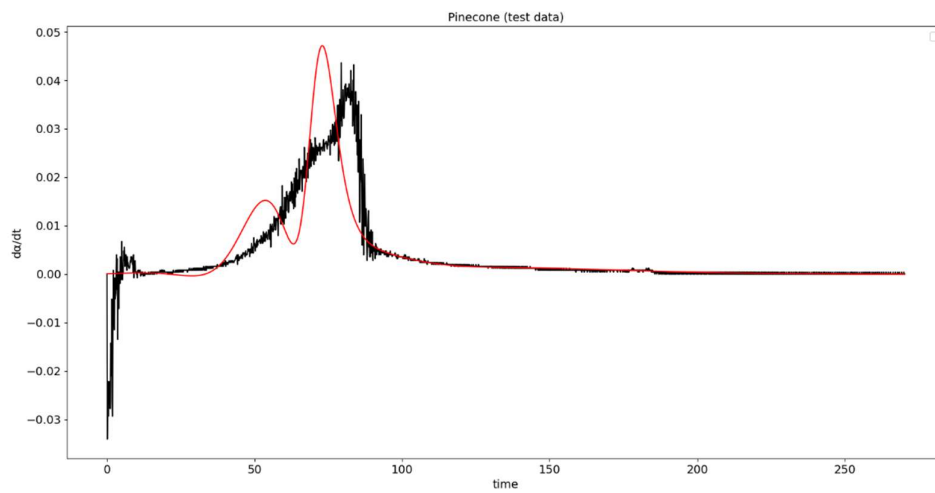


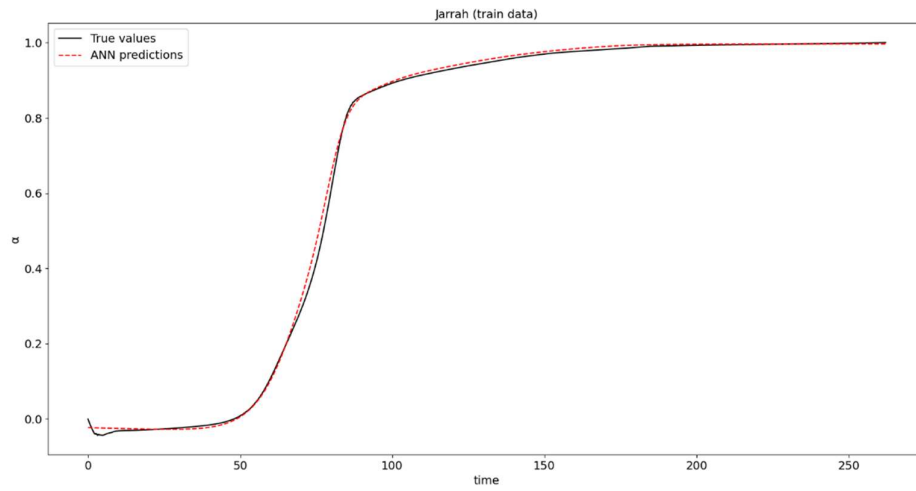*Figure 4.7 Prediction of rate of conversion for Pinecone (test data) for 9 samples*

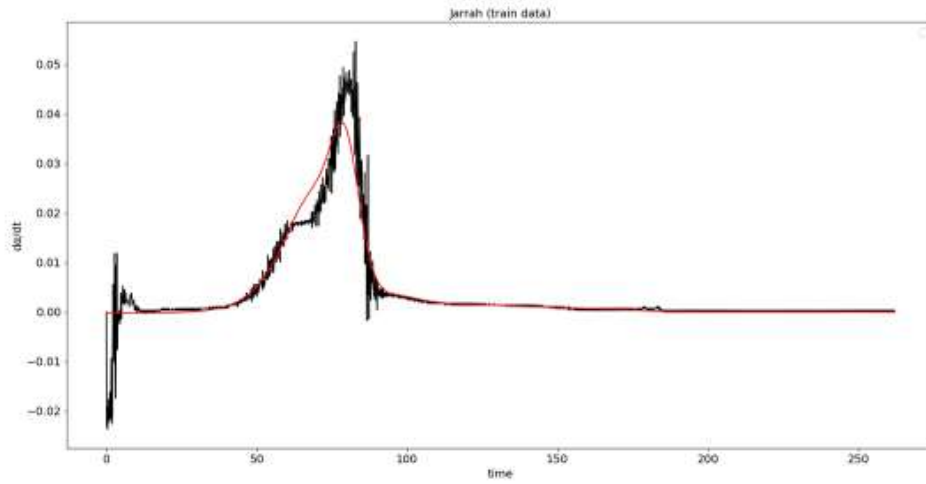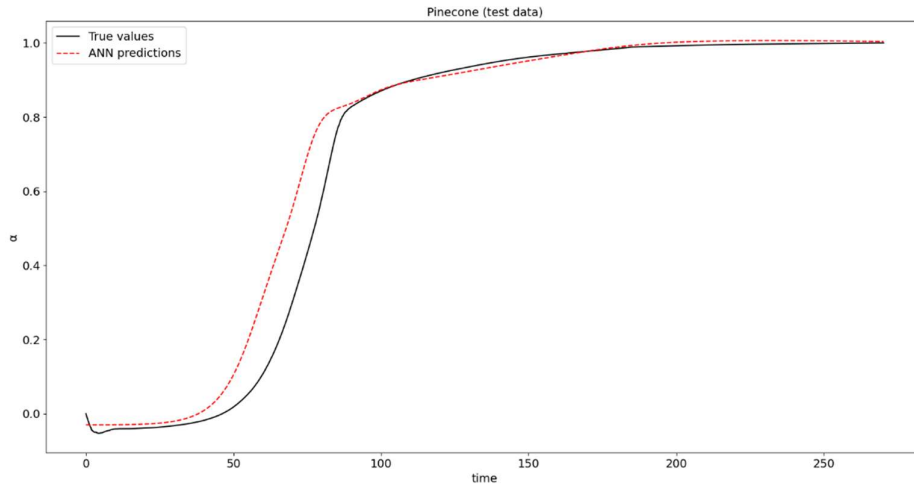*Figure 4.8 Prediction of conversion using regularized approach for Jarrah (train data) for 9 samples*



*Figure 4.9 Prediction of rate of conversion using regularized approach for Jarrah (train data) for 9 samples*

*Figure 4.10 Prediction of conversion using regularized approach for Pinecone (test data) using 9 samples*
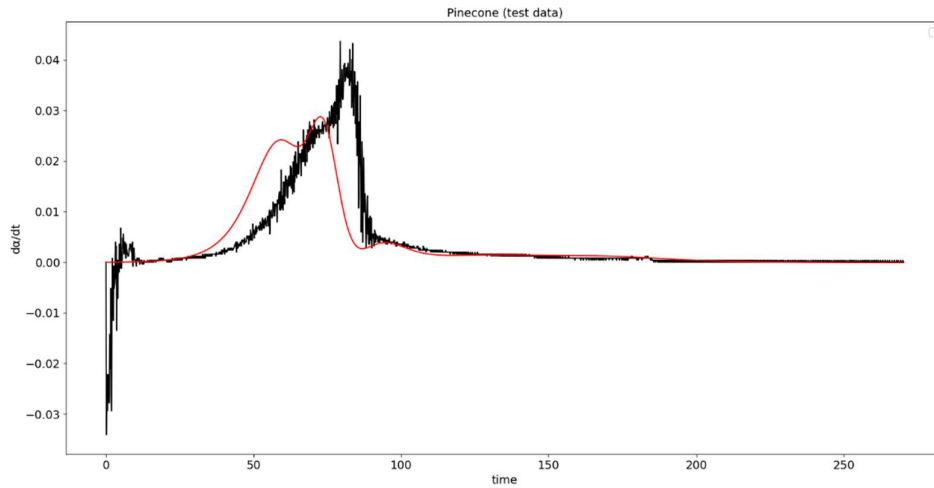


*Figure 4.11  Prediction of rate of conversion using regularized approach for Pinecone (test data) for 9 samples*

To establish confidence about model's learning ability, the model is tested on training data samples. The training results for alpha for model with 50 neurons as well as models with 100, 200 and 500 neurons yield good match. The model training results for dα/dt also show agreeable match with experimental data. The shoulders are not captured in unregularized model but the dα/dt max value is predicted with reasonable accuracy. After adding regularization to the model, the shoulders start becoming apparent in the predictions but the max value for dα/dt starts reducing. The test results for training data for model with 100, 200

and 500 neurons and an additional 5th hidden layer also show accurate match with experimental data. This helps establish the confidence on models learning abilities. The models' predictive capabilities are re-tested using experimental data for unknown (not used for training) biomass samples. Note: the unknown biomass sample for machine is known to the experimenter.

The predictive capability of the model trained using 9 biomass samples and having 4 hidden layers with 50 neurons each is poor. It predicts the general form of conversion function but does not predict the rate of reaction function with great accuracy. To improve the predictive capability of the model, we train it further by adding pure cellulose, hemicellulose, and lignin samples. We also add samples for 9 biomass samples used earlier for an additional particle size 250-300 μm. We also incorporate an additional hidden layer so that the model has 5 hidden layers and increased the number of neurons to 200 neurons per hidden layer. The prediction capability of the model improves from a MSE loss value of 0.0067 to 0.0036 for conversion function. Assuming pyrolysis reaction to be function of biomass composition, we keep the hidden layers at 5 and neurons per hidden layer at 200 and train the model with 6 new biomass mixed samples with varying cellulose, hemicellulose, and lignin values. Upon testing the model for an unknown sample, the MSE improves from 0.0036 to 0.0021. The model shows improvement in predicting conversion function as well as reaction rate function. To test the hypothesis further, we train the model using 3 new mixed biomass samples (Figures 4.16 and 4.17) and test its prediction for an unknown sample (Figure 4.18 and 4.19). This improves the machine's prediction MSE from 0.0021 to 0.0017. We checked the effect of regularization for this model (Figures 4.20 & 4.21) and find only a minor improvement of 0.0001 in MSE. Lastly, the maximum number of samples is kept the same and only the number of neurons is changed – first to 100 neurons (Figures 4.22, 4.24, 4.26, 4.28) and then to 500 neurons (Figures 4.23, 4.25, 4.27 and 4.29). Keeping the number of biomass samples used for training constant and reducing the number of neurons to 100 from 200, we see a decrease in MSE of 0.0001. Whereas, for the same number of training biomass samples and increasing the number of neurons from 200 to 500, we get an increase in MSE for test prediction of 0.0001.
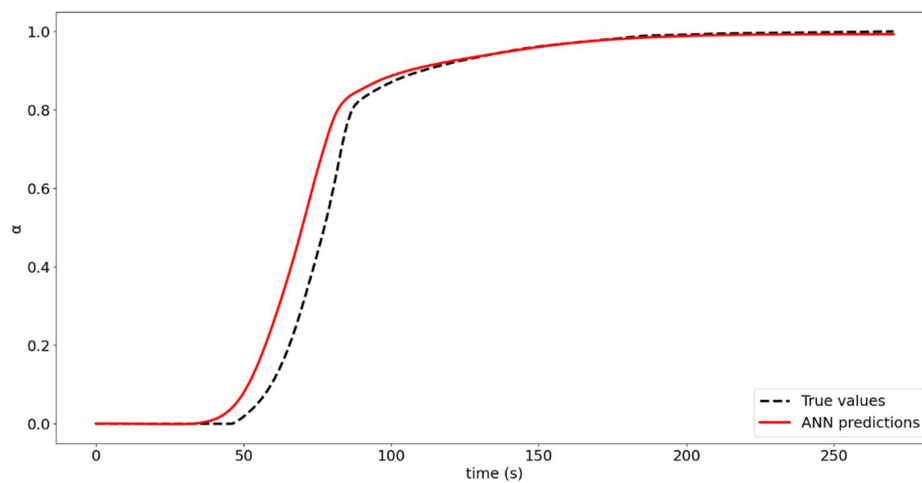
*Figure 4.12 Results for model trained using pure cellulose, hemicellulose, lignin and new particle size range samples – unknown sample test data*
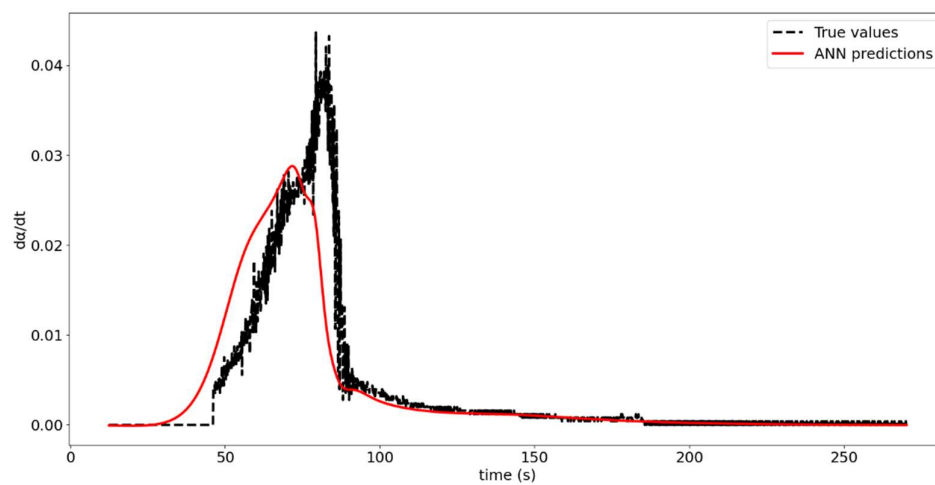


*Figure 4.13 Results for model trained using pure cellulose, hemicellulose, lignin and new particle size range samples – unknown sample test data; unregularized*
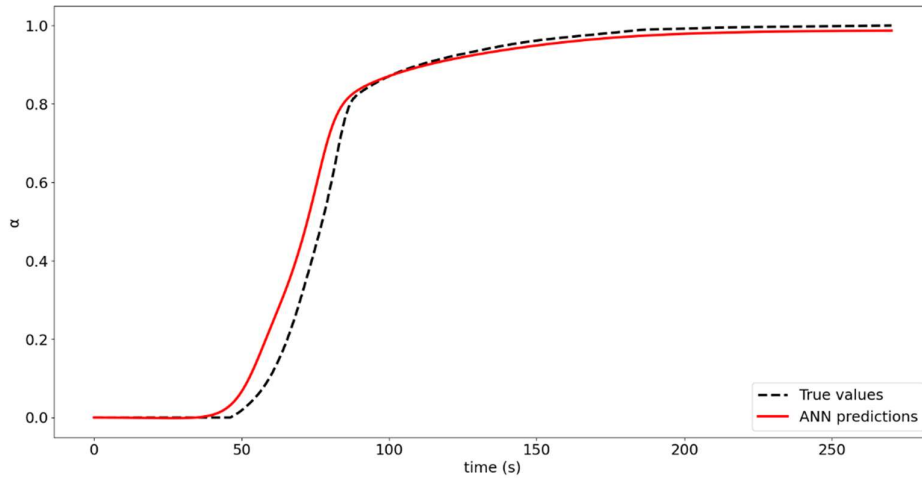
*Figure 4.14 Prediction results for unknown sample trained using 6 additional samples - test data results*
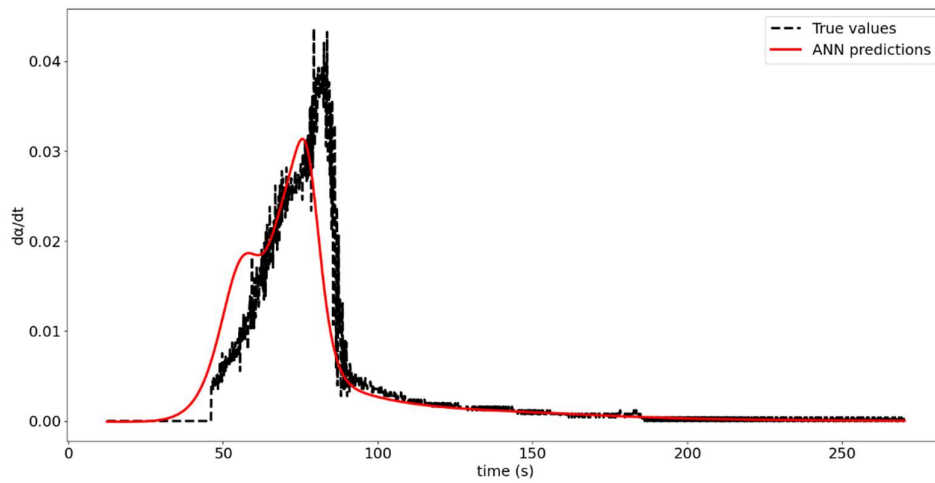


*Figure 4.15 Prediction results for unknown sample trained using 6 additional samples - test data results; 5 hidden layers and 200 neurons per hidden layer*
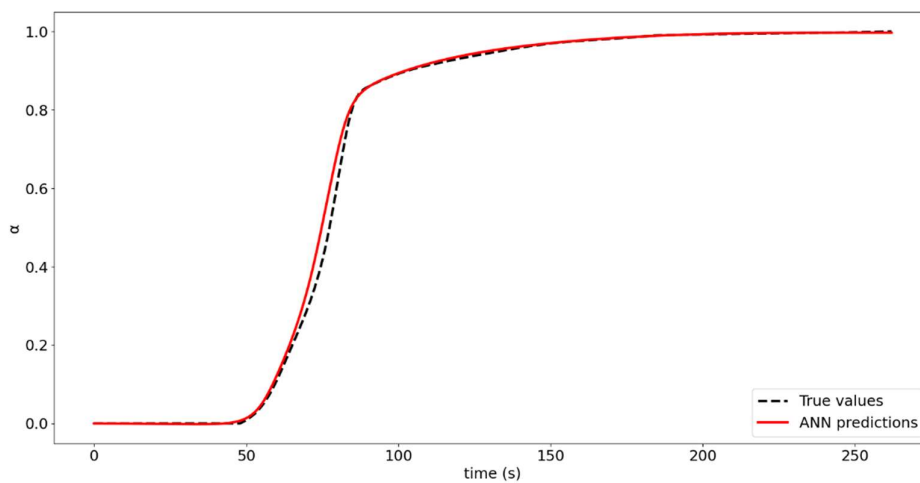
111

*Figure 4.16 Prediction of conversion function using training data after training using 9 additional samples; 5 hidden layers and 200 neurons per hidden layer*
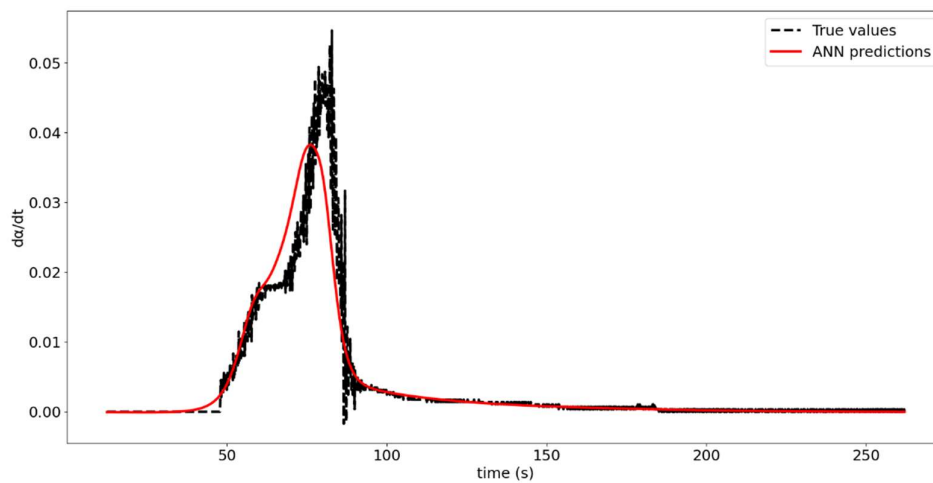


*Figure 4.17 Prediction of reaction rate function using training data after training using 9 additional samples; 5 hidden layers and 200 neurons per hidden layer*
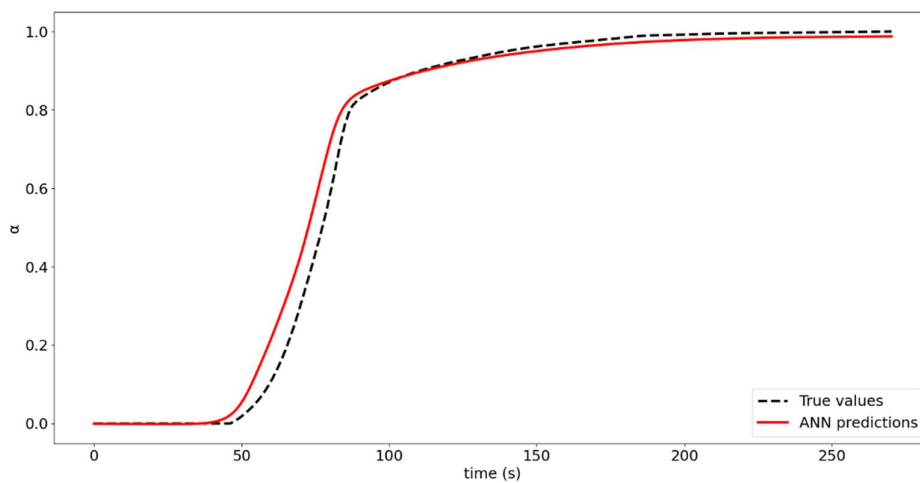
*Figure 4.18 Prediction of conversion function for unknown sample after training using 9 additional samples; 5 hidden layers and 200 neurons per hidden layer*
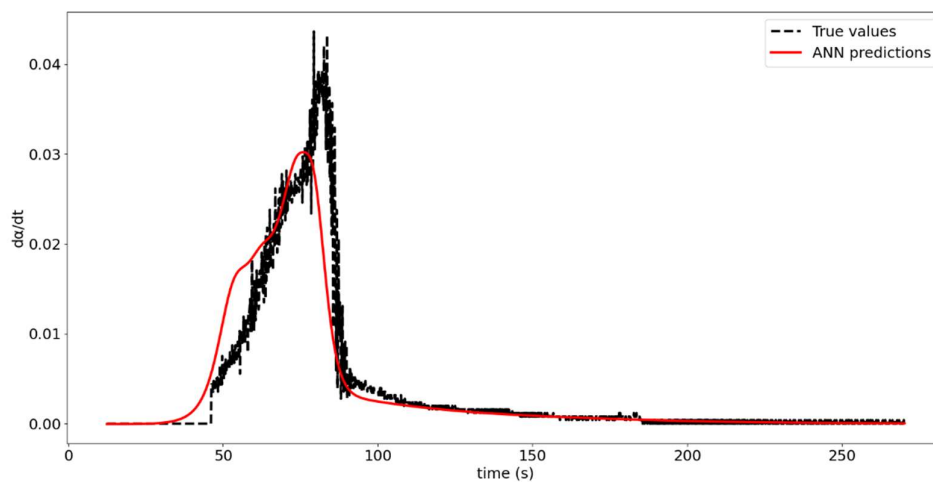


*Figure 4.19 Prediction of reaction rate function for unknown sample after training using 9 additional samples; 5 hidden layers and 200 neurons per hidden layer*
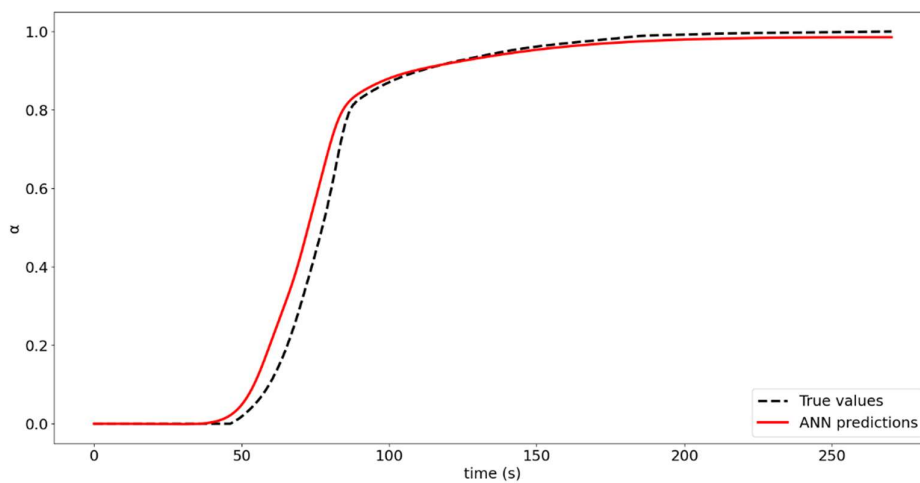
*Figure 4.20 Prediction of conversion function for unknown sample after training using 9 additional samples and using regularization - test data results; 5 hidden layers and 200 neurons per hidden layer*
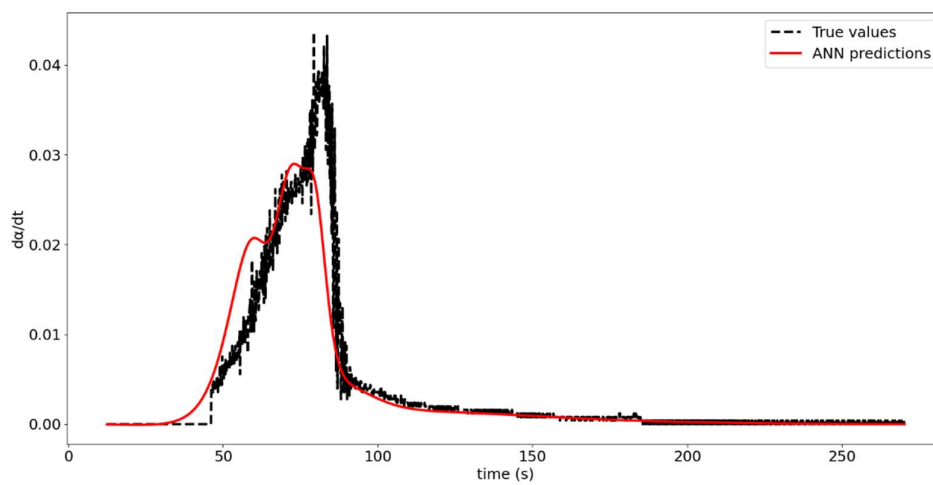


*Figure 4.21 Prediction of reaction rate function for unknown sample after training using 9 additional samples and using regularization - test data results; 5 hidden layers and 200 neurons per hidden layer*
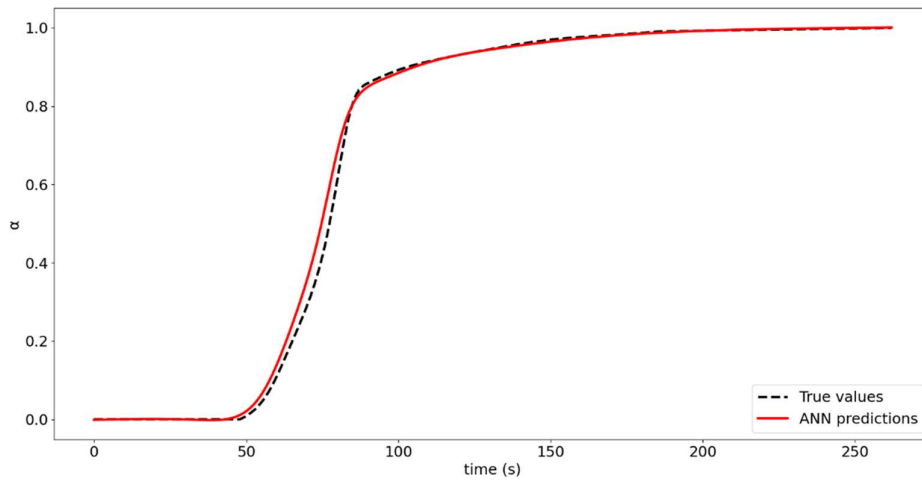
*Figure 4.22 Training data result for conversion function for model with 100 neurons, 5 HL and all training samples*
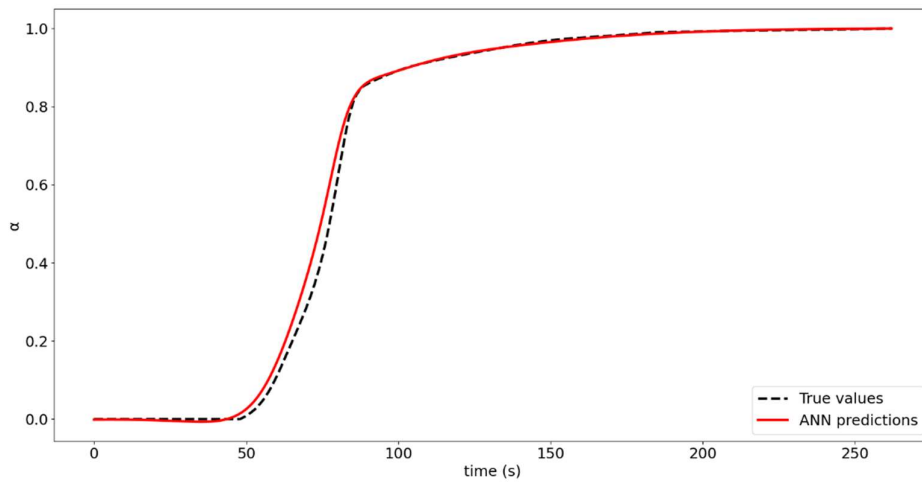


*Figure 4.23 Training data result for conversion function for model with 500 neurons, 5 HL and all training samples*

*Figure 4.24 Training data result for rate of reaction function for model with 100 neurons, 5 HL and all training samples*



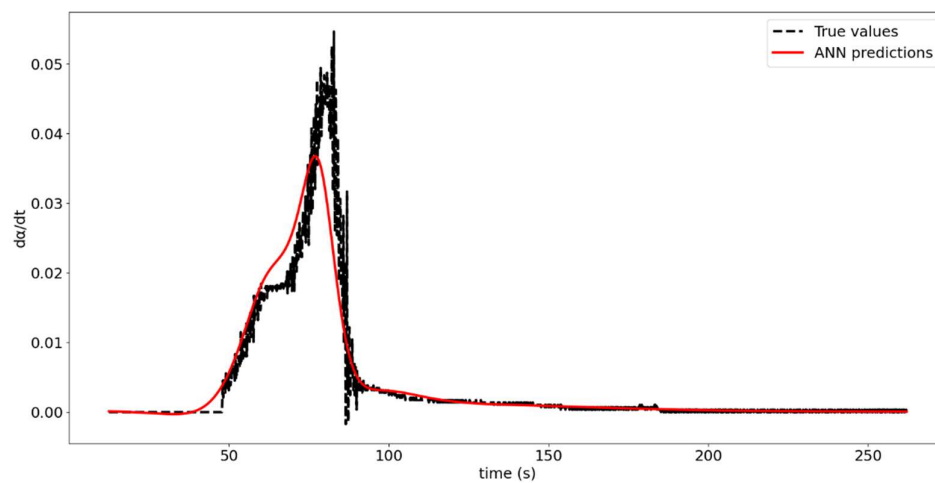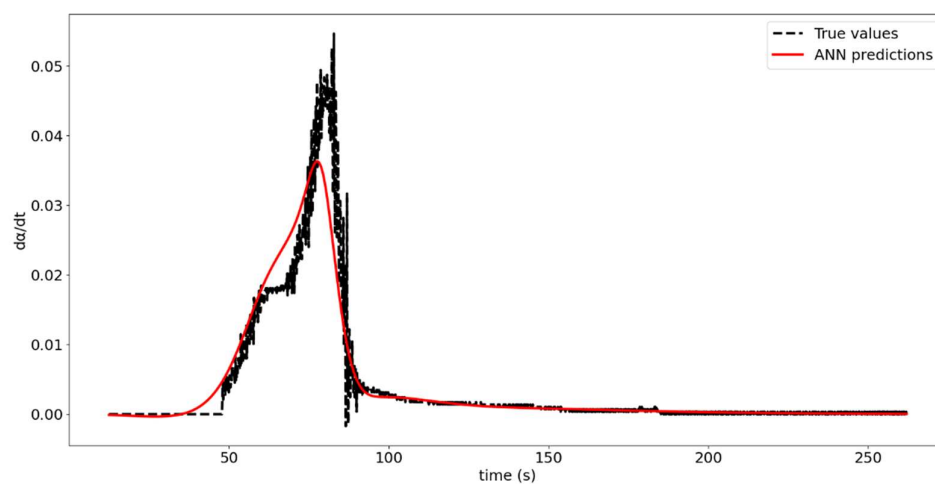*Figure 4.25 Training data result for rate of reaction function for model with 500 neurons, 5 HL and all training samples*

*Figure 4.26 Test result of conversion function for unknown sample by model with 100 neurons, 5 HL and all training samples*
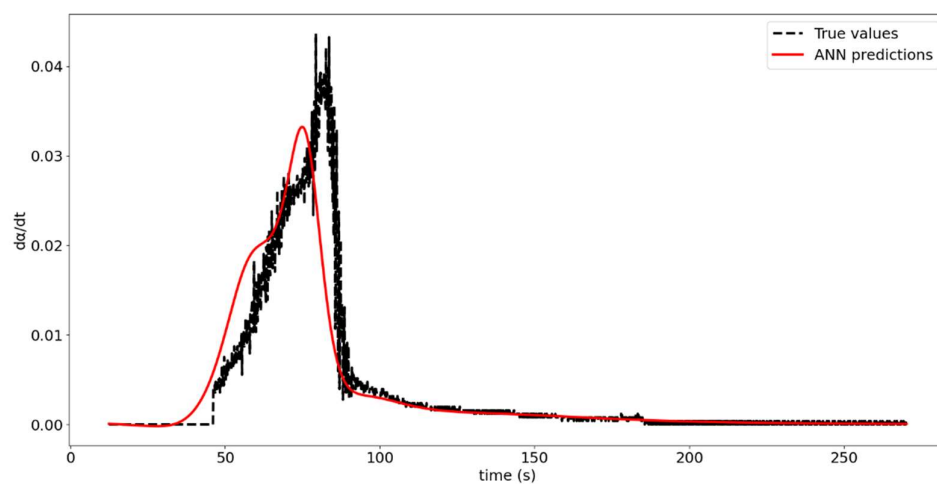


*Figure 4.27 Test result of rate of reaction function for unknown sample by model with 100 neurons, 5 HL and all training samples*
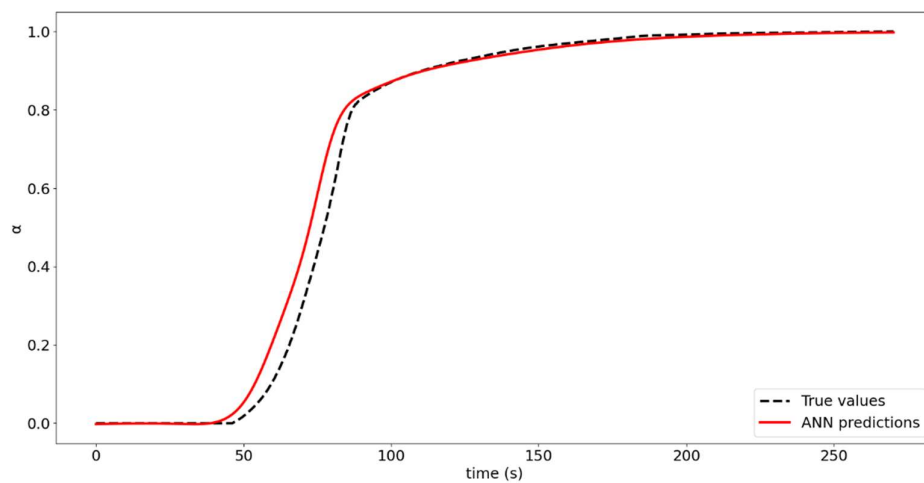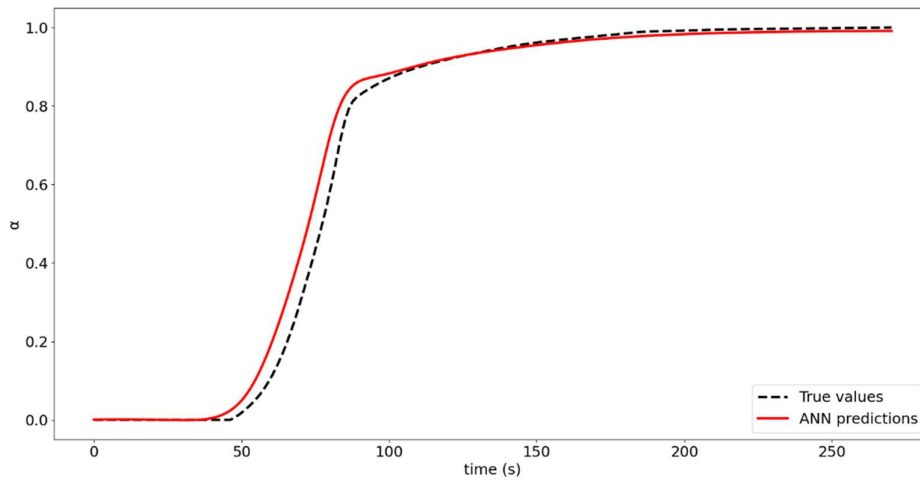
*Figure 4.28 Test result of conversion function for unknown sample by model with 500 neurons, 5 HL and all training samples*
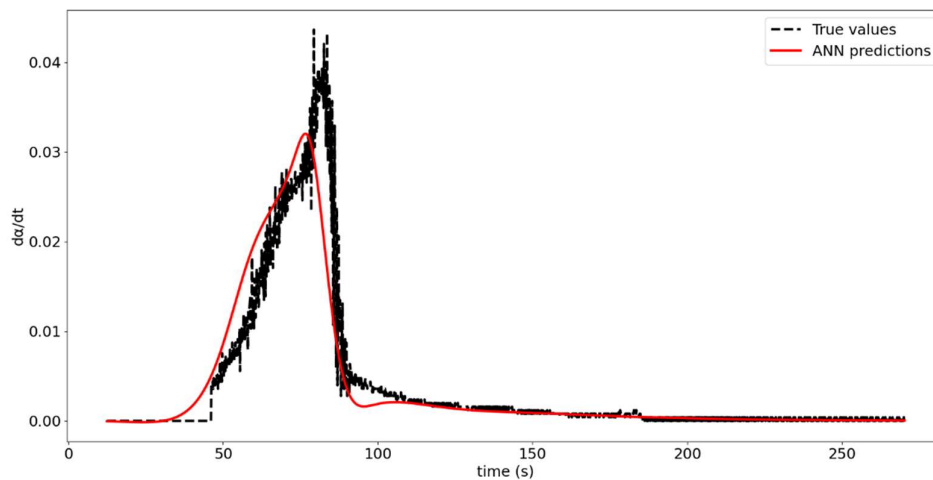


*Figure 4.29 Test result of rate of reaction function for unknown sample by model with 500 neurons, 5 HL and all training samples*

Using ANN model, the compositional heterogeneity of biomass is accounted for and can be dealt with better by providing better process control to the variation in feedstock. The accuracy of ANN model depends on both the volume and quality of spread of data sets on which it is trained. The prediction ability of ANN model bears strong dependence on number of samples used for training and variation in compositional heterogeneity. The ANN models prediction is improved by increasing the number of neurons and hidden layers, however this has a milder effect on prediction capability as compared to compositional variation and

number of training samples. The higher the number of neurons and hidden layers, more is the computational time necessary for training and testing the model. ANN model with 200 neurons and 5 hidden layers shows good prediction capability with reasonable computation duty. The artificial neural network models having incorporated the effect of composition on reaction kinetics, bear the potential for further improvement by increasing the variation and quantity of training sets.

The range of validity and prediction accuracy of the developed model will be improved by training it with more varied experimental data. Other parameters such as number of hidden layers, number of neurons in each layer, weight of the residual loss function, optimizers and learning rates could be tuned to improve the results of ANN predictions. However, those investigations lie beyond the purview of current thesis work and shall be dealt with in future work.

## Further scope of work

To improve the predictive capability of the model within the domain specified in this work, it should be trained with newer biomass samples mass loss data at 250 °K/min heating rate. This would improve the rigour of model within specified boundaries. It is also possible to incorporate newer dimensions such as multiple heating rates and catalytic effect into the model. However, without enough variety in each newly added domain, the model fails to predict unknow samples. To ensure uniqueness in the value of predicted kinetic parameters, the prediction accuracy needs to be improved and the model needs to be trained on a profusion of data generated from experimental work and literature.The understanding from current work is summarised in the final chapter 5. Some aspects of reactor design and incorporation of current modelling approach to achieve dynamic reactor control are also touched upon in the concluding chapter.

# References

(1) Vyazovkin, S. *Isoconversional Kinetics of Thermally Stimulated Processes*; Springer International Publishing: Cham, 2015. https://doi.org/10.1007/978-3-319-14175-6.

(2) Goodfellow, I.; Bengio, Y.; Courville, A. *Deep Learning*; MIT press, 2016.

(3) Conesa, J. A.; Caballero, J. A.; Reyes-Labarta, J. A. Artificial Neural Network for Modelling Thermal Decompositions. *J. Anal. Appl. Pyrolysis* **2004**, *71* (1), 343–352. https://doi.org/10.1016/S0165-2370(03)00093-7.

(4) Puig-Arnavat, M.; Hernández, J. A.; Bruno, J. C.; Coronas, A. Artificial Neural Network Models for Biomass Gasification in Fluidized Bed Gasifiers. *Biomass Bioenergy* **2013**, *49*, 279–289. https://doi.org/10.1016/j.biombioe.2012.12.012.

(5) Puig-Arnavat, M.; Bruno, J. C. Artificial Neural Networks for Thermochemical Conversion of Biomass. In *Recent advances in thermo-chemical conversion of biomass*; Elsevier, 2015; pp 133–156.

(6) Sunphorka, S.; Chalermsinsuwan, B.; Piumsomboon, P. Application of Artificial Neural Network for Kinetic Parameters Prediction of Biomass Oxidation from Biomass Properties. *J. Energy Inst.* **2017**, *90* (1), 51–61. https://doi.org/10.1016/j.joei.2015.10.007.

(7) Sunphorka, S.; Chalermsinsuwan, B.; Piumsomboon, P. Artificial Neural Network Model for the Prediction of Kinetic Parameters of Biomass Pyrolysis from Its Constituents. *Fuel* **2017**, *193*, 142–158. https://doi.org/10.1016/j.fuel.2016.12.046.

(8) Liu, J.; Jia, H.; Mairaj Deen, K.; Xu, Z.; Cheng, C.; Zhang, W. Application of Machine Learning Methods for Lignocellulose Biomass Pyrolysis: Activation Energy Prediction from Preliminary Analysis and Conversion Degree. *Fuel* **2023**, *343*, 128005. https://doi.org/10.1016/j.fuel.2023.128005.

(9) Balsora, H. K.; Kartik, S.; Dua, V.; Joshi, J. B.; Kataria, G.; Sharma, A.; Chakinala, A. G. Machine Learning Approach for the Prediction of Biomass Pyrolysis Kinetics from Preliminary Analysis. *J. Environ. Chem. Eng.* **2022**, *10* (3), 108025.

(10) Nawaz, A.; Kumar, P. Pyrolysis Behavior of Low Value Biomass (Sesbania Bispinosa) to Elucidate Its Bioenergy Potential: Kinetic, Thermodynamic and Prediction Modelling Using Artificial Neural Network. *Renew. Energy* **2022**, *200*, 257–270. https://doi.org/10.1016/j.renene.2022.09.110.

(11) Rasool, T.; Srivastava, V. C.; Khan, M. N. S. Utilisation of a Waste Biomass, Walnut Shells, to Produce Bio-Products via Pyrolysis: Investigation Using ISO-Conversional and Neural Network Methods. *Biomass Convers. Biorefinery* **2018**, *8* (3), 647–657. https://doi.org/10.1007/s13399-018-0311-0.

(12) Ji, W.; Richter, F.; Gollner, M. J.; Deng, S. Autonomous Kinetic Modeling of Biomass Pyrolysis Using Chemical Reaction Neural Networks. *Combust. Flame* **2022**, *240*, 111992. https://doi.org/10.1016/j.combustflame.2022.111992.

(13)    Zhu, H.; Dong, Z.; Yu, X.; Cunningham, G.; Umashanker, J.; Zhang, X.; Bridgwater, A. V.; Cai, J. A Predictive PBM-DEAM Model for Lignocellulosic Biomass Pyrolysis. *J. Anal. Appl. Pyrolysis* **2021**, *157*, 105231.

(14)    Zhu, L.-T.; Chen, X.-Z.; Ouyang, B.; Yan, W.-C.; Lei, H.; Chen, Z.; Luo, Z.-H. Review of Machine Learning for Hydrodynamics, Transport, and Reactions in Multiphase Flows and Reactors. *Ind. Eng. Chem. Res.* **2022**, *61* (28), 9901–9949.

(15)    Reyes-Urrutia, A.; Capossio, J. P.; Venier, C.; Torres, E.; Rodriguez, R.; Mazza, G. Artificial Neural Network Prediction of Minimum Fluidization Velocity for Mixtures of Biomass and Inert Solid Particles. *Fluids* **2023**, *8* (4), 128.

(16)    Sun, Y.; Liu, L.; Wang, Q.; Yang, X.; Tu, X. Pyrolysis Products from Industrial Waste Biomass Based on a Neural Network Model. *J. Anal. Appl. Pyrolysis* **2016**, *120*, 94–102. https://doi.org/10.1016/j.jaap.2016.04.013.

(17)    Mutlu, İ.; Yaman, S.; Haykiri-Acma, H. A Study to Predict Pyrolytic Behaviors of Refuse-Derived Fuel (RDF): Artificial Neural Network Application. *J. Anal. Appl. Pyrolysis* **2016**, *122*, 84–94. https://doi.org/10.1016/j.jaap.2016.10.013.

(18)    Ascher, S.; Watson, I.; You, S. Machine Learning Methods for Modelling the Gasification and Pyrolysis of Biomass and Waste. *Renew. Sustain. Energy Rev.* **2022**, *155*, 111902.

(19)    Yucel, O.; Aydin, E. S.; Sadikoglu, H. Comparison of the Different Artificial Neural Networks in Prediction of Biomass Gasification Products. *Int. J. Energy Res.* **2019**, *43* (11), 5992–6003. https://doi.org/10.1002/er.4682.

(20)    Kargbo, H. O.; Zhang, J.; Phan, A. N. Optimisation of Two-Stage Biomass Gasification for Hydrogen Production via Artificial Neural Network. *Appl. Energy* **2021**, *302*, 117567. https://doi.org/10.1016/j.apenergy.2021.117567.

(21)    Alabdrabalnabi, A.; Gautam, R.; Sarathy, S. M. Machine Learning to Predict Biochar and Bio-Oil Yields from Co-Pyrolysis of Biomass and Plastics. *Fuel* **2022**, *328*, 125303.

(22)    Wei, H.; Luo, K.; Xing, J.; Fan, J. Predicting Co-Pyrolysis of Coal and Biomass Using Machine Learning Approaches. *Fuel* **2022**, *310*, 122248.

(23)    Bi, H.; Wang, C.; Lin, Q.; Jiang, X.; Jiang, C.; Bao, L. Pyrolysis Characteristics, Artificial Neural Network Modeling and Environmental Impact of Coal Gangue and Biomass by TG-FTIR. *Sci. Total Environ.* **2021**, *751*, 142293. https://doi.org/10.1016/j.scitotenv.2020.142293.

(24)    Hough, B. R.; Beck, D. A. C.; Schwartz, D. T.; Pfaendtner, J. Application of Machine Learning to Pyrolysis Reaction Networks: Reducing Model Solution Time to Enable Process Optimization. *Comput. Chem. Eng.* **2017**, *104*, 56–63. https://doi.org/10.1016/j.compchemeng.2017.04.012.

(25)    Lu, L.; Pecha, M. B.; Wiggins, G. M.; Xu, Y.; Gao, X.; Hughes, B.; Shahnam, M.; Rogers, W. A.; Carpenter, D.; Parks II, J. E. Multiscale CFD Simulation of Biomass Fast Pyrolysis with a Machine Learning Derived Intra-Particle Model and Detailed Pyrolysis Kinetics. *Chem. Eng. J.* **2022**, *431*, 133853.

(26)     Zhong, H.; Xiong, Q.; Yin, L.; Zhang, J.; Zhu, Y.; Liang, S.; Niu, B.; Zhang, X. CFD-Based Reduced-Order Modeling of Fluidized-Bed Biomass Fast Pyrolysis Using Artificial Neural Network. *Renew. Energy* **2020**, *152*, 613–626. https://doi.org/10.1016/j.renene.2020.01.057.

(27)     Li, T. Y.; Xiang, H.; Yang, Y.; Wang, J.; Yildiz, G. Prediction of Char Production from Slow Pyrolysis of Lignocellulosic Biomass Using Multiple Nonlinear Regression and Artificial Neural Network. *J. Anal. Appl. Pyrolysis* **2021**, *159*, 105286. https://doi.org/10.1016/j.jaap.2021.105286.

(28)     Liew, Y. W.; Arumugasamy, S. K.; Selvarajoo, A. Potential of Biochar as Soil Amendment: Prediction of Elemental Ratios from Pyrolysis of Agriculture Biomass Using Artificial Neural Network. *Water. Air. Soil Pollut.* **2022**, *233* (2), 54. https://doi.org/10.1007/s11270-022-05510-2.

(29)     Kanthasamy, R.; Almatrafi, E.; Ali, I.; Hussain Sait, H.; Zwawi, M.; Abnisa, F.; Choe Peng, L.; Victor Ayodele, B. Bayesian Optimized Multilayer Perceptron Neural Network Modelling of Biochar and Syngas Production from Pyrolysis of Biomass-Derived Wastes. *Fuel* **2023**, *350*, 128832. https://doi.org/10.1016/j.fuel.2023.128832.

(30)     Aniza, R.; Chen, W.-H.; Yang, F.-C.; Pugazhendh, A.; Singh, Y. Integrating Taguchi Method and Artificial Neural Network for Predicting and Maximizing Biofuel Production via Torrefaction and Pyrolysis. *Bioresour. Technol.* **2022**, *343*, 126140. https://doi.org/10.1016/j.biortech.2021.126140.

(31)     Debiagi, P.; Gentile, G.; Cuoci, A.; Frassoldati, A.; Ranzi, E.; Faravelli, T. A Predictive Model of Biochar Formation and Characterization. *J. Anal. Appl. Pyrolysis* **2018**, *134*, 326–335.

(32)     Ighalo, J. O.; Adeniyi, A. G.; Marques, G. Application of Artificial Neural Networks in Predicting Biomass Higher Heating Value: An Early Appraisal. *Energy Sources Part Recovery Util. Environ. Eff.* 1–8. https://doi.org/10.1080/15567036.2020.1809567.

(33)     Tsekos, C.; Tandurella, S.; de Jong, W. Estimation of Lignocellulosic Biomass Pyrolysis Product Yields Using Artificial Neural Networks. *J. Anal. Appl. Pyrolysis* **2021**, *157*, 105180. https://doi.org/10.1016/j.jaap.2021.105180.

(34)     Tang, Q.; Chen, Y.; Yang, H.; Liu, M.; Xiao, H.; Wu, Z.; Chen, H.; Naqvi, S. R. Prediction of Bio-Oil Yield and Hydrogen Contents Based on Machine Learning Method: Effect of Biomass Compositions and Pyrolysis Conditions. *Energy Fuels* **2020**, *34* (9), 11050–11060.

# Chapter 5 Reflections and future directions

## Summary

A set of experiments to determine the composition of biomass samples were performed. Conversion profiles and rate of reaction profiles for biomass samples at different heating rates were studied. Existing kinetic methods were used to study the reaction kinetics of biomass pyrolysis. A novel predictive modelling approach was developed for biomass pyrolysis. Artificial neural networks were used to develop models capable of predicting conversion and rate of reaction profiles for unknown biomass samples. This approach has the potential for dynamic control of heterogenous feedstock and is applicable over wider heating rate range.

## Conclusion

It is evident that biomass slow pyrolysis and biomass fast pyrolysis are qualitatively different phenomena. For low $\Delta T/\Delta t$ values or slow heating rates or slow pyrolysis condition, the thermal breakdown reactions of biomass are lumped together. As opposed to this, discrete reaction regimes are observed in case of higher heating rates or fast pyrolysis conditions or large $\Delta T/\Delta t$ values. To perform biomass fast pyrolysis, two conditions must be ensured, kinetically controlled reaction regime and minimization of secondary and tertiary reactions. Pyrolysis reaction can either assume an endothermic route or an exothermic route. Endothermic control of reaction leads to optimization of crude oil formation. Exothermic control of reaction leads to formation of char and syngas. Kinetic control of reaction would promote endothermicity and optimise oil yield. Whether a reaction pathway is via kinetic control or thermodynamic control is determined by total reaction and vapour residence time under fixed operating conditions. Higher $\Delta t/\Delta T$ ratios will favour thermodynamic control whereas lower $\Delta t/\Delta T$ ratios will favour kinetic control of reaction pathway. A reactor in which heat transfer is facilitated via conduction is suitable for obtaining char and gas yield. For optimizing crude oil yield (qualitatively and quantitatively) dominant mode(s) of heat transfer need to be convection and radiation. Biomass fast pyrolysis is not just a function of temperature but also of its composition. Existing kinetic methods do not take composition into consideration. Such an assumption works in case of homogenous feedstock. Existing methods as such are based on the implicit assumption that solid feedstock is homogeneous. Biomass is inherently heterogeneous. To address this, in this work, artificial neural network models are trained to predict the conversion and rate of reaction profiles for unknown biomass samples. These models incorporate the biochemical composition of biomass, show good predictions for unknown biomass samples and are applicable over wider heating rate range.

123

## Highlights

- The modelling approach presented in this work captures in terms of mass quantification the compositional heterogeneity of biomass in pyrolysis kinetics.

- The model(s) are also extendable to higher heating rates.

- The models have the capacity to predict conversion profiles of unknown biomass samples.

- The models show promise in predicting the rate of reaction profile for unknown biomass samples with some accuracy. This accuracy in prediction for unknown biomass samples is shown to increase upon training with more varied composition data.

- The current model has cellulose (wt%), hemicellulose (wt%), lignin (wt%) and heating rate ($^{\circ}$K/s) as dimensions. Given enough variation in each dimension, the current model can be trained to incorporate newer dimensions.

## Recommendations

It is recommended that to realise the potential of biomass pyrolysis for bio-oil production, major areas of focus and investigation should be novel reactor designs, experiments to elucidate the multi-scale variation in reaction mechanism and developing predictive models capable of handling a variable heterogenous feedstock with process control. Incorporating pretreatment and down-streaming aspects into design considerations is also recommended since these aspects influence the bio-oil yield.

To achieve heat transfer rates sufficient for fast pyrolysis it is recommended that the dominant form of heat transfer be either convection or radiation. It is also recommended that the vapour residence times be kept to minimal, not more than 5 second in reaction regime. As such a reactor with mechanism to facilitate rapid vapour transport and immediate quenching to stop further vapour phase reactions is recommended. Particle size reduction prior to pyrolysis is also recommended.

Experimental investigations to determine bio-yield composition at different temperature and vapour residence times are recommended. The experiments should be performed at

isothermal conditions with small particle sizes and with rapid transport and quenching of pyrolysis vapours, preferably in a series of chilled organic and inorganic solvents. A study of bio-oil yields at different isothermal temperatures with varying vapour residence times will allow for the integration of reaction mechanism and kinetic study.

It is recommended that the model presented in this work is trained further using more varied biomass compositions to improve the prediction of rate of reaction profile for unknown biomass samples. Ultimately, if the potential of biomass pyrolysis for oil generation is to be realized fully, a concerted effort which makes use of open-source software and platforms to bring together the research of various groups and institutes engaged in investigating biomass fast pyrolysis is recommended.